# SHEAR TRANSFER STRENGTH OF CONCRETE PLACED AGAINST HARDENED CONCRETE

A Thesis

Presented to

The Graduate Faculty of The University of Akron

In Partial Fulfillment

of the Requirements for the Degree

Master of Science

Mohamed Habouh

August, 2015

SHEAR TRANSFER STRENGTH OF CONCRETE PLACED AGAINST HARDENED CONCRETE

Mohamed Habouh

Thesis

| Approved: | Accepted: |
| --- | --- |
| Advisor<br>Dr. Anil Patnaik | Department Chair<br>Dr. Wieslaw K. Binienda |
| Committee Member<br>Dr. David Roke | Acting Dean of the College<br>Dr. Rex Ramsier |
| Committee Member<br>Dr. Ala Abbas | Interim Dean of the Graduate school<br>Dr. Chand Midha |
| | Date |

# ABSTRACT

Shear transfer strength of concrete placed against hardened concrete has been of interest because of the unavoidable joints between structural elements. Failed joints in adjacent box beam girder bridges cause premature aging of these bridges and financial liabilities. There are no design guidelines for such joints. This research was performed to understand the joint behavior and vertical shear transfer mechanism of as-cast concrete joints. Three sets of reinforced, un-reinforced along with specimens with precompression were tested. Finite element analyses models were developed. It was established that (a) ACI 318-2011 over-estimates the shear strength of joints with high clamping force. (b) The shear strength expression introduced by Patnaik 2001 for horizontal shear for smooth interface is applicable for vertical shear with a well defined upper bound for shear strength at clamping forces larger than 800 psi. (c) Lateral stresses and lateral spread of joints are generated due to vertical shear. Lateral supports and the application of normal compressive forces to shear interface will increase the joint strength. (d) Larger vertical slip at the shear interfaces at failure load is possible when external normal force is applied.

ACKNOWLEDGMENTS

I would like to express my deepest and sincere appreciation to my advisor Dr. Anil Patnaik for his persistent guidance and continued support throughout the research; He has been a constant source of great inspiration for me. I am also very thankful to my committee members, Dr. D. Roke and Dr. A. Abbas for their valuable suggestions and corrections. I would like to thank all my friends; the graduate students for their help and valuable advices throughout the entire research process, I would like to thank my family and friends for their continued support in this challenging experience.

TABLE OF CONTENTS

Page

LIST OF TABLES

LIST OF FIGURES

Figure Page

# CHAPTER I

# INTRODUCTION

## 1.1 Background and Problem Statement

In reinforced concrete structures, the integrity of the structural elements is important; the highest load carrying capacity will be achieved if there are no joints between different concrete units, and the entire structure is made as a monolithic concrete structure assuring that the structure will act as a single unit. However making a structure completely monolithic is not always the practical or economical. Therefore, joints are unavoidable in construction. Cost, time, ease of construction, and safety are important factors that will influence the location and number of planned and controlled construction joints. Construction joints may result from unexpected circumstances that can be due to the breakdown of construction equipment, unsuitable materials (e.g., concrete with properties outside the acceptable QA/QC limits), or bad weather condition. It is important to avoid the joints in the locations of high bending or shear stresses. Joints can be vertical or horizontal while the loads acting in these joints can be perpendicular or parallel to the joint interface. Some examples of the expected joints are the joints between the web and the flange in T-sections, joints between columns and their footings, joints between the columns and the beams, the longitudinal joints in the adjacent prestressed concrete box

beam girders. Such joints can be reinforced joints with transverse rebar or unreinforced joints. The capacity of the unreinforced joints can be significantly low in comparison with the reinforced joints. The overall design of a structure including the joints is to ensure that the structure acts as one monolithic unit.

In adjacent prestressed box beam girders, when joints are exposed to the weather and loading conditions, the failure of the shear key between the adjacent girders is usually accompanied with failure in the waterproofing membranes. The key way joints are grouted with cementitious grouts. The water leaking through the key way of a typical longitudinal joint will corrode the internal reinforcement and the prestressing strands leading to spalling of the concrete cover in the box beams. This problem is a very common problem as reported by many state departments of transportation in the United States.

Figure 1: Water Leakage at a Typical Joint in Adjacent Box Beams

In bridges, failure of the joints can cause deterioration because the girders will act individually under the applied loads resulting in higher vertical deflection and larger horizontal movements that can cause the reported waterproofing membrane failure, usually the cracks propagates to the asphalt pavement on the surface. The corroded strands within the box beams can suffer reduced cross-sectional area and loss of prestress leading to higher deflection than expected. In order to understand the joint behavior, the shear transfer strength of the grout placed against the hardened concrete surface of the adjacent precast concrete box beams needs to be evaluated.

Figure 2: Box Beams with Corroded Strands at the Bottom

In this research project, the interface shear transfer strength was investigated for concrete placed against hardened concrete with and without reinforcement when a static

load is applied parallel to the interface to develop the required basis for establishing the failure criteria and the quantify the effects of the factors influencing the joint shear transfer capacity at the key way joints of adjacent box beam bridges.

## 1.2 ACI Current Practice

The American Concrete Institute Code (ACI 318, 2011) adopted the shear-friction concept to evaluate the shear strength of the cracked concrete and the concrete placed against hardened concrete. It is assumed that such a crack will form, and that reinforcement must be provided across the crack to resist relative displacement by dowel action. When shear acts along a crack, one crack face slips relative to the other. If the crack faces are rough and irregular, this slip is accompanied by separation of the crack faces. At ultimate, the separation is sufficient to stress the reinforcement crossing the crack to its yield point. The reinforcement provides a clamping force ($A_{vf}\ f_y$) across the crack faces. The applied shear is then resisted by friction between the crack faces, and by dowel action of the reinforcement crossing the crack.

When the shear-friction reinforcement is perpendicular to the shear plane, the nominal shear strength $V_n$ is given by

$$V_n = 0.8A_{vf}f_y + A_cK_1$$

where Ac is the area of concrete section resisting shear transfer ($in^2$ ) and $K_1$ = 400 psi for normal weight concrete, 200 psi for all-lightweight concrete, and 250 psi for sand lightweight concrete. These values of $K_1$ apply to both monolithically cast concrete and to concrete cast against hardened concrete with a rough surface.

Another ACI equation to determine the shear capacity for concrete placed against hardened concrete with rough surface

$Vn = A_{vf} f_y \mu$. Where μ is coefficient of friction = 1.0 λ

$\lambda = 1$ for normal weight concrete, for the case of concrete placed against the hardened concrete with rough interface, a coefficient of 1.0 is used. And three upper limits are applied to the shear capacity, and the smallest limit governs.

$$V_n \leq (0.2f'_c A_c \; or \; (480 + 0.08f'c) A_c \; or \; 1600A_c)$$

The Horizontal shear strength was defined by the ACI 318-11 in section 11.4.6.3 when the contact surfaces are clean, free of laitance, and intentionally roughened to a full amplitude of approximately 1/4 in., $V_{nh}$ shall be taken equal to $(260 + 0.6\rho_v f_y)\lambda b_v d$, but not greater than $500 b_v d$.

The expression accounts only for the surface area of the interface and the steel ties crossing the interface, that reinforcement was defined in section 17.6.1, 17.6.2, 17.6.3 as

- Where ties are provided to transfer horizontal shear, tie area shall not be less than $0.75\sqrt{f'_c}\,(b_V * s/f_{yt})$, and tie spacing shall not exceed four times the least dimension of supported element, nor exceeding 24 in.
- Ties for horizontal shear shall consist of single bars or wire, multiple leg stirrups, or vertical legs of welded wire reinforcement.
- All ties shall be fully anchored into interconnected elements.

The design expression doesn't account for the compressive strength of the concrete if $[V_{nh} < 500 b_v d]$. If $(V_{nh} > 500 b_v d)$ vertical shear using the shear friction theory will apply as discussed earlier.

## 1.3 Study Objective

The ACI doesn't differentiate between the cracked concrete and the concrete placed against hardened concrete with a rough interface. Considering the weak bond strength between the concrete placed against hardened concrete. The design expressions account for the area of reinforcement crossing the section without considering the distribution of that rebar in the section. The previous studies considered many factors that affect the shear strength of concrete interface but all of them are concrete related factors accounting for the area of steel crossing the interface, the effect of the rebar distribution of the bars in the concrete were not studied. A secondary objective is to develop a well-defined state of stresses using finite element models to understand the load paths and the effect of the different distribution of the reinforcement on the interface performance. Also needed is a validation of the horizontal shear strength expressions for the prediction of interface shear strength. The effect of the clamping force on the shear strength of concrete joined using grout material is also needed. The following is a summary of the objectives of the study:

- Evaluation of the ACI current expression
- Evaluate the previous expressions by researchers
- Determine the behavior of joints under applied loads
- Study the effects of steel area, rebar distribution of the steel crossing the shear interface, and the effects of concrete interface area
- Study effects of lateral restraints at the interface, and normal forces acting on the interface

# CHAPTER II

# LITERATURE REVIEW

The shear capacity of reinforced concrete has been subject to research since the fifties of 20$^{th}$ century, with that extensive research for the last 60 years, the design codes had changed over time to reach the current shear strength expressions stated in ACI 318-11. The current practices at the time of each study and the interest of different researchers varied in the context of structural concrete in different earlier studies. In this literature review, the developments, theories, and test results from previous research are explained within the following classification.

1. The differences between the shear capacities for monolithic concrete, the concrete placed against hardened concrete, the cracked concrete, concrete interface with smooth or rough interface, and the application of shear keys and its effect on the ultimate shear strength.
2. The factors affecting the bond strength between concrete layers with different ages.
3. The study of the ultimate shear strength for the case of horizontal and vertical shear.

## 2.1 The factors affecting the bond strength between concrete layers with different ages.

There are many parameters which are often neglected by the design codes that can affect the strength of the interface by affecting the bond strength at the interface

Between concrete layers cast at different ages (Birkeland H. W., 1968). The factors adopted under this study are described in the following sections of this chapter.

2.1.1 Surface Preparation.

Roughness of concrete interface will change the friction coefficient of the concrete interface.

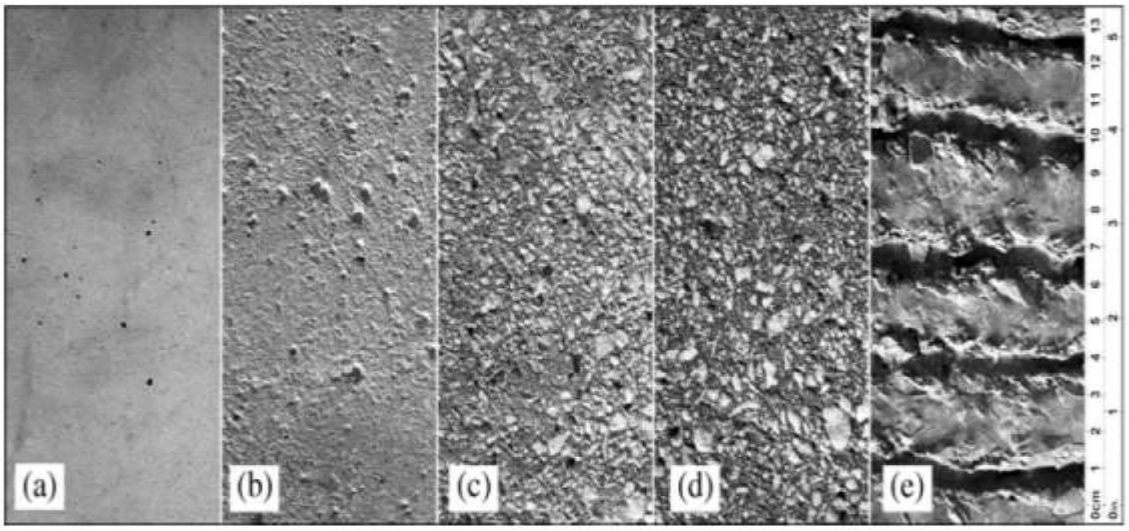


Figure 3 : Roughness of Concrete Surface (Pedro & Eduardo, 2011)

In Figure 3 on surface preparation the following are the descriptions of each surface (a) left as-cast; (b) wire-brushing; (c) sandblasting; (d) shot blasting; and (e) hand-scrubbing.

A laser roughness analyzer was used to quantify the roughness parameter and to measure the maximum valley depth $R_v$. The valley depth varies from 0.005 inch for concrete placed against steel formwork to 0.093 inch for the hand scrubbed concrete.

The bond strength of the concrete-to-concrete interface increased with the increase of the surface roughness, therefore that the higher the roughness of the interface the higher the shear strength (Pedro & Eduardo, 2011).

Table 1 : Roughness Classification (Pedro & Eduardo, 2011)

| Surface preparation Maximum valley depth $R_v$, mm (inch) | |
|---|---|
| Left as-cast | 0.119 (0.005) |
| Wire-brushing | 0.473 (0.019) |
| Sand blasting | 0.604 (0.024) |
| Shot blasting | 0.899 (0.035) |
| Hand-scrubbing | 2.350 (0.093) |

2.1.2 Shrinkage

Stresses increase with the increase of the differential shrinkage between concrete layers.

2.1.3 Stiffness

The differential stiffness between the concrete layers is an important factor that will affect the friction between the concrete interface. In the study by Pedro & Eduardo (2011), four specimens each having two layers of concrete were tested to understand the effects of differential stiffness, the base (bottom) layer for the 4 specimens was $E_s = 4351$ ksi, and the top layer with four different modulus of elasticity values $E_c = 4351, 4496, 5076, and\ 6382\ ksi$. These experiments showed that the differential stiffness could have influence in the bond strength of the interface.

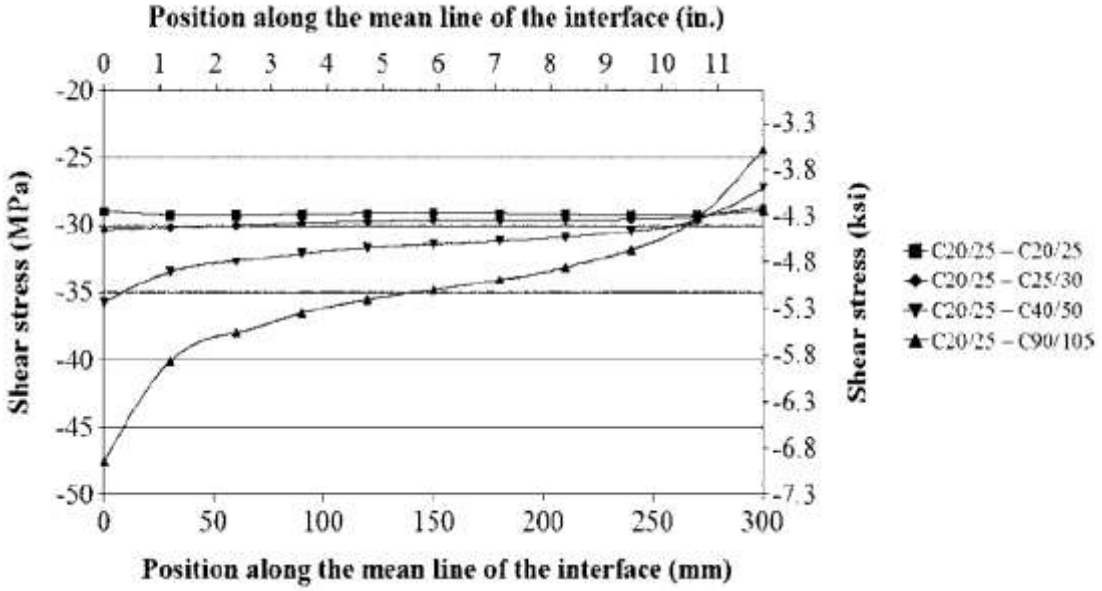


Figure 4 : Shear Distribution at Interface Due To Differential Stiffness (Pedro & Eduardo, 2011).

The stress distribution at the interface, for both shear and normal stresses, is influenced by the differential stiffness of the two units on either side of the interface. With the increase of the differential stiffness, stress concentrations occur at both ends and the stress distribution assumes an S-shaped form. For the concrete layers with the same modulus of elasticity, the stress distributions are linear along the interface.

### 2.1.4 Curing

Two curing conditions were considered in the study by Pedro & Eduardo (2011). One set of concrete specimens was stored in the laboratory and another set was stored outside, directly exposed to the environmental conditions such as solar radiation, rain, and wind. For both curing conditions, inside and outside the laboratory, the average values of temperature and relative humidity were very similar, whereas the coefficient of variation for the inside condition was approximately the double relative to the outside condition, due to higher daily fluctuations of both parameters.

## 2.2 The Study of the Ultimate Shear Strength for Horizontal shear.

The shear strength in concrete can be classified in the two major different categories, the horizontal shear strength and the vertical shear strength, both of these two categories can be subdivided by the combination of rough vs. smooth interface, reinforced vs. non reinforced, with or without shear key, monolithic vs. concrete placed against hardened concrete.

### 2.2.1 The Shear Strength in Horizontal Rough Interface for Composite Concrete Beams.

The shear strength of the composite beam specimens for the rough interface is discussed below.

#### 2.2.1.1 Horizontal Shear with Rough Interface by (Loov & Patnaik, 1994).

In this study the authors introduced a new parabolic design equation to replace four of the ACI equations based on 16 beam tests which account for the effect of the concrete strength and the clamping stress. This equation is equally applicable for lightweight concrete and semi-lightweight concrete. The test results indicated that (1) stirrups are unstressed and ineffective until the horizontal shear stresses exceed 1.5 to $2\,MPa$, (2) without special effort to produce roughness, the interface can develop adequate shear resistance and that will simplify the production of the precast concrete beams. That also eases the onsite production of concrete when it is tedious to add roughness to the interface in the concrete inside the formwork with heavy reinforcement. A normally vibrated concrete presents an as-cast surface in most of the horizontal joints. Vertical joints that are cast against wooden or steel formwork will have smooth surface. Many variables like the width and the length of the flange, different areas of longitudinal steel, variable effective depth; variable yield stress of the reinforcement leading to

clamping stresses varying from $0.4\ to\ 6.06\ MPa$ and a varying concrete compressive strength. Using an upper limit for shear strength of

$V_n = 0.25f'c$. The proposed design expression is

$$V_n = \lambda_к * \sqrt{(15 + \rho_v f_y) f'_c} \leq 0.25 f'c \text{ (psi)}$$

$$V_n = \lambda_к * \sqrt{(0.1 + \rho_v f_y) f'_c} \leq 0.25 f'_c \text{(MPa)}$$

A recommended range for the clamping stress is 0 psi to 800 psi or 0 MPa to 5.5 $MPa$, where $V_n$ is the ultimate horizontal shear stress strength at an interface.

2.2.1.2 Horizontal Shear Transfer across a Roughened Surface (Mitchell, 2002).

In the research carried out by (Mitchell, 2002), a total of 90 concrete composite members were tested to determine the horizontal shear strength along the interface of a roughened surface. The ‘‘push-off’’ method of testing was implemented to determine the capacity. It was ascertained that the roughness of the surface had a profound effect on the shear capacity and is a far better indicator of strength than the compressive strength of the concrete. Design curves were provided based on the surface roughness and the compressive strength of the in-situ concrete.

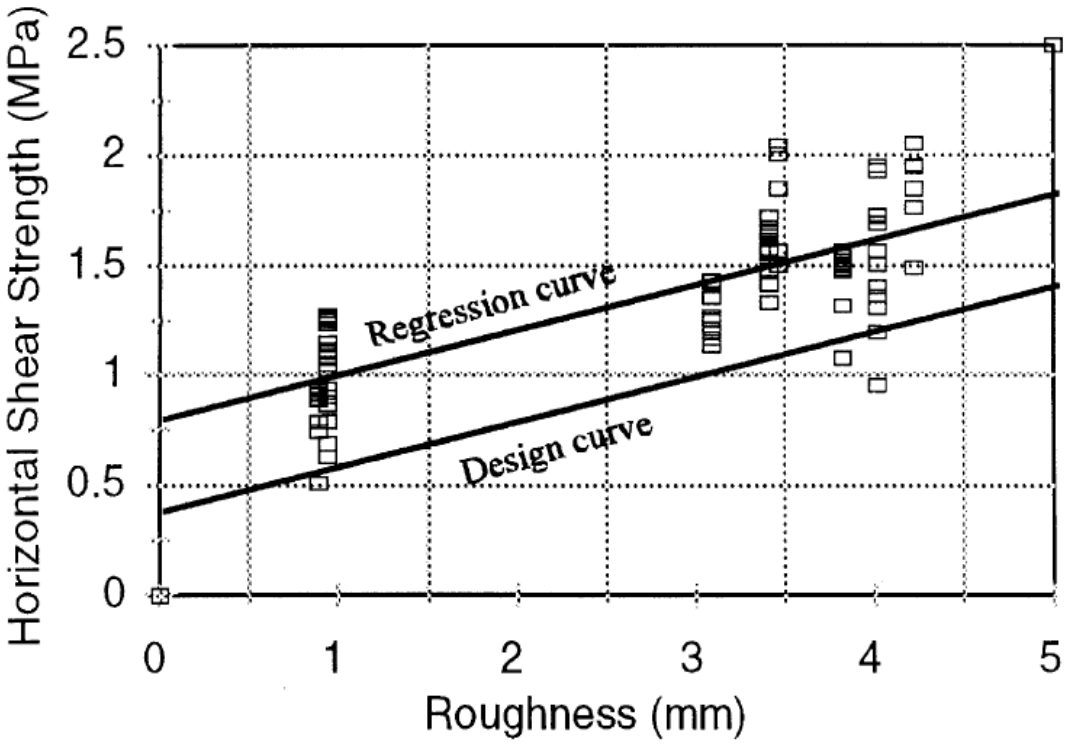


Figure 5: Horizontal Shear Strength for Rough Interface by (Mitchell, 2002)

They introduced four equations to evaluate the design values for the horizontal shear strength; two of them relate the shear strength to the roughness and two to calculate the shear strength using the concrete compressive strength as shown in Table 2.

Table 2: Design Equations (Mitchell, 2002)

| | Horizontal shear for the regression curve | Horizontal shear At 95% one side confidence interval. |
|---|---|---|
| Horizontal shear based on concrete strength | $0.0286f_{cu} + 0.5701$ | $(0.0286f_{cu} - 0.0544)/\text{ɛ}_m$ |
| Horizontal shear based on roughness | $0.2090R_z + 0.7719$ | $(0.2090R_z + 0.3762)/\text{ɛ}_m$ |

Where $\gamma_m$ is a material or safety factor applied as recommended in BS 8110 and other similar standards. A material factor of 1.4 is used for shear. $R_z$ is the surface roughness in mm. Upon close inspection of the roughness equation $V_h = 0.2090R_z + 0.7719$, for every millimeter change in roughness, the shear capacity changes by $0.2\ MPa$. The change in shear capacity is significant. The roughness of a brushed or raked surface can vary significantly according to the amount of pressure applied on the brush and rake. In a few of the specimens tested, the surface was brushed but the roughness did not exceed 1 mm. It was also reported that the concrete compressive strength doesn't have big influence on the horizontal shear strength, and also reported by (Patnaik, 2001). The concrete strength of composite concrete beams with a smooth interface does not affect the horizontal shear strength of such beams. The effective depth to tie spacing ratio $(d/s)$ of composite beams also does not have any effect on the horizontal shear strength of such beams.

2.2.2 The Shear Strength in Horizontal Smooth Interface for Composite Concrete Beams.

The first nonlinear design expression was $(v_u = 33.5\sqrt{\rho f_y}$ proposed by (Birkeland H. W., 1968) and cited by (Patnaik, 2001). In previous studies by (Hanson, 1960) and (Mattock, 1974) a push-off test results for 18 specimens were reported for bonded and unbounded beams with a smooth interface while the failure in horizontal shear is considered at a slip = 0.005" or 1.3 mm that 18 beams were reported in addition to another 24 beams by Patnaik, 2001 presenting a wide range of variables such as concrete strength, effective depth, area of ties crossing the interface, and horizontal area resisting the shear. Table 3 summarizes the values of the variables taken in consideration,

a shear strength expression was introduces by (Patnaik, 2001) evaluating the horizontal shear to be calculated as $v_n = 0.5\rho_{vf}\sqrt{f'_c E_c} \leq \rho_{vf} f_{yf}$

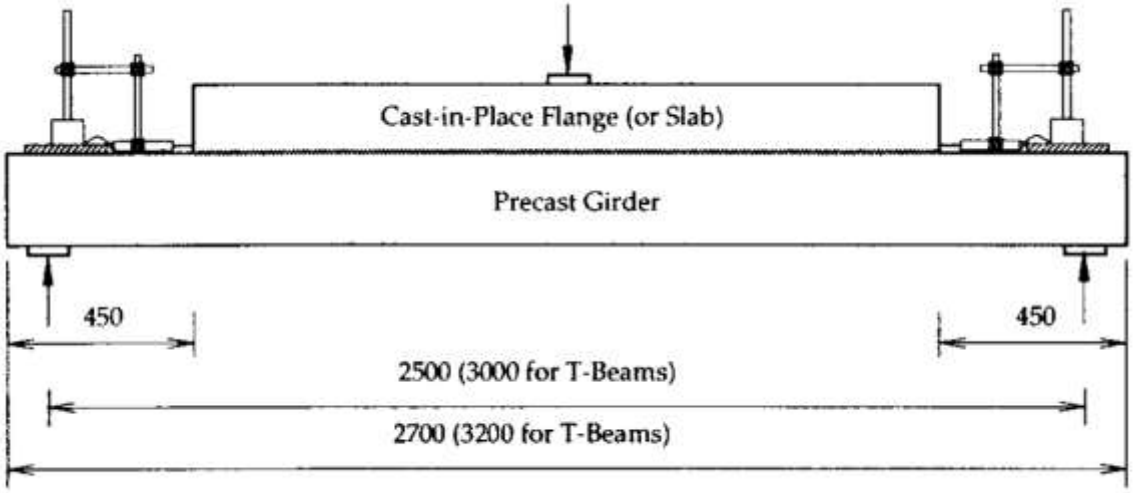


Typical Beam Elevation

Figure 6 : Test Specimen **(Patnaik, 2001)**

Table 3: Details of 24 Test Beams for a Smooth Interface (Patnaik, 2001)

TABLE 2. Details of Test Beams of Present Study

| Beam number (1) | Interface width $b_v$ (mm) (2) | Area of long. steel $A_s$ (mm²) (3) | Effective depth $d$ (mm) (4) | Concrete Strength (MPa) | | Ties Crossing Interface | | | | Clamping stress $P_{cr}$ (MPa) (11) |
|---|---|---|---|---|---|---|---|---|---|---|
| | | | | Web (5) | Flange (6) | Area (mm²) (7) | Spacing (mm) (8) | $f_{yt}$ (MPa) (9) | $f_{at}$ (MPa) (10) | |
| SR1.1 | 250 | 2,410 | 309 | 25.5 | 19.8 | 60 | 450 | 558 | 604 | 0.30 |
| SR1.2 | 250 | 2,410 | 309 | 25.5 | 19.8 | 60 | 450 | 558 | 604 | 0.30 |
| SR2.1 | 100 | 2,410 | 309 | 23.5 | 27.8 | 60 | 450 | 520 | NA | 0.75 |
| SR2.2 | 100 | 2,410 | 309 | 23.5 | 27.8 | 60 | 450 | 520 | NA | 0.75 |
| SR3.1 | 100 | 2,410 | 309 | 17.0 | 22.5 | 25 | 300 | 704 | 748 | 0.59 |
| SR3.2 | 100 | 2,410 | 309 | 17.0 | 22.5 | 25 | 300 | 704 | 748 | 0.59 |
| SR4.1 | 100 | 400 | 317 | 35.7 | 34.8 | 31 | 450 | 641 | 686 | 0.44 |
| SR4.2 | 100 | 400 | 317 | 26.7 | 31.0 | 31 | 450 | 641 | 686 | 0.44 |
| SR4.3 | 100 | 400 | 317 | 35.7 | 34.8 | 31 | 250 | 641 | 686 | 0.79 |
| SR4.4 | 100 | 400 | 317 | 26.7 | 31.0 | 31 | 250 | 641 | 686 | 0.79 |
| SR4.5 | 100 | 510 | 317 | 35.7 | 34.8 | 62 | 350 | 641 | 686 | 1.14 |
| SR4.6 | 100 | 510 | 317 | 26.7 | 31.0 | 62 | 350 | 641 | 686 | 1.14 |
| SR5.1 | 100 | 510 | 317 | 35.7 | 34.8 | 62 | 250 | 641 | 686 | 1.59 |
| SR5.2 | 100 | 510 | 317 | 26.7 | 31.0 | 62 | 350 | 641 | 686 | 1.59 |
| SR5.3 | 100 | 600 | 317 | 35.7 | 34.8 | 62 | 200 | 641 | 686 | 1.99 |
| SR5.4 | 100 | 600 | 317 | 26.7 | 31.0 | 62 | 200 | 641 | 686 | 1.99 |
| SR5.5 | 100 | 1,010 | 314 | 35.7 | 34.8 | 62 | 150 | 641 | 686 | 2.65 |
| SR5.6 | 100 | 1,010 | 314 | 26.7 | 31.0 | 62 | 150 | 641 | 686 | 2.65 |
| ST1.1 | 150 | 1,800 | 289 | 36.4 | 34.4 | 157 | 200 | 340 | 447 | 1.78 |
| ST1.2 | 150 | 1,800 | 289 | 35.9 | 32.4 | 157 | 200 | 340 | 447 | 1.78 |
| ST2.1 | 150 | 3,200 | 277 | 38.0 | 33.9 | 157 | 150 | 340 | 447 | 2.37 |
| ST2.2 | 150 | 3,200 | 277 | 35.1 | 31.6 | 157 | 150 | 340 | 447 | 2.37 |
| ST3.1 | 150 | 3,200 | 277 | 33.9 | 26.9 | 157 | 100 | 340 | 447 | 3.56 |
| ST3.2 | 150 | 3,200 | 277 | 34.2 | 30.3 | 157 | 100 | 340 | 447 | 3.56 |

Table 4: Previous Test Results for 18 Beams for a Smooth Interface

**TABLE 1. Details of Test Beams of Previous Studies**

| Source (1) | Beam number (2) | Interface width $b_v$ (mm) (3) | Effective depth $d$ (mm) (4) | Concrete Strength (MPa) | | Ties Crossing Interface | | | Clamping stress $\rho_{vf} f_{yf}$ (MPa) (10) | Horizontal shear strength (MPa) (11) |
|---|---|---|---|---|---|---|---|---|---|---|
| | | | | Web (5) | Flange (6) | Area ($mm^2$) (7) | Spacing (mm) (8) | $f_{yf}$ (MPa) (9) | | |
| "Composite" (1976) | S-7-S | 610 | 179 | 48.7 | 37.9 | — | — | — | 0 | 2.96 |
| | S-8-S | 610 | 179 | 48.7 | 28.0 | — | — | — | 0 | 2.74 |
| Nossier and Murtha (1971) | S0.0 | 38 | 152 | 30.1 | 25.7 | — | — | — | 0 | 3.23 |
| | S0.3 | 38 | 152 | 35.0 | 24.7 | 11.3 | 98 | 170 | 0.51 | 3.16 |
| | S0.7 | 38 | 152 | 34.1 | 29.7 | 11.3 | 41.3 | 170 | 1.22 | 4.09 |
| Bryson and Carpenter (1970) | SG-2 | 76 | 373 | 33.1 | 16.5 | — | — | — | 0 | 2.18 |
| Saemann and Washa (1964) | 4A | 89 | 356 | 19.4 | 18.8 | 127 | 127 | 294 | 3.30 | 3.99 |
| | 12A | 89 | 356 | 21.2 | 19.2 | 127 | 127 | 294 | 3.30 | 3.84 |
| | 7C | 89 | 356 | 23.0 | 19.4 | 127 | 508 | 294 | 0.83 | 2.87 |
| | 3D | 89 | 356 | 25.7 | 24.8 | 71 | 508 | 370 | 0.58 | 2.74 |
| | 1A | 89 | 356 | 19.7 | 18.7 | 127 | 127 | 294 | 3.30 | 5.75 |
| | 4C | 89 | 356 | 21.9 | 22.9 | 127 | 254 | 294 | 1.65 | 4.64 |
| | 9C | 89 | 356 | 21.3 | 21.9 | 127 | 508 | 294 | 0.83 | 3.69 |
| | 7D | 89 | 356 | 26.2 | 25.9 | 71 | 508 | 370 | 0.58 | 3.98 |
| Grossfield and Birnstiel (1962) | Beam 1 | 64 | 308 | 30.3 | 30.3 | 71 | 127 | 345 | 3.04 | 3.93 |
| Hanson (1960a,b) | BS-I | 203 | 508 | 32.3 | 20.7 | 142 | 152 | 340 | 1.56 | 3.39 |
| | BS-II | 203 | 508 | 33.2 | 24.3 | 142 | 406 | 368 | 0.63 | 3.21 |
| Revesz (1953) | J | 76 | 179 | 46.0 | 21.8 | — | — | — | 0 | 0.84 |

Comparing the strength provided by ACI 318-99, Canadian code, PCI expression, Test results and the newly proposed expression it was found that the ACI and Canadian codes underestimate the strength of the interface while the PCI expression under estimate the sections with high clamping stresses and not accurate for low clamping stresses (Figure 7).

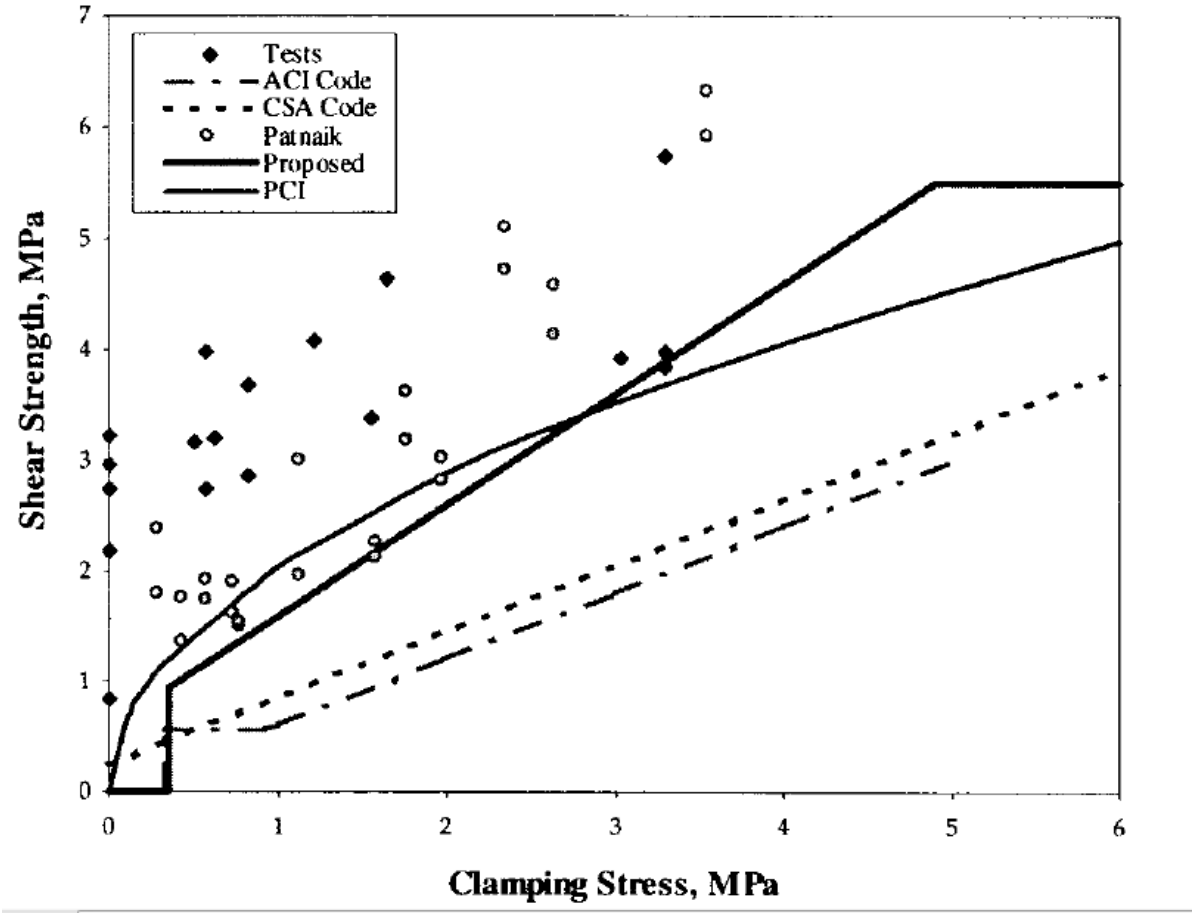


Figure 7 : Comparison between Different Design Expressions for Smooth Interface (Patnaik, 2001)

2.2.3 The use of keys for horizontal shear

The use of shear key and different shear key design have a significant influence on the shear strength, in a research study by (Arafjo & E1 Debs, 2005) considering the cast in-situ concrete is one of the simplest and cost effective ways to connect two concrete elements, the connections proposed by these authors in that research are shown in Figure 8: Shear connections and Figure 9.

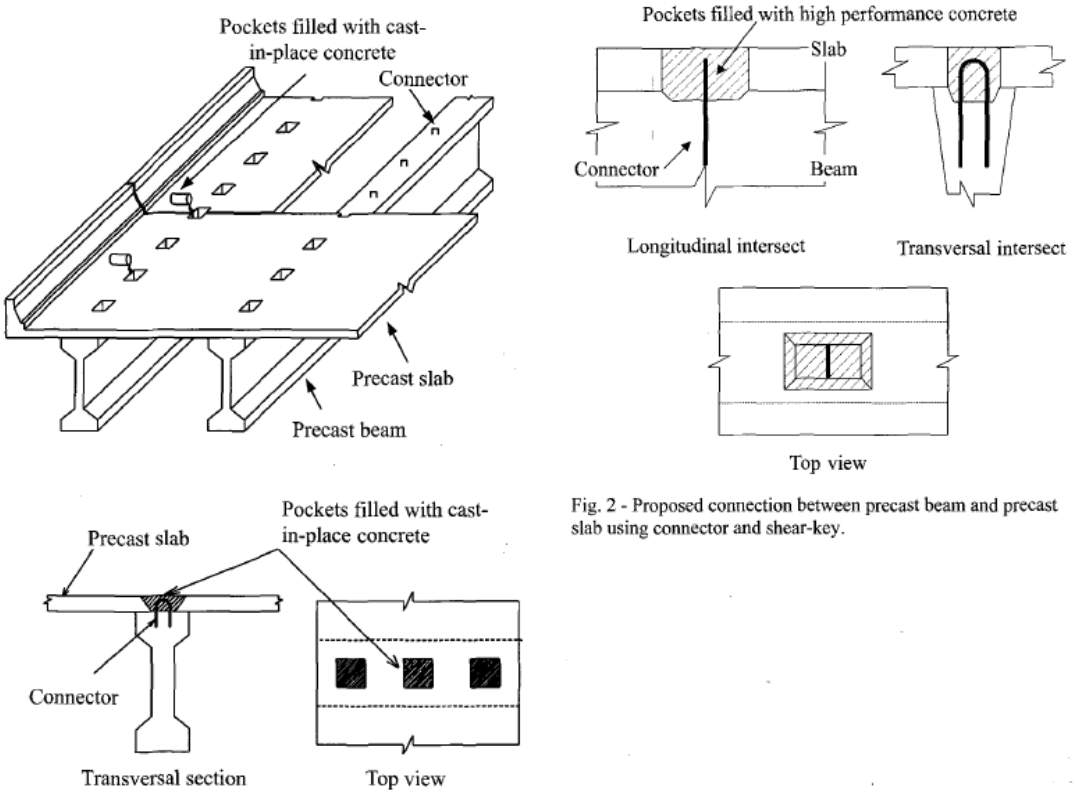


Fig. 2 - Proposed connection between precast beam and precast slab using connector and shear-key.

Figure 8: Shear connections (Arafjo & E1 Debs, 2005)

They concluded that a 35% increase in the connection strength can be achieved by increasing the compressive strength of the pocket filling concrete, and further increase in the connection strength can be obtained by increasing the pocket diameter, the application of fiber to the filling concrete increased the connection strength by 62%. They proposed two expressions to evaluate the strength of the precast slabs and beams made composite by this type of connection.

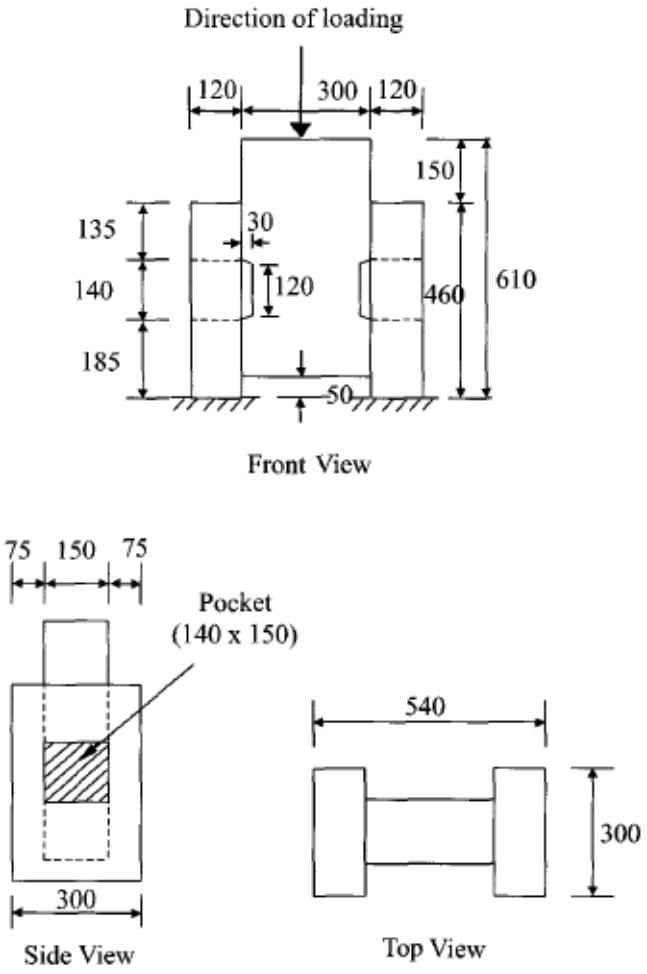


Figure 9: Push-out test (Arafjo & E1 Debs, 2005)

Empirical expression to evaluate the connection strength with shear-key and fibers.

$$\tau_u = 1.238\sqrt{f_{cm}} + 1.791\sigma_n \le 2.6\sqrt{f_{cm}},$$
$$\text{if } 0.75\% \le V_f \le 1.50\% \quad (R = 0.92)$$

$$\tau_u = 1.730 f_{cm}^{0.708} \left(\rho\sqrt{f_y}\right)^{0.415} \le 2.6\sqrt{f_{cm}},$$
$$\text{if } 0.75\% \le V_f \le 1.50\% \quad (R = 0.95)$$

Empirical expression to evaluate the connection strength with shear-key and without fibers.

$$\tau_u = 1.270\sqrt{f_{cm}} + 0.798\rho f_y \le 1.8\sqrt{f_{cm}} \quad \text{(MPa)}$$
$$\text{if } V_f = 0\% \ (R = 0.93)$$

## 2.3 The Study of the Ultimate Shear Strength for Vertical shear

This section deals with the discussion of ultimate shear strength of vertical shear.

### 2.3.1 Shear Capacity of Monolithic Concrete vs. the Concrete Placed Against Hardened Concrete, the Cracked Concrete (Aziz, 2010).

In an experimental study by Aziz (2010), 14 Specimens were tested to compare the shear capacity of concrete surface considering seven specimen configurations.

1- Reinforced monolithic concrete

2- Plain concrete with smooth interface

3- Smooth interface with reinforcement across the shear resisting plane

4- Plain concrete with rough interface

5- Rough interface with reinforcement across shear plane

6- Plain concrete with shear key

7- Reinforced shear key across the shear interface.

Figure 10 and 11 show the specimens and the different cases used in the study by Aziz (2010).

| Specimens Designation | No. of Specimens | Shape |
|---|---|---|
| Control specimen, no joints, with 3-Ø10 shear reinforcement | 2 | 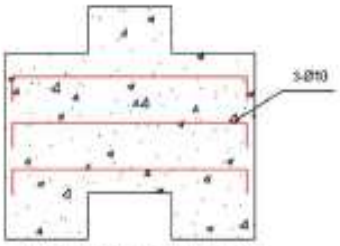 Reinforced Concrete Specimen |
| Smooth surfaces, no shear reinforcement | 2 | 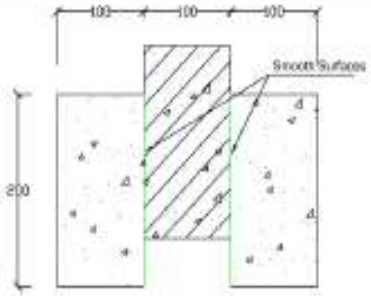 Specimen with Smooth Surfaces |
| Intentionally roughened surfaces to 6mm amplitude, no shear reinforcement | 2 | 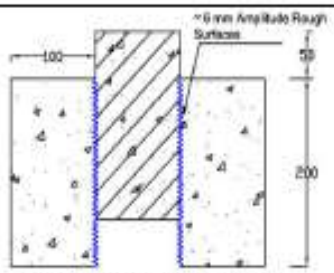 Reinforced Specimen with Rough Surfaces |
| Shear key specimens with smooth surfaces, | 2 | 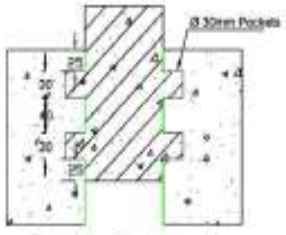 Shear Key Specimen with Smooth Surfaces |

Figure 10: Sampling Details (Aziz, 2010) - (A)

| Specimens Designation | No. of Specimens | Shape |
|---|---|---|
| Shear key specimens with intentionally roughened surfaces to 6mm amplitude | 2 | 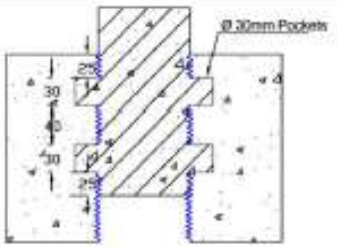 Shear Key Specimen with Rough Surfaces |
| Smooth surfaces with shear reinforcement | 2 | 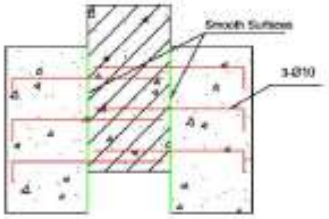 Reinforced Specimen with Smooth Surfaces |
| Intentionally roughened surfaces to 6mm amplitude, with shear reinforcement | 2 | 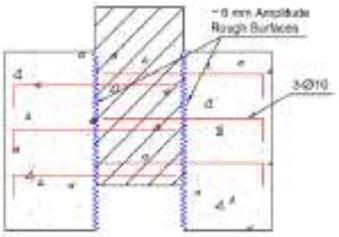 Specimen with Rough Surfaces |

Figure 11 : Sampling Details (Aziz, 2010) - (B)

All the reinforced specimens contain 3 # 3 reinforcing bars (10 mm diameter).

The test results reproduced from the original publication are tabulated in Table 5. The results indicate that there is a large variation of shear strengths for different types of specimens.

Table 5: Interface Shear Transfer Capacity (Aziz, 2010)

| Specimen Designation | $V_n$ (kN) | $V_n$ (kN) Average | $V_{capacity} / V_{control}$ |
|---|---|---|---|
| Unreinforced 1 (control) | 290 | 225 | control |
| Unreinforced 2 (control) | 160 | | |
| Smooth 1 | 40 | 20 | 0.085 |
| Smooth 2 | 0 | | |
| Rough 1 | 85 | 101 | 0.43 |
| Rough 2 | 117 | | |
| Shear key Smooth 1 | 110 | 123 | 0.52 |
| Shear key Smooth 2 | 136 | | |
| Shear key Rough 1 | 114 | 129 | 0.55 |
| Shear key Rough 2 | 144 | | |
| Rein. 1 (control) | 464 | 404 | control |
| Rein. 2 (control) | 344 | | |
| Smooth Rein. 1 | 72 | 82 | 0.20 |
| Smooth Rein. 2 | 92 | | |
| Rough Rein. 1 | 142 | 145 | 0.36 |
| Rough Rein. 2 | 148 | | |

The maximum shear strength can be obtained by the control specimen which is made from monolithic reinforced concrete. The roughness, reinforcement, and shear key contribute to the development of strength contribution for smooth unreinforced specimens. The interface roughness provides frictional resistance that leads to an increase in the shear capacity. Shear keys will provide bearing compressive stresses to the external concrete blocks and add to shear transfer strength at the interface. The steel reinforcement crossing resists large amount of interface shear depending on its area and the yield stress.

2.3.2 Shear Strength for Vertical Shear Interface.

The ‘‘shear-friction theory’’ was first presented in 1966 and was adopted in all design codes for reinforced concrete structures to predict the shear strength of different types of concrete-to-concrete interface such as:

(a) The interface between a precast element and a cast-in-place units

(b) The interface between two parts of an element cast at different times

(c) The interface between an element and a support

(d) The interface between an existing element and a repairing/strengthening layer

(e) The interface between two parts of an element generated by a crack.

Two different situations can be considered:

a) interface shear strength without loss of adhesion.

b) Interface shear strength with relative slip between both concrete parts. Where the ‘‘shear-friction theory’’ can be applied, where the interfacial behavior is assumed to be controlled by cohesion (sometime called aggregate interlock), friction and dowel action. All design expressions have been calibrated from experimental results, mostly using push-off test specimens (Pedro & Eduardo, 2012).

The development of ultimate shear strength expressions on test results and empirical equations. In a study by Gaston and Kriz (1964) design expressions to estimate the ultimate longitudinal shear stress in scarf joints of precast concrete were suggested. This expression accounts only for the normal force without reinforcement or frictional contribution for a smooth interface expression and was as follows:

$$Vu = 43 + 0.78\,бn\ (psi)$$

Another expression for smooth bonded interfaces the design expression was suggested as follows:

$$Vu = 110 + 0.7\,б n \text{ (psi)}$$

Where Vu is the ultimate longitudinal shear stress at the interface and $б n$ is the normal stress at the interface.

2.3.2.1 Equations by (Anderson, 1960)

Anderson was one of the first to propose a design expression to predict the longitudinal shear strength of concrete interfaces. The proposed expressions are as follows:

$$v_u = 640 + 33180 * \rho \text{ For } (f'_c < 3000) \text{ psi}$$

$$v_u = 800 + 40000 * \rho \text{ For } (f'_c > 3000) \text{ psi}$$

2.3.2.2 Equations by (Mattock & Kaar, 1961)

These authors proposed a design expression based on the shear span/effective depth ratio to determine the ultimate longitudinal shear stress at the interface of composite reinforced concrete beams. The proposed expression is as follows:

$$V_u = \frac{2700}{\frac{x}{d}+5} + 17500\rho\ psi$$

2.3.2.3 Equation by (Saemann & Washa, 1964)

The surface condition was not considered in the proposed expression because the authors concluded that its contribution to the shear strength is variable and decreases with the increase of the shear reinforcement ratio.

$$V_u = \frac{2700}{x+5} + 30{,}000\rho\frac{33-X}{X^2+6X+5} \text{ (psi)}$$

2.3.2.4 Equations by (Gaston & Kriz, 1964)

The authors suggested the following design expressions to estimate the ultimate longitudinal shear stress in scarf joints of precast concrete. For smooth un-bonded interfaces the design

$$V_u = 43 + 0.78\,бn$$

Smooth bonded interfaces the design expression is as follows:

$$V_u = 110 + 0.70\,бn$$

2.3.2.5 Equations by (Birkeland & Birkeland, 1966)

They were the first to propose a linear expression to evaluate the ultimate longitudinal shear stress of concrete interfaces. The proposed expression is as follows:

$$V_u = \rho f_y \tan\emptyset = \rho f_y \mu$$

Where $V_u$ is the ultimate longitudinal shear stress at the interface; $\rho$ is the reinforcement ratio; $fy$ is the yield strength of the reinforcement; and Ø is the internal friction angle. The tangent of the internal friction angle is also designated as coefficient of friction "$\mu$", and the term $\rho f_y$ is the clamping stresses. This expression was proposed for smooth concrete surfaces, and intentionally roughened concrete surfaces. The coefficient of friction was empirically determined, varying with the surface preparation, and it was defined for several situations.

Table 6 : Surface Condition and Friction Coefficient.

| Surface condition | Ø | μ |
|---|---|---|
| Monolithic concrete | 59.5 | 1.7 |
| Intentionally roughened construction joints | 54.5 | 1.4 |
| For ordinary construction joints and for concrete to steel interfaces | 38.7 to 45 | 0.8 to 1.0 |

2.3.2.6 Modified Equation by (Mattock A. H., 1974)

Presented a modified expression calibrated with average values from experimental results, given by:

$$V_u = 400 + 0.8\ (\rho fy\ + б n)\ \text{(psi)}$$

2.3.2.7 Equation by (Hermansen & Cowan, 1974)

$$V_u = 580 + 0.8\rho fy \quad \text{(psi)}$$

2.3.2.8 (Mattock A. H., 2001)

Four expressions were introduced to evaluate the ultimate shear strength accounting for the surface roughness, steel area, concrete area, and weight of concrete. The following charts show the design expressions with the proposed limits for different conditions.

Table 7: Mattock Design Expression (A)

| | | Condition If | | | Vu = |
|---|---|---|---|---|---|
| 1 | Intentionally roughened conc. Placed against hardened conc. | $б_n \geq K_1/1.45$ | or | $V_n \geq 1.55 * K1$ | $K_1 + 0.8\ (\rho f_y + б_n)$ |
| | | $б_n < K_1/1.45$ | or | $V_n < 1.55 * K1$ | $2.25\ (\rho f_y + б_n\ )$ |

Limited to $K_2\ f'_c$ or $K_3$

Table 8: K Factors

| | Normal weight monolithic conc. | Intentionally roughened conc. placed against hardened conc. | Sand light weight | All light weight concrete |
|---|---|---|---|---|
| K1 | $0.1f_c$ or 800 psi | 400 psi | 250 | 200 psi |
| K2 | 0.3 | 0.3 | 0.2 | 0.2 |
| K3 | 2400 psi | 2400 psi | 1200 psi | 1200 psi |

Table 9: Revised Mattock Design Expressions (B)

| | | | |
|---|---|---|---|
| 2 | For conc. Placed against hardened conc. not intentionally roughened surface | $V_u = 0.6\lambda\rho f_y$ | $0.2f_c'$Or 800 psi |
| 3 | For concrete anchored to clean, unpainted, as-rolled steel by headed studs or by reinforcing bars | $V_u = 0.7\lambda\rho f_y$ | |

Table 10: λ Factor

| | Normal weight concrete | Sand light weight | All light weight concrete |
|---|---|---|---|
| λ | 1 | 0.85 | 0.75 |

2.3.3 Shear transfer across a crack in reinforced high strength concrete.

The modulus of elasticity, ductility, stiffness, and behavior of concrete depend on the concrete compressive strength. The design expressions introduced by many researchers in earlier studies limit the use of those expressions to a certain percent values of the concrete compressive strength in the range of normal strength concrete for their expressions to be applicable. In a study by (Mansur, Vinayagam, & Tan, 2008), the authors investigated many of the available expressions for high strength concrete for the shear transfer strength of a concrete interface, both analytically and experimentally. A comparison was made between several design expressions, including the ones proposed in the ACI 318-05 and PCI Design Handbook (1992) and those suggested by Mattock and his co-workers, Walraven et al., Mau and Hsu, Lin and Chen, and Loov and Patnaik (1994). It was concluded that the design expressions proposed by Walraven et al. and by Mau and Hsu give unsafe predictions of the interface shear strength. Moreover, the design expression proposed by (Loov & Patnaik, 1994), similar to the one proposed by

Mau and Hsu, although with different values for the coefficients, presented similar and unconservative predictions.

A single curve formulation was proposed by (Mansur, Vinayagam, & Tan, 2008) based on the design expression by Mau and Hsu and calibrated with a set of 154 test results. The compressive strength of the concrete adopted in the experimental study was between 18 $MPa$ (2,611 $psi$) and 100 $MPa$ (14,504 $psi$), while the normalized clamping forces ($\rho f_y/f_c$) were between 0.02 and 0.39. The proposed expression is given by:

$$V_u/f_c = 0.566\sqrt{\rho f_y/f_c} \leq 0.3$$

Where $V_u$ is the ultimate longitudinal shear stress at the interface; fc is the concrete compressive strength; ρ is the reinforcement ratio; and $f_y$ is the yield strength of the reinforcement. The yield strength of the reinforcement bars crossing the interface was $of$ 300 $MPa$ (43.5 $ksi$) and 530 $MPa$ (76.9 $ksi$). Comparing the proposed expression with the experimental data, and they concluded that their equation could be unsafe for low values of the normalized clamping forces. Therefore, a tri-linear formulation was proposed

Table 11:Proposed horizontal shear expressions by (Mansur, Vinayagam, & Tan, 2008)

| Clamping force( CF) | $0.075 > CF$ | $0.075 < CF < 0.270$ | $CF > 0.270$ |
|---|---|---|---|
| $V_u/fc_u =$ | $2.5\ \rho f_y/f_c$ | $\frac{3.80}{f_c^{0.385}} + 0.55\ \rho f_y/f_c$ | 0.3 |

## 2.4 Summary

In this chapter, a summary of some of the common design equations for the shear transfer strength of a concrete interface suggested by several researchers in the past studies is outlined. A distinction between horizontal shear in composite concrete beams and interface shear transfer strength needs to be made in applying these design equations.

# CHAPTER III

# METHODOLOGY

This chapter explains how the experimental plan was developed to address the research objectives. The following methodology was adopted to address the objectives of this study. The test plan includes the development of suitable details for the test specimens, specimen preparation, test set-up and the related shear tests.

## 3.1 Study Parameters

The parameters considered for study are discussed below.

### 3.1.1 Reinforcement and Concrete

Three sets of specimens were made for comparisons between smooth and rough concrete interfaces, different reinforcement ratios, and different reinforcement distribution on the joint. A smooth interface was obtained by casting concrete against ply-wood, and a rough interface was obtained as an as-cast surface without smoothing or intentionally roughening the interface.

The three sets of 12 specimens each were made in this test program. The reinforcement crossing the interface and specimen geometry were symmetric. Each test specimen comprised three concrete units resulting in two shear planes. The first of the three sets of

tests represents a smooth interface with two specimens (S12, S14) reinforced with two and four #3 bars crossing each shear plane. In the designation of the test specimens, the first number stands for the set number (1, 2, or 3) and the second number stands for the number of reinforcing bars crossing each shear plane, the second set comprised five specimens with rough concrete surface reinforced using # 3 rebar , the number of bars crossing each interface varied from two through six bars in each plane (S22, S23, S24, S25, and S26), and the third set comprised five specimens with rough interface reinforced using # 3 bars, The number of bars crossing each interface varied from two through six bars with larger shear area and different reinforcement ratios $\rho = As/Ac$ Where $A_s$ is the area of steel crossing the interface, $A_c$ is the area of concrete interface. Set # 2 and # 3 had equal number of bars crossing the interface with different rebar distribution. The concrete and rebar areas for all the specimens are given in Table 12: Study Parameters2 accounting for the two the shear interfaces in each test specimen.

Table 12: Study Parameters

| Set No. | Specimen Name | No. of #3 bars | Concrete Surface | Area of Concrete surface | As ($in^2$) | $\rho = A_s/A_c$ |
|---|---|---|---|---|---|---|
| 1 | S12 | 2 | smooth | 116 | 0.44 | 0.0038 |
| | S14 | 4 | | 116 | 0.88 | 0.0076 |
| 2 | S22 | 2 | Rough | 90 | 0.44 | 0.0049 |
| | S23 | 3 | | 90 | 0.66 | 0.0073 |
| | S24 | 4 | | 90 | 0.88 | 0.0098 |
| | S25 | 5 | | 90 | 1.1 | 0.0122 |
| | S26 | 6 | | 90 | 1.32 | 0.0147 |
| 3 | S32 | 2 | Rough | 150 | 0.44 | 0.0029 |
| | S33 | 3 | | 150 | 0.66 | 0.0044 |
| | S34 | 4 | | 150 | 0.88 | 0.0059 |
| | S35 | 5 | | 150 | 1.1 | 0.0073 |
| | S36 | 6 | | 150 | 1.32 | 0.0088 |

3.1.2 Development Length for Rebar

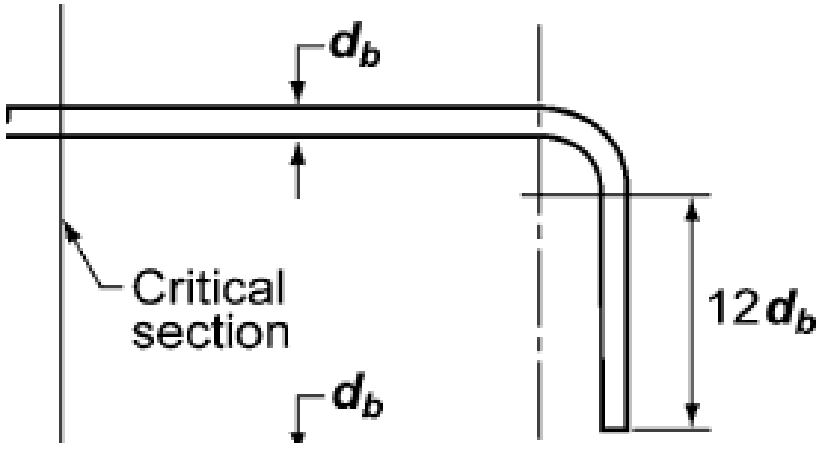


Figure 12 : Development Length (ACI, 2011)

According to ACI 318-11 (Section R12.5), the development length of the hook for the bars in tension should be $12d$. If #3 bars with diameter of 0.375" are used, $12d = 12 \text{ x } 0.375 = 4.5$"

Five inches are used as development length for the rebar in the Specimens.

### 3.1.3 Mix Design

The concrete mix design used for the 3 sets of specimens is given in Table 13.

Table 13: Mix Design.

| | | | |
|---|---|---|---|
| 1 | Cement content | 675 | $lb/yd^3$ |
| 2 | Water at (W/C = 0.5) | 338 | $lb/yd^3$ |
| 3 | Coarse aggregate # 8 | 1424 | $lb/yd^3$ |
| 4 | Coarse aggregate # 3/8 | 427 | $lb/yd^3$ |
| 5 | Fine Aggregate River sand | 997 | $lb/yd^3$ |

### 3.1.4 Compressive Strength

The concrete was mixed in room temperature of about 70° F in a laboratory scale concrete mixer. The test specimens were made in plywood molds and place in the curing room after 24 hours of setting for moist curing. Compressive strength tests on standard cylinders were conducted to determine the compressive strength of the concrete on the day of the testing. The compressive strength for the weakest block in each Specimen at the time of testing was determined based on the average of 3 cylinder tests and reported in Table 14: Compressive Strength.

Table 14: Compressive Strength

| # | Specimen | Compressive strength, psi | # | Specimen | Compressive strength, psi |
|---|---|---|---|---|---|
| 1 | S12 | 6158 | 7 | S26 | 6690 |
| 2 | S14 | 6158 | 8 | S32 | 6158 |
| 3 | S22 | 6023 | 9 | S33 | 6158 |
| 4 | S23 | 6625 | 10 | S34 | 6158 |
| 5 | S24 | 6155 | 11 | S35 | 6158 |
| 6 | S25 | 6625 | 12 | S36 | 6158 |

3.1.5 Rebar Arrangement

According to the study by (Aziz, 2010), the non-reinforced smooth concrete interface can resist 0 to 7% of the shear strength of monolithic concrete and up to 30 or 40% of the shear strength with a rough interface. It is well known that reinforced joints can develop larger shear strength than those without any interface reinforcement. Therefore, in this research project, the following three factors were studied:

Figure 13: Test Specimen's reinforcement

a) Reinforcement area $As$

b) Area of concrete interface $Ac$

c) Arrangement of the reinforcement in the section

Different values of the ratio $\rho = As/Ac$ were used to account for the first two factors. Specimens S23 and S35 have the same steel ratio ρ value of 0.0073. However, the number of rebar and the concrete surface area are not the same for the two specimens. Specimens S25 and S35 had the same rebar area in the joint with different arrangement to study the effect of different rebar distribution.

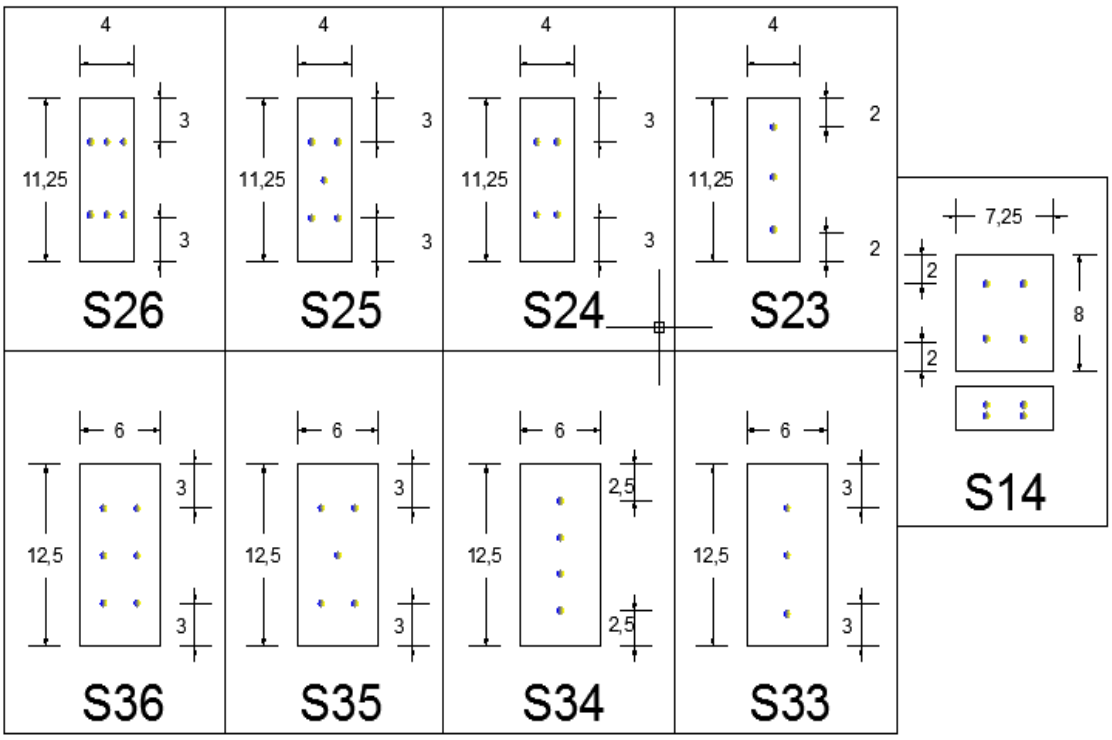


Figure 14: Test Specimens Interface Details

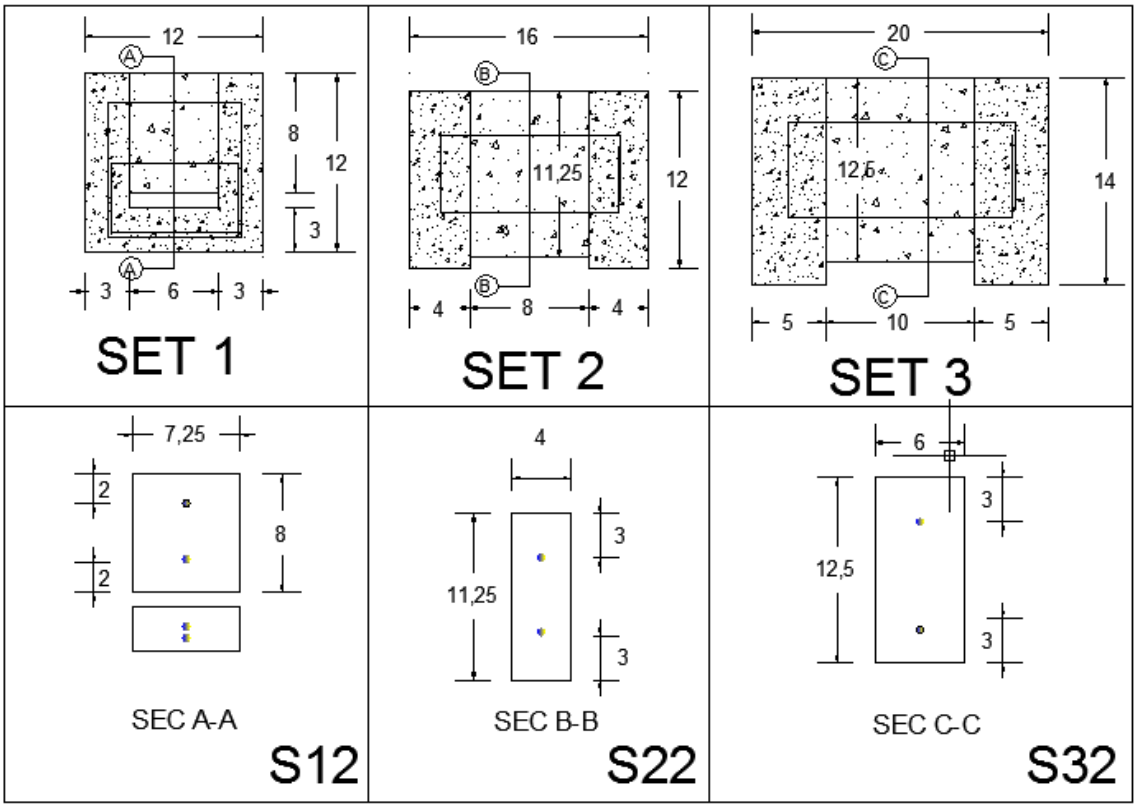


Figure 15: Test Specimen Details (continued)

3.2 Preparation of Specimens.

For the first set; concrete units were cast 6 days apart where the first part U-shaped units with the rebar were cast first on smooth plywood surface, and subsequently the second (or the middle) unit was cast.

The second and the third set were casted 2 days apart without smoothening for a natural vibrated rough surface that gives full amplitude of ¼ in or more was obtained to match the normal construction practice as shown in Figure 16 : Rough Interface in the Current Test.

Figure 16 : Rough Interface in the Current Tests

The horizontal bars at the corners were provided to prevent the pull out of the reinforcement from the concrete and to improve the stress distribution in the concrete that can be expected in real structures. This detailing is assumed to provide adequate

confinement for the steel in the concrete section and adequate development length for the reinforcing bars one either side of the interface. Each specimen consists of three concrete units with a suitable rough or smooth concrete interface and a recess under in the middle block (reduced height) to allow for slip during the shear tests.

## 3.3 Shear Test Setup and Procedure

The testing machine used for the test is a hydraulic machine with a capacity of 300 kips, while the maximum applied load to the specimens was less than 130 kips. Loading was continued beyond the initial slip and subsequent failure to capture the final failure mode and the deformation of the reinforcement. A loading rate of 70 lb/sec was applied to the specimens to demonstrate static load.


Figure 17: Test setup

Each test lasted 20 to 30 minutes to reach the maximum load depending on the amount of load needed to fail a particular specimen. Dial gages were fixed at the top of the moving (left and right) concrete units to measure the relative slip of the middle block and the corresponding applied load at 1,000 lb load intervals initially and at every 500 lb interval closer to the failure. Load-slip relationship was developed by calculating average slip from the two gages (one at each interface). The test set-up is shown in Figure 17: Test setup.

Each specimen of the second and third sets had 3 different casting dates and different compressive strength. As per ACI 318-11, the least strength should be the governing strength used in the design equations. Compression tests were performed on three 4" x 8" standard cylinders to determine the average strength of the concrete for each batch.

# CHAPTER IV

# RESULTS AND DISCUSSION

## 4.1 Test Results.

The steel ratio in the test specimens varies from 0.3% to 1.2%. The test results show that the interface shear strength can be increased by increasing the reinforcement ratio ρ with significantly lower relative slip at the interface.

Table 15: Shear Test Results

| SN. | Specimen no. | # of bars | Max load (lb) | Shear strength (psi) | Slip (in) | concrete Sec. | Shear Area ($in^2$) | ρ = As/Ac | As |
|---|---|---|---|---|---|---|---|---|---|
| 1 | S12 | 2 | 28944 | 249.52 | 0.257 | 3*7.25= 21.75 | 116 | 0.003793 | 0.44 |
| 2 | S14 | 4 | 38105 | 328.49 | 0.01925 | | 116 | 0.007586 | 0.88 |
| 3 | S22 | 2 | 33227 | 369.19 | 0.038 | 4*4=16 $in^2$ | 90 | 0.004889 | 0.44 |
| 4 | S23 | 3 | 55171 | 613.01 | 0.04275 | | 90 | 0.007333 | 0.66 |
| 5 | S24 | 4 | 62945 | 699.39 | 0.041 | | 90 | 0.009778 | 0.88 |
| 6 | S25 | 5 | 80799 | 897.77 | 0.041 | | 90 | 0.012222 | 1.10 |
| 7 | S26 | 6 | 71000 | 788.89 | 0.05725 | | 90 | 0.014667 | 1.32 |
| 8 | S32 | 2 | 47314 | 315.43 | 0.06375 | 5*6=30 $in^2$ | 150 | 0.002933 | 0.44 |
| 9 | S33 | 3 | 61233 | 408.22 | 0.1825 | | 150 | 0.0044 | 0.66 |
| 10 | S34 | 4 | 60835 | 405.57 | 0.0445 | | 150 | 0.005867 | 0.88 |
| 11 | S35 | 5 | 112201 | 748.0067 | 0.089 | | 150 | 0.007333 | 1.10 |
| 12 | S36 | 6 | 126445 | 842.9667 | 0.0975 | | 150 | 0.0088 | 1.32 |

4.2 Rebar Distribution and Failure Mode.

The arrangement of the rebar defines the load path and affects the stress distribution in the concrete section and the failure mode Figure 19: Splitting and Failure of S33. Splitting and subsequent failure of S33 shows that the concrete was crushed and totally damaged while the rebar was still in place Figure 19. Failure can result from yielding in the steel, excessive stresses in concrete, or pullout for the rebar due to inadequate development length and/or lack of confinement for the reinforcement.

Figure 18 : Development Length in Specimens

The case of S33 when the 3 bars are vertically above each other, the failure happened at the same section containing the 3 bars due to the splitting of the specimen in the middle.

Figure 19: Splitting and Failure of S33

ACI 318 –11 equation using the shear friction theory for the case of concrete placed against hardened concrete with μ = 1 for concrete placed against hardened concrete and μ = 0.6 for cracked concrete and λ = 1 for normal weight concrete predicts the nominal shear strength $Vn = Avf\ fy\mu$

This expression takes only the area of the interface reinforcement into consideration while the distribution of the rebar in the section is not considered; the upper limit for concrete strength is the least value determined from three expressions.

For normal weight concrete either placed monolithically or placed against hardened concrete with surface intentionally roughened, $V_n$ shall not exceed the smallest of

$$Vn \leq 0.2\ f'c\ Ac$$

$$Vn \leq (480 + 0.08f'c)Ac$$

$$Vn \leq 1600Ac.$$

Comparing test results to ACI and the horizontal shear expressions

Table 16 below shows the calculation of shear strength according to ACI expression and the applied limitations for each test specimen.

Table 16: Shear Strength by ACI Expressions

| Specimen | f'c psi | Ac ($in^2$) | As ($in^2$) | ρ= As/Ac | ACI 1 (0.8Av*Fy+ AcK1) | ACI 11 $A_{vf}$*$F_{yf}$*μ (lb) | 0.2f'c*Ac (lb) | 1600*Ac (lb) | (480+0.08f'c)*Ac (lb) | V= ACI (lb) | ν = ACI (psi) |
|---|---|---|---|---|---|---|---|---|---|---|---|
| S12 | 6,158 | 116 | 0.44 | 0.0038 | 67,520 | 26,400 | 142,866 | 185,600 | 112,826 | 26,400 | 228 |
| S22 | 5,086 | 90 | 0.44 | 0.0049 | 57,120 | 26,400 | 91,548 | 144,000 | 79,819 | 26,400 | 293 |
| S32 | 6,158 | 150 | 0.44 | 0.0029 | 81,120 | 26,400 | 184,740 | 240,000 | 145,896 | 26,400 | 176 |
| S23 | 5,086 | 90 | 0.66 | 0.0073 | 67,680 | 39,600 | 91,548 | 144,000 | 79,819 | 39,600 | 440 |
| S33 | 6,158 | 150 | 0.66 | 0.0044 | 91,680 | 39,600 | 184,740 | 240,000 | 145,896 | 39,600 | 264 |
| S14 | 6,158 | 116 | 0.66 | 0.0057 | 78,080 | 39,600 | 142,866 | 185,600 | 112,826 | 39,600 | 341 |
| S24 | 5,086 | 90 | 0.88 | 0.0098 | 78,240 | 52,800 | 91,548 | 144,000 | 79,819 | 52,800 | 587 |
| S34 | 6,158 | 150 | 0.88 | 0.0059 | 102,240 | 52,800 | 184,740 | 240,000 | 145,896 | 52,800 | 352 |
| S25 | 5,086 | 90 | 1.1 | 0.0122 | 88,800 | 66,000 | 91,548 | 144,000 | 79,819 | 66,000 | 733 |
| S35 | 6,158 | 150 | 1.1 | 0.0073 | 112,800 | 66,000 | 184,740 | 240,000 | 145,896 | 66,000 | 440 |
| S26 | 5,086 | 90 | 1.32 | 0.0147 | 99,360 | 79,200 | 91,548 | 144,000 | 79,819 | 79,200 | 880 |
| S36 | 6,158 | 150 | 1.32 | 0.0088 | 123,360 | 79,200 | 184,740 | 240,000 | 145,896 | 79,200 | 528 |

Comparing the test results of Specimen S12, S14 to the (ACI, 2011) to the expressions by (Patnaik, 2001)for the horizontal shear strength for concrete with smooth interface $V_n = 0.4\rho_{vf}\sqrt{f'c * Ec} \leq 1.1\,\rho_{vf}\,f_{yf}$ shows that ACI expression is safe and conservative when the smooth interface expression by Patnaik 2001 may not be applicable for interface shear other than for horizontal shear in composite concrete

beams with a smooth interface.

Comparing the test results of 12 Specimens with rough interface to the ACI expression and the expression of horizontal shear for concrete with rough interface using the expression by (Loov & Patnaik, 1994)

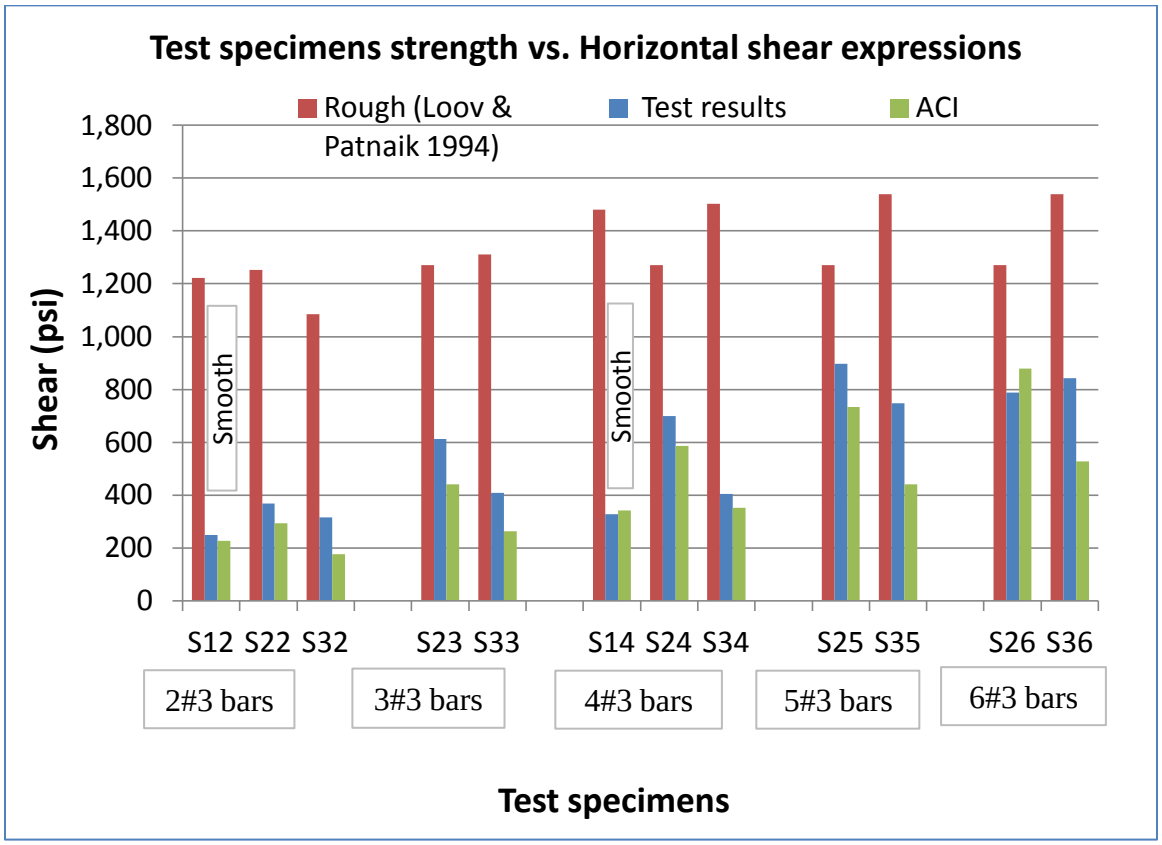


Figure 20: Comparing test results with Horizontal Shear Expression for rough interface by (Loov & Patnaik, 1994)

The roughness of the concrete has a considerable contribution to shear strength, the test specimens were not intentionally roughened to match the suggested roughness condition, it was vibrated with as-cast surface but without smoothing or roughening of the surface. Figure 15 shows the application of the expression introduced by Patnaik 2001 for the horizontal shear strength with a smooth interface.

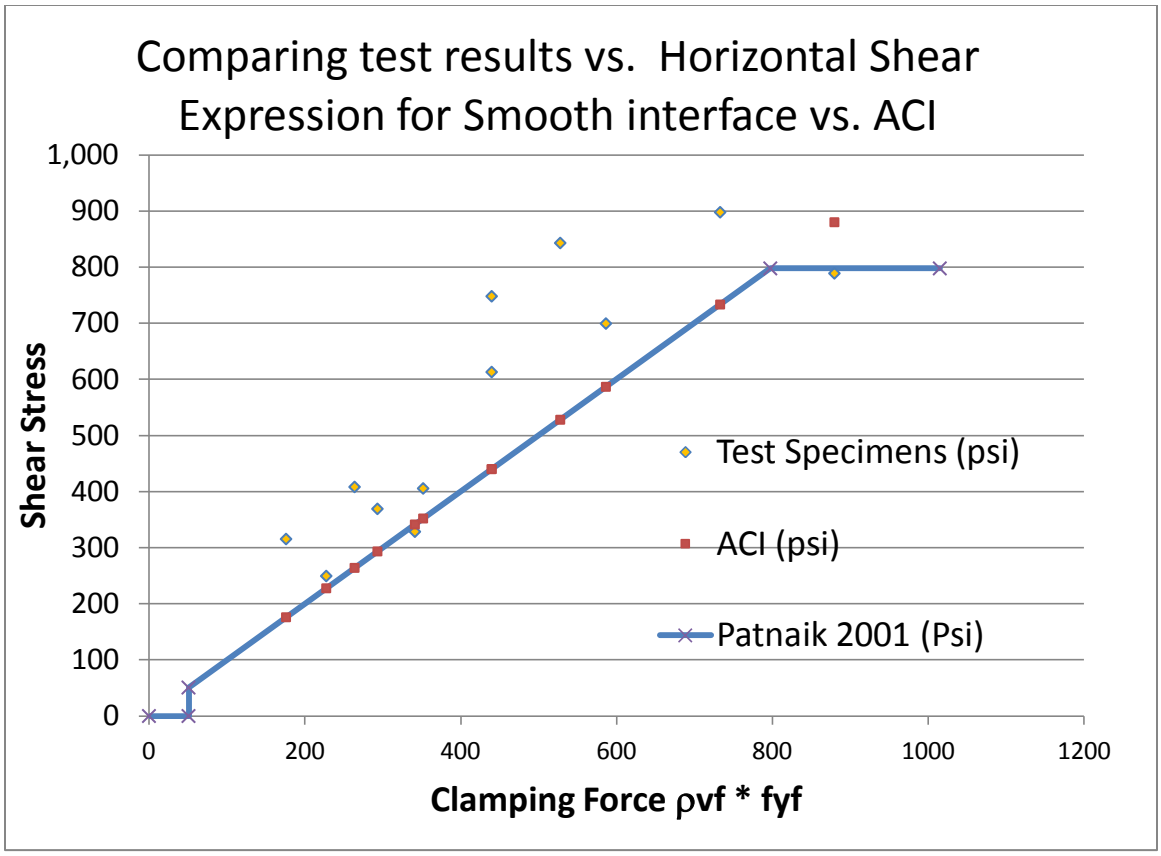


Figure 21: Comparing test results with Horizontal Shear Expression for Smooth interface (Patnaik, 2001) – A (psi)

It was found that the expressions proposed for the horizontal shear strength of composite concrete beams can be applicable to the vertical shear in as cast and smooth interface. Most of the previously proposed design expressions account for the strength of concrete by setting upper limit to the design value. Patnaik 2001 indicated that the shear strength is equal to zero with low clamping force when $\rho_{vf} f_{yf} < 51\, psi$ ($0.35\, Mpa$) and an upper limit for clamping force larger than 798 psi (5.5 Mpa). For S26 with clamping force equal to 880 psi the ACI design expression is overestimating the shear strength and the upper bound of the proposed expression by Patnaik 2001 is appropriate. It was reported that the design expressions are not accurate in evaluating the shear strength. Shear strength depends on three forces acting together to resist the shear stress,

(a) the bond between the concrete accompanied with relatively small slip depending on the elasticity of concrete, (b) the friction between the concrete at the interface which can be increased by restraining the lateral movements of the concrete units in the tension region, and/or by applying external normal forces to increase the friction and to balance the tensile force developed in the rebar (c) the rebar area and $f_y$ crossing the interface which may also affect dowel-action. Most of the test specimens could resist shear greater than the ACI design expression$V_n = A_{vf}\ f_y\ \mu$. Except for S14 with clamping force equal 341 psi with smooth interface. This expression allows stresses to reach the yield stress, the actual yield stress was determined from a tensile test of the rebar. Figure 47 : Stress Strain Diagram of Rebar shows that the ultimate stress is around 50% above the yield stress, however limiting the allowable strength to the yield stress is convenient to control the slip and to provide safety margin.

4.3 Load-Slip Diagram

Figures 25 to 34 demonstrate the effect of the confinement of the rebar and effect of the distribution of the bars in the section from the test results. In specimen S34 with compressive strength $f'c$ 6,158 $psi$ was almost equal to 6,155 psi for $S24$. $Ac = 150\ in^2$ which is greater than $90\ in^2$ for S24. The failure load for S34 was $60{,}835\ lb$ which is less than the failrue load of $62945\ lb\ for\ S24$.

In S14 and S24 with the same rebar distribution, S14 had smooth interface, better confinement for the rebar and higher $f'c$ with a concrete cover of 2 inches. Three inch concrete cover for S24 is smaller than that of S14. The failure load for S24 was $62{,}945\ lb$ which is greater than $39{,}400\ lb$ which is the failure load of S14.

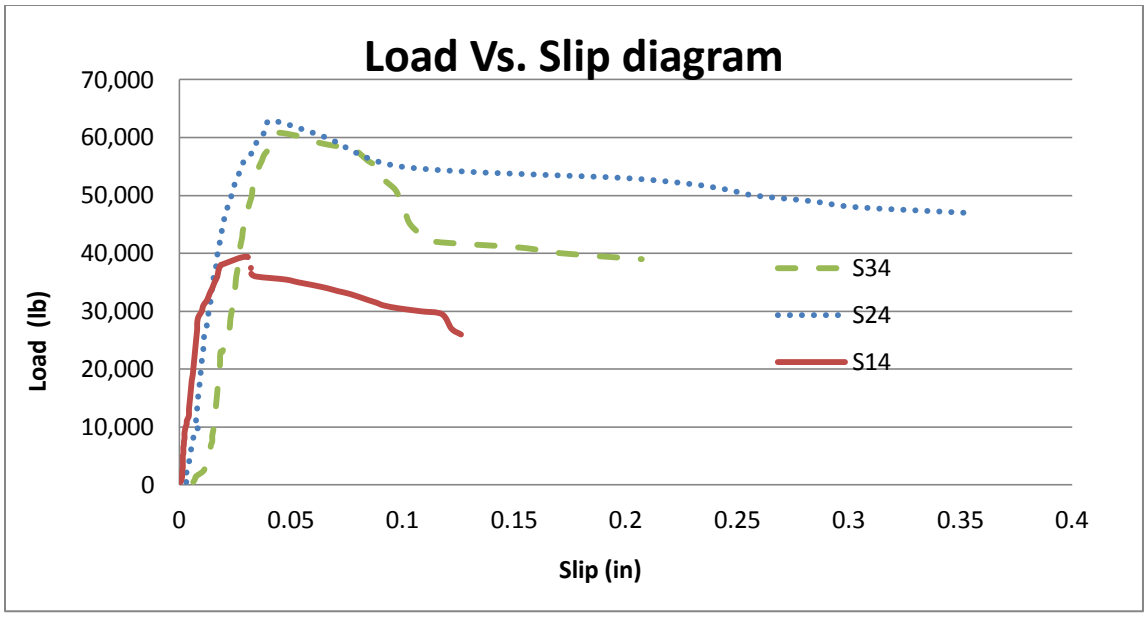


Figure 22 : Load Slip Diagram

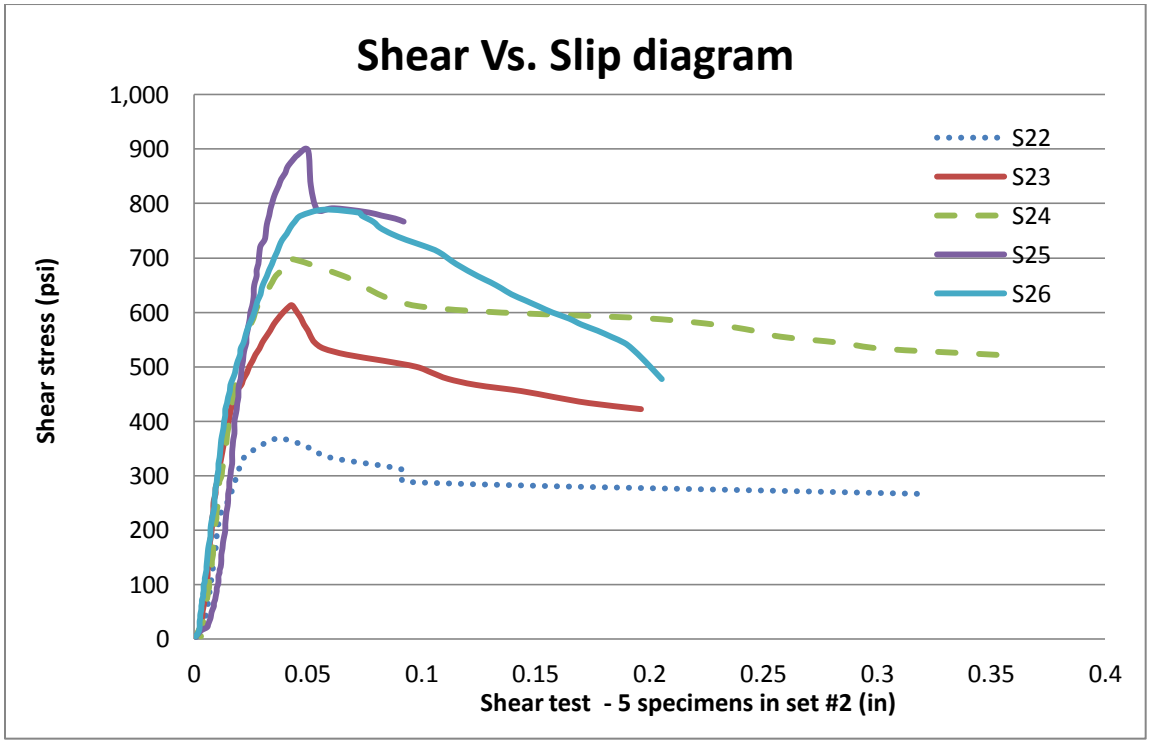


Figure 23: Shear-Slip Diagram for Set # 2

The common result is that the ultimate shear capacity at failure happens at a slip of around 0.05 in. and the higher the steel ratio, the higher the shear strength.

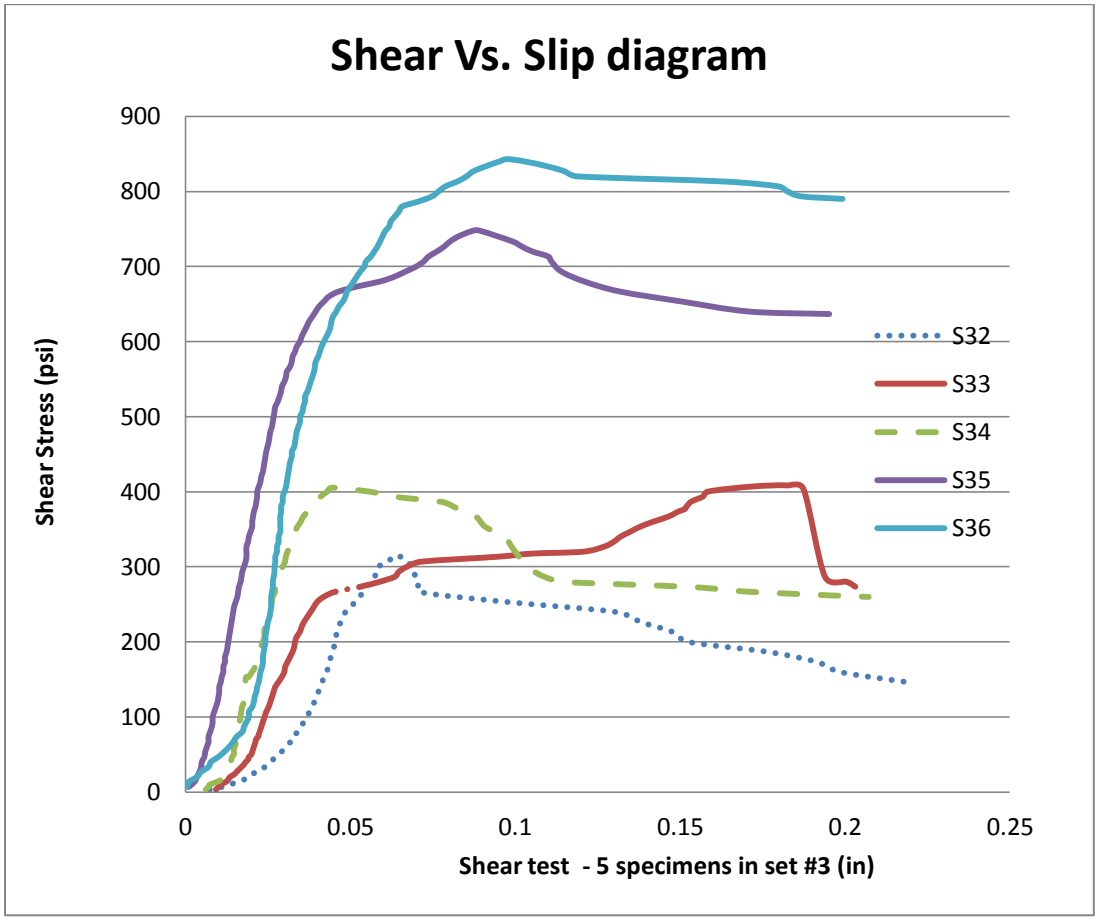


Figure 24: Shear-Slip Diagram for Set # 3

The shear capacity of the specimen S36 with six bars was greater than the shear strength of S35. However the initial slip is larger in S36 than in S35. The reason for large slip might be the uneven surface of specimen S36. The general trend in the test results were that the higher the reinforcement ratio, the less the slip and the higher the ultimate shear capacity of the specimen.


Figure 25: Failure in S14

The external concrete units with cross section of 4"x 3" didn't provide enough confinement for the reinforcement. The movement of the rebar from its original location and bending of the rebar appears in Figure 25: Failure in S145. The rebar appeared to have transferred the load to the middle concrete block thereby splitting the concrete above the reinforcement. Because of the distribution of the 4 bars in the section, the middle block for specimen S33 did not split in the case of S33 Figure 19: Splitting and Failure of S33.

Specimen S26: The first cracks to appear while loading the test specimen and are vertical cracks between the concrete blocks when the applied load broke the bond between the concrete blocks. Some cracks regularly appeared in all the specimen under the loading point due to the concentration of the stresses which is considered a disturbed region. When the slip started between the concrete blocks, the interface reinforcement is mobilized and the loads were transferred to the interface rebar connecting the blocks together.

The third type of cracks appears at the level of the rebar which appears first in the external blocks due to the lack of concrete confinement for the rebar.

Figure 26: Cracks in S26

S26: Loading on the specimen was continued manually after the failure of the specimen and reaching the ultimate load capacity and recording the shear strength to observe the final failure mode. Figure 26 shows the external blocks that failed due to low confinement of the rebar and the lateral split in the middle block, the second failure pattern at the rebar level.

Figure 27: Failure mode of S26

Specimen S14: Figure 28 shows the crack in the middle in the bottom concrete block that connects the edges due to the high tensile stresses that developed in the rebar due to the vertical loading.

Figure 28: Splitting tensile stresses in S14

Specimen S22: when the reinforcing bars are all in one vertical plane, the stress concentration in the section containing the rebar splits the specimen at this section.

Figure 29: Splitting tensile stresses in S22

Furthermore, for specimen S22, the middle concrete block had no cracks while the external block was split at the middle as shown in Figure 30.


Figure 30: Specimen S22 with no cracking in the middle concrete block

Specimen S26: With larger area of reinforcement and more than one bar in the shear interface in the vertical plane, the effects of the concrete confinement is observed to increase the shear capacity and to avoid the splitting tensile failure in the specimen Figure 31: Failure mode of specimen S26.

Figure 31: Failure mode of specimen S26

Specimen S14: the picture shows the back side of the specimen that is similar to the front view in (Figure 25: Failure in S14) when the cover concrete spalled on both sides around the rebar, bigger concrete cover and rebar confinement may help to avoid this type of failure.

Figure 32: Failure mode of specimen S14

Specimen S34: using steel plate under the loading cell provides a uniform loading on the middle block and eliminates cracks in the middle block under the applied loading.

Figure 33: distribution of applied load

Specimen S26: The cracks developed at the location of the rebar through the height of the specimen as it appears in Figure 36 in the left external concrete block with 3

cracks at different levels indicating a disturbed region at the location of the rebar. The use of strut and tie model to follow the load path and stresses distribution in the specimen can be explained based on these cracks.


Figure 34: Failure mode of specimen S26

4.4 Comparisons of Test Specimens

The most common situation for cold joint in projects is when the hardened concrete is cast against formwork, which is defined in this research as concrete with smooth surface, or "as-cast" concrete surface when the concrete is cast and vibrated without intentional roughness or smoothing, three comparisons were made between the specimens with rough interface (1) constant steel area with variable interface surface area, (2) constant interface area with variable steel area for set # 2 with a constant $A_c$ =90 $in^2$ with variable area of shear reinforcement and set # 3 with constant $A_c$ =150 $in^2$ but with variable area of shear reinforcement, and (3) constant reinforcement areas with different rebar distribution (S24 vs. S34 and S26 vs. S36).

Table 17: Test Variables

| Rough interface | | | | | | | |
|---|---|---|---|---|---|---|---|
| Constant $A_s$ | Variable $A_c$ | Specimen ID | Ultimate load | Constant $A_c$ | Variable $A_s$ | Specimen ID | Ultimate load |
| 2#3 | 90 | S22 | 33,227 | 90 | 2#3 | S22 | 33,227 |
| | 150 | S32 | 47,314 | | 3#3 | S23 | 55,171 |
| 3#3 | 90 | S23 | 55,171 | | 4#3 | S24 | 62,945 |
| | 150 | S33 | 61,233 | | 5#3 | S25 | 80,799 |
| 4#3 | 90 | S24 | 62,945 | | 6#3 | S26 | 71,000 |
| | 150 | S34 | 60,835 | 150 | 2#3 | S32 | 47,314 |
| 5#3 | 90 | S25 | 80,799 | | 3#3 | S33 | 61,233 |
| | 150 | S35 | 112,201 | | 4#3 | S34 | 60,835 |
| 6#3 | 90 | S26 | 71,000 | | 5#3 | S35 | 112,201 |
| | 150 | S36 | 126,445 | | 6#3 | S36 | 126,445 |

Comparing S23 to S33 with the same rebar area and increased interface area from 90 $in^2$ to 150 $in^2$, the load capacity increased from 55,171 lb to 61,233 lb, however the

shear stress strength decreased from 613 psi to 408 psi. Comparing specimens S22 with interface area equal to 90 $in^2$ with S32 with interface area equal to 150 $in^2$ at constant reinforcement area of 2#3 bars, the shear stress strength was reduced from 369 psi to 315 psi. Also in the case of S34 compared to s34 at constant reinforcement area, the shear stress strength was reduced from 699 psi to 406 psi. Increasing the interface area might increase the load carrying capacity but will not increase the shear stress strength.

When the steel area is constant the increase of interface area increased the shear strength (shear load carrying capacity) except for the case of 4#3.

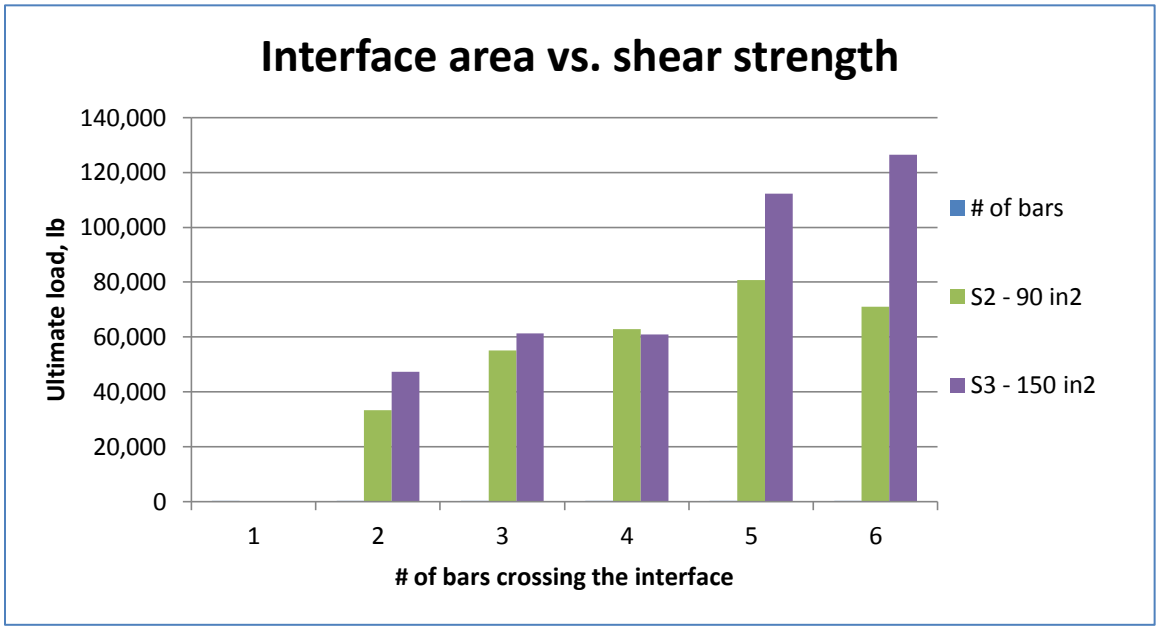


Figure 35: Interface Area vs. Shear Strength Constant Area of Steel - A

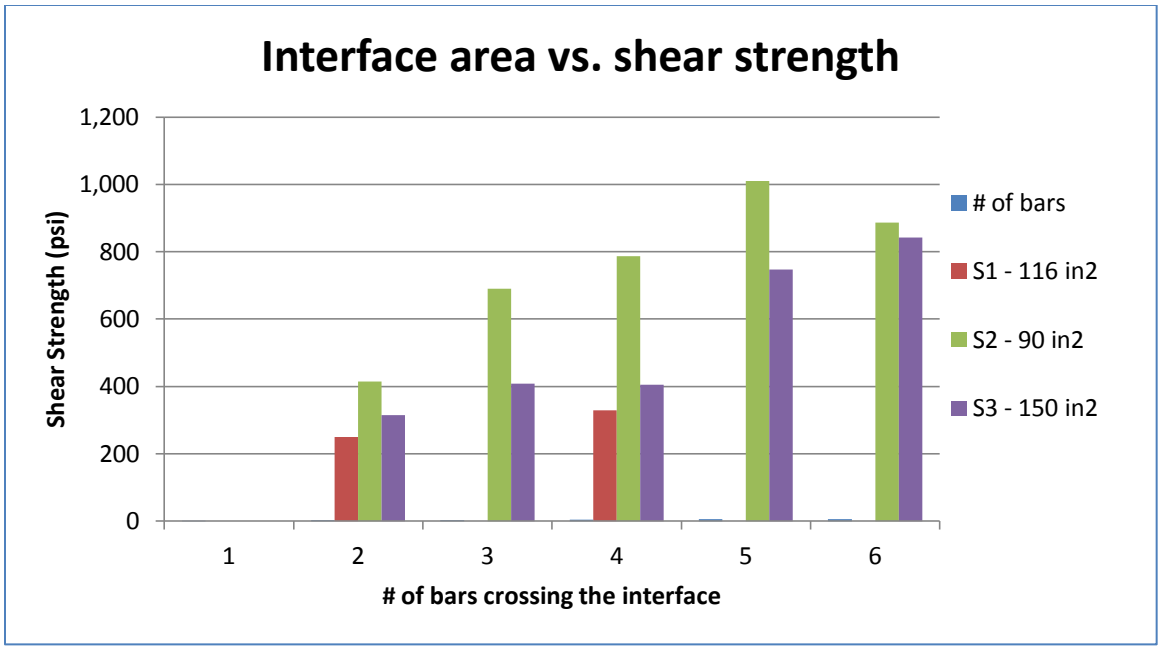


Figure 36: Interface Area vs. Shear Strength Constant Area of Steel - B

Increasing the reinforcement area increased load and shear capacities for all the specimens except S26.

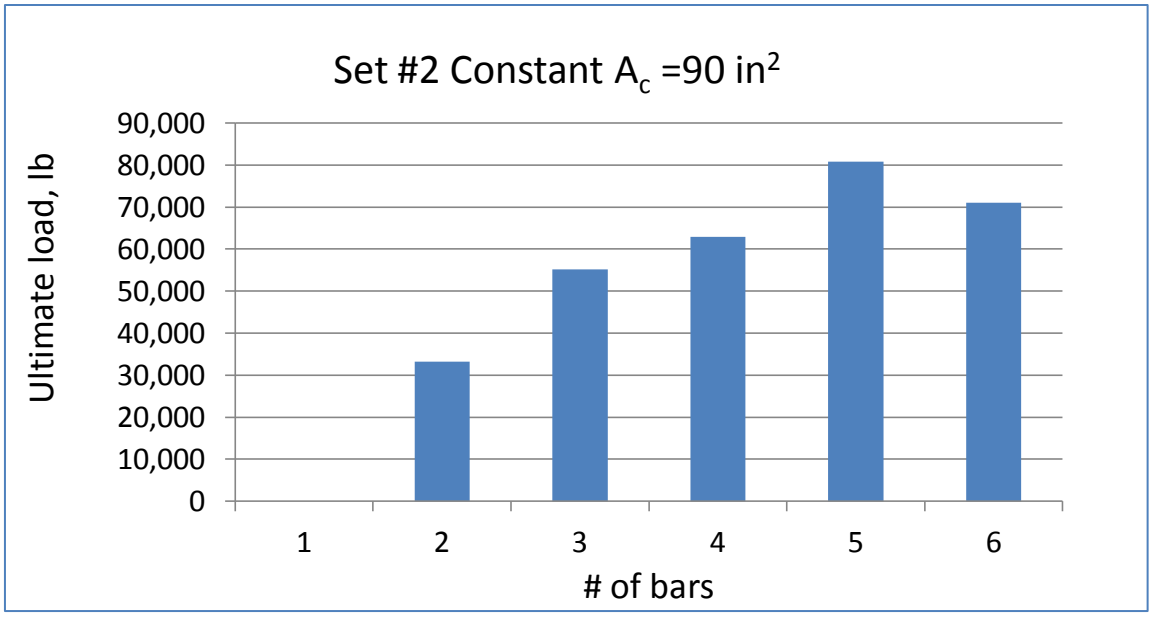


Figure 37: Set #2 Constant $A_c$ =90 $in^2$ with variable area of shear reinforcement - A

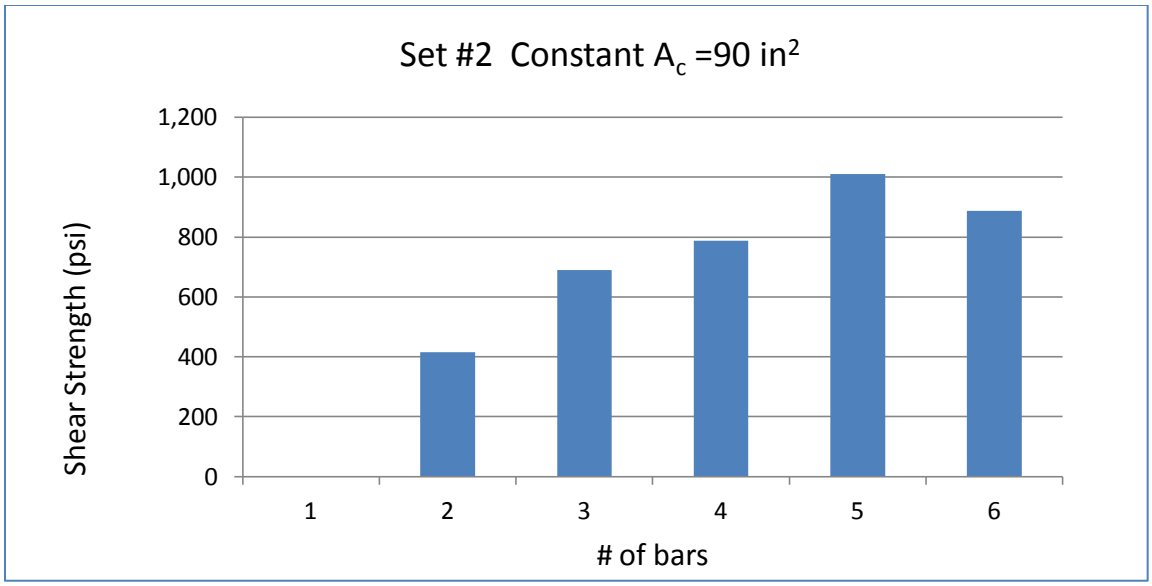


Figure 38: Set #2 Constant $A_c$ =90 $in^2$ with variable area of shear reinforcement - B

For Set# 3 increasing the steel area with constant concrete area (150 $in^2$) increased the shear strength except for S24 with 4 bars Figure 39.

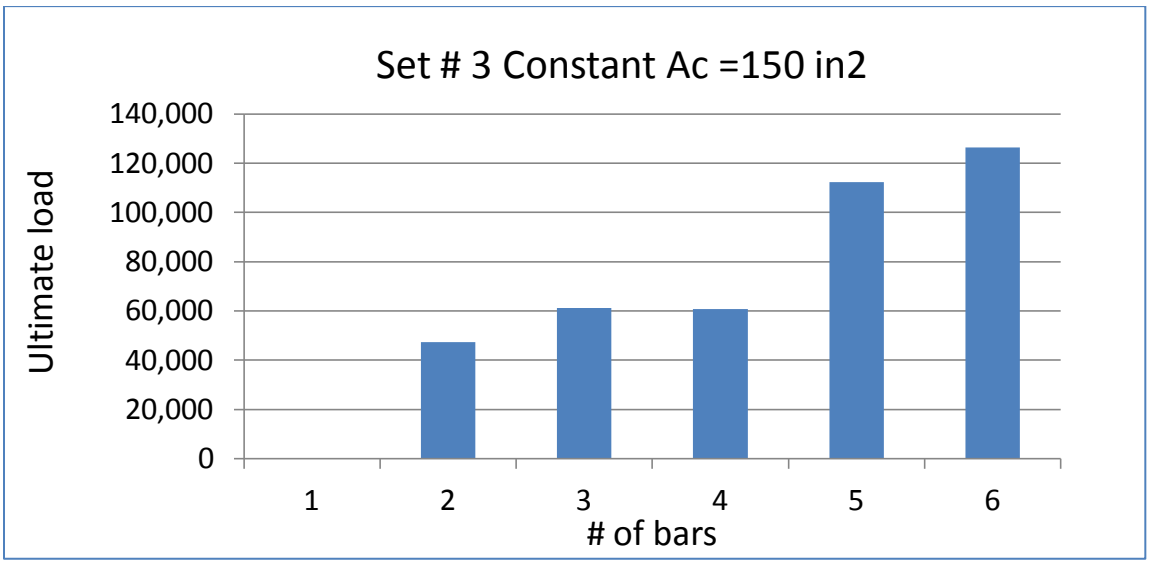


Figure 39: Set #3 Constant $A_c$ =150 $in^2$ with variable area of shear reinforcement - A

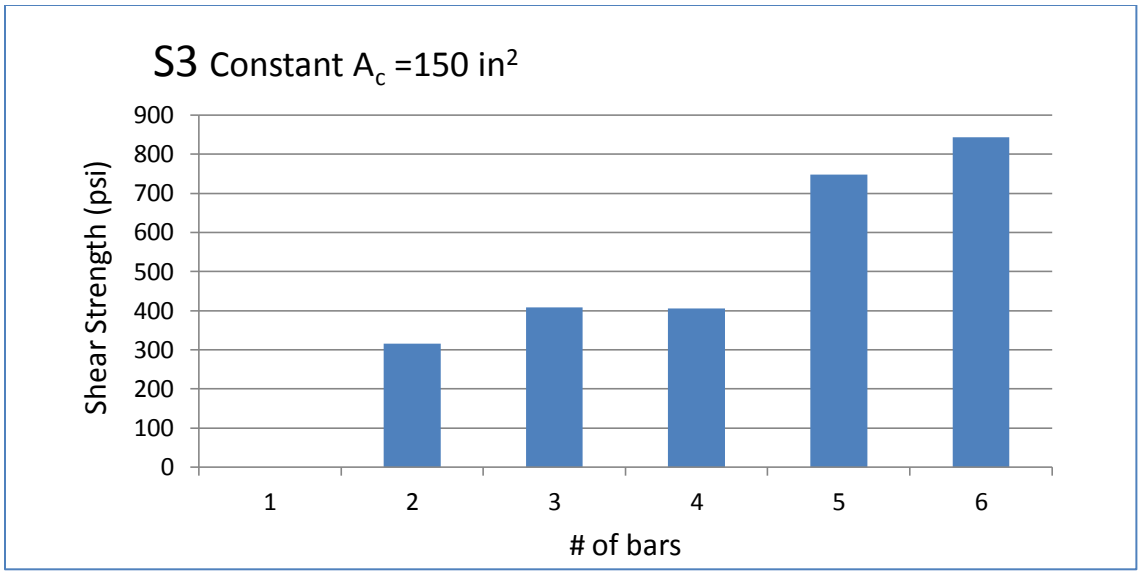


Figure 40: Set #3 Constant $A_c$ =150 in$^2$ with variable area of shear reinforcement - B

Rebar distribution defines the load path through the concrete units to form struts and ties forcing the specimen to fail in crushing if the compressive stresses of the struts reaches the compressive strength of the concrete unit, or in tensile splitting if the tensile stresses around the ties reach the tensile strength of the concrete.

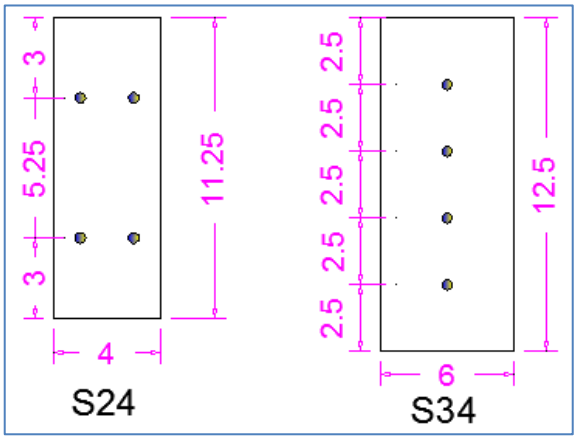


Figure 42: Rebar distribution for $A_s$ = 4#3

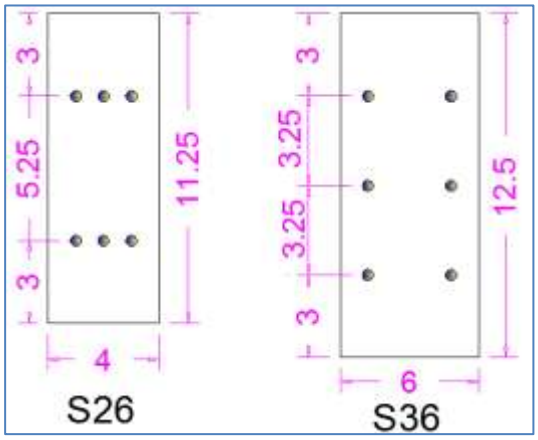


Figure 41: Rebar distribution for $A_s$ = 6#3

The rebar distribution in S24 is better than S34 that increased the shear stress strength of the specimen from 406 psi to 700 psi despite a larger interface area in Set#3 than in Set#2. Better comparison could be achieved with constant area of concrete interface.

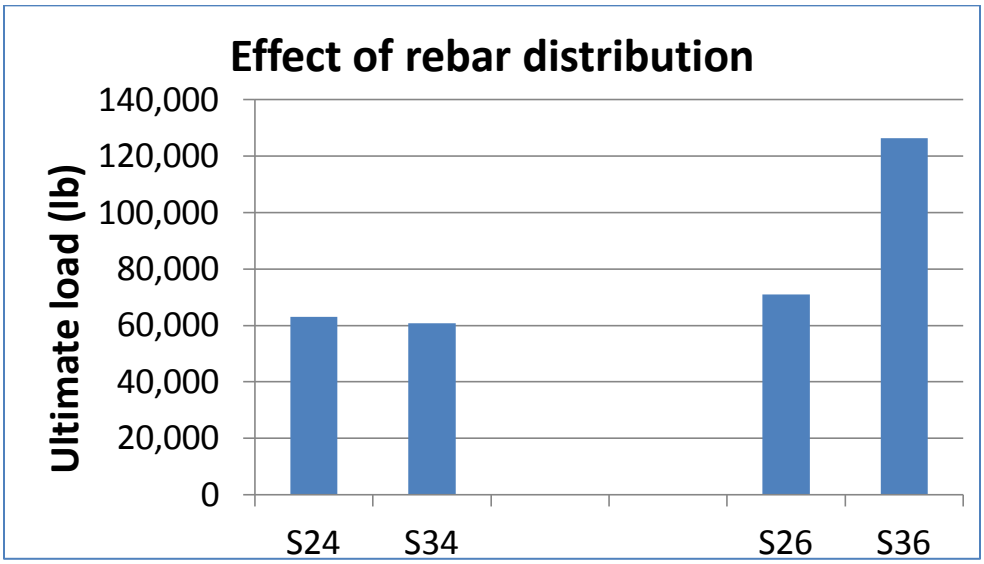


Figure 43: Rebar distribution - A

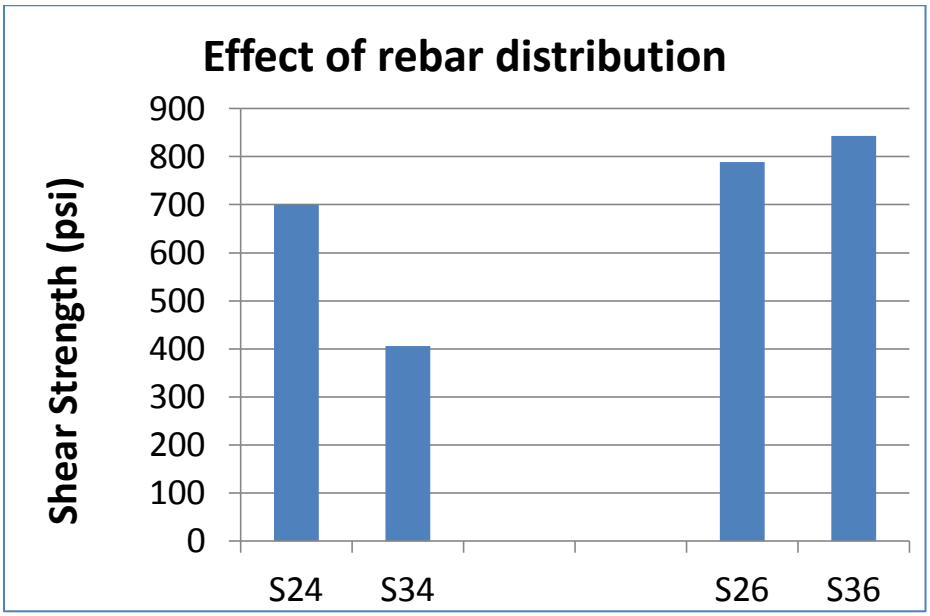


Figure 44: Rebar distribution - B

## 4.5 Finite Element Analysis

Three dimensional finite element models were used to compare the laboratory test results and to analyze the stress in the steel and the concrete due to static load using ABAQUS 6.11 / STANDARD

### 4.5.1 Material Properties.

Tensile test was conducted on a used rebar to determine the actual stress strain curve for the input file ABAQUS. Three tensile specimens were tested using # 4 bars and machined in the mid-length to reduce the diameter to 0.3" instead of the actual bar diameter of 0.5 inch to control the location of failure then applying tensile load. Displacement at a rate 0.05 in/min or 0.0008 inch/sec was applied for the first and second specimens and a displacement rate of 0.1 inch/min applied for the third Specimen.


Figure 45 : Tensile Test Steup of Rebar

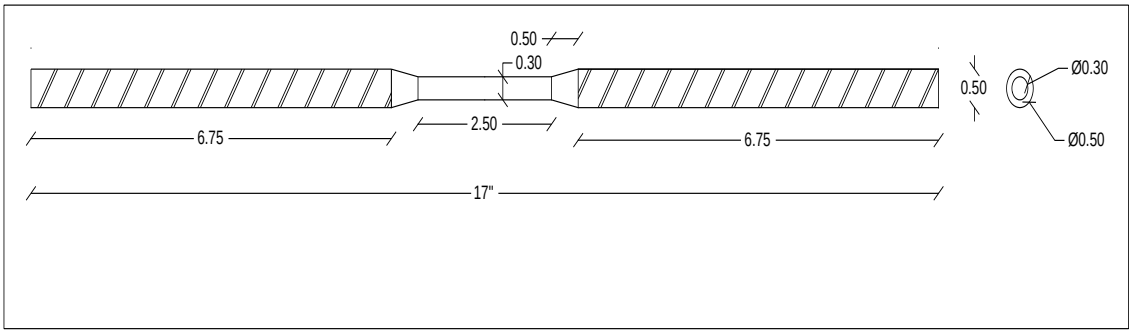


Dimensions in inches

Figure 46 : Preparation of Tensile Test Specimen

All three specimens failed in the expected location with significantly higher stresses compared to the $60\ ksi$ specified strength that was recommended by the manufacturer, with ultimate stresses reaching 130 ksi. The following table shows the test results for the three specimens.

Table 18: Tensile Test Results.

| | Specimen # 1 | Specimen # 2 | Specimen # 3 |
|---|---|---|---|
| Loading rate (in/sec) | 0.0008 | 0.0008 | 0.0016 |
| Loading rate (lb/sec) | 52 | 52 | 104 |
| Yield stress (ksi) | 88.9 | 81.5 | 68.6 |
| Strain at yield | 0.00269 | 0.0027 | 0.00356 |
| ultimate stress (ksi) | 135.7 | 128.9 | 116.8 |
| Strain at ultimate stress | 0.10172 | 0.09115 | 0.09928 |
| Load at failure (kips) | 111.7 | 105.201 | 87.0871 |
| Strain at failure | 0.18088 | 0.19762 | 0.16418 |

The data of specimen # 1 was used in the finite element modeling. A stress–strain diagram for specimen # 1 is shown in Figure 45 : Tensile Test Steup of Rebar.

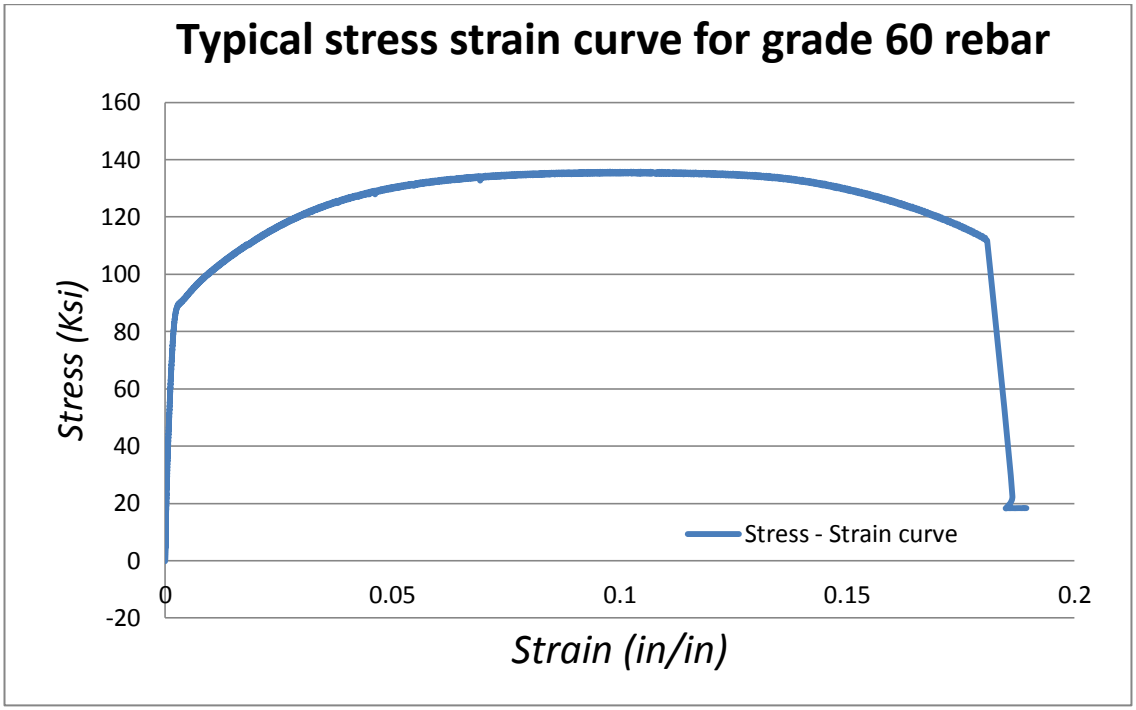


Figure 47 : Stress Strain Diagram of Rebar

4.5.2 Displacement control approach

A displacement control approach was used in modeling the test specimens using ABAQUS implicit for static analysis. Load control approach is used to apply loads in the test. The program calculates the corresponding displacement and stress. This will not be true representation of the loading condition in developing the actual stress-strain curves used for steel and concrete because applied stressed can have two different values of strains causing the program to abort without completing the analysis. In such a situation we can use the displacement control approach to apply continuous displacement to the structure and the program will calculate the corresponding required load and stress. In other types of analysis like static Riks or dynamic analysis, ABAQUS can handle this type of stress-strain curves with descending values in a load or displacement controlled analysis.

A tremendous amount of data were obtained by the computerized test machine for the stress strain tensile test of the rebar including loading and unloading cycles to maintain a loading rate of $0.005\ inch/min$. Aa select and calculated set of values that will define the stress-strain curve were used in ABAQUS input files. ABAQUS also requires in the input file separated elastic and plastic regions for the material properties. The numbers in Table 18 were used in the input file which defines the elastic region of the mild steel as the linear part of the curve with a stress of $89.1\ ksi$ with the corresponding elastic strain of $0.00275\ in/in$; then the plastic stresses from $89.1\ ksi$ until it reaches the ultimate stress бu = $135.6\ ksi$ with corresponding plastic $strain = total\ strain - \epsilon y$ that vary from 0 to 0.00507 in/in. The unloading and failure region

to reach a maximum plastic strain = 0.00642 that corresponds to a total strain = 0.00642+0.00275 = 0.00917 in/in.

Table 19: Input File for Steel "Stress-Strain Curve"

| Steel | | | |
|---|---|---|---|
| $E_s$ | 29,000 ksi | $\epsilon_y$ | 0.00275 in/in |
| Stress | Plastic strain | Stress | Plastic strain |
| 89096 | 0 | 119034 | 0.00297 |
| 89096 | 9.00E-05 | 120209 | 0.00307 |
| 89695 | 0.00018 | 121324 | 0.00316 |
| 90145 | 0.00026 | 122008 | 0.00328 |
| 91151 | 0.00038 | 123845 | 0.00337 |
| 92347 | 0.00049 | 125115 | 0.00347 |
| 93497 | 0.00058 | 126945 | 0.00359 |
| 94188 | 0.00072 | 127487 | 0.00369 |
| 95163 | 0.00083 | 128434 | 0.00378 |
| 95699 | 0.00093 | 128556 | 0.00391 |
| 96796 | 0.00106 | 129978 | 0.00401 |
| 98301 | 0.00116 | 130278 | 0.0041 |
| 99801 | 0.00126 | 131929 | 0.00441 |
| 100768 | 0.00139 | 132495 | 0.00454 |
| 102136 | 0.0015 | 133116 | 0.00465 |
| 103495 | 0.00159 | 134966 | 0.00487 |
| 104776 | 0.00172 | 135595 | 0.00507 |
| 105590 | 0.00183 | 135025 | 0.0052 |
| 107313 | 0.00191 | 134879 | 0.0053 |
| 108074 | 0.00204 | 134304 | 0.00541 |
| 109610 | 0.00213 | 132461 | 0.00554 |
| 110817 | 0.00223 | 130956 | 0.00564 |
| 111923 | 0.00235 | 129229 | 0.00574 |
| 113484 | 0.00245 | 127214 | 0.00588 |
| 114506 | 0.00255 | 124857 | 0.00598 |
| 115386 | 0.00266 | 120601 | 0.00608 |
| 116882 | 0.00276 | 117733 | 0.00621 |
| 117716 | 0.00285 | 113339 | 0.00632 |
| | | 18346 | 0.00642 |

Table 20: Input File of Concrete "Stress-Strain Curve"

| Concrete | | | | | |
|---|---|---|---|---|---|
| $f'_c$ = 6,500 psi | | $E_c$ = 4,645 ksi | | Elastic = 0.00063 | |
| Stress | Plastic strain | Total strain | Stress | Plastic strain | Total strain |
| 2925 | 0 | 0.00063 | 6325 | 0.0019 | 0.00253 |
| 3724 | 0.00005 | 0.00068 | 6264 | 0.002 | 0.00263 |
| 4186 | 0.0001 | 0.00073 | 6198 | 0.0021 | 0.00273 |
| 4601 | 0.0002 | 0.00083 | 6127 | 0.0022 | 0.00283 |
| 4969 | 0.0003 | 0.00093 | 6054 | 0.0023 | 0.00293 |
| 5291 | 0.0004 | 0.00103 | 5977 | 0.0024 | 0.00303 |
| 5567 | 0.0005 | 0.00113 | 5899 | 0.0025 | 0.00313 |
| 5800 | 0.0006 | 0.00123 | 5819 | 0.0026 | 0.00323 |
| 5994 | 0.0007 | 0.00133 | 5738 | 0.0027 | 0.00333 |
| 6150 | 0.0008 | 0.00143 | 5657 | 0.0028 | 0.00343 |
| 6273 | 0.0009 | 0.00153 | 5576 | 0.0029 | 0.00353 |
| 6366 | 0.001 | 0.00163 | 5495 | 0.003 | 0.00363 |
| 6432 | 0.0011 | 0.00173 | 5414 | 0.0031 | 0.00373 |
| 6474 | 0.0012 | 0.00183 | 5334 | 0.0032 | 0.00383 |
| 6496 | 0.0013 | 0.00193 | 5255 | 0.0033 | 0.00393 |
| 6499 | 0.0014 | 0.00203 | 5177 | 0.0034 | 0.00403 |
| 6487 | 0.0015 | 0.00213 | 5100 | 0.0035 | 0.00413 |
| 6462 | 0.0016 | 0.00223 | 5024 | 0.0036 | 0.00423 |
| 6425 | 0.0017 | 0.00233 | 4949 | 0.0037 | 0.00433 |
| 6379 | 0.0018 | 0.00243 | | | |

4.5.3 ABAQUS Analysis Plan

Finite element analysis was performed to determine (i) the ultimate shear capacity of the reinforced concrete with rough interface (ii) study the effects of rebar distribution, $A_s$, $A_c$, boundary conditions and the lateral supports effect on the ultimate shear capacity. The parameters taken into consideration in the analysis are given in Table 21. The rebar distribution considered in the analysis is shown in Figure 50. All the reinforcing bars used in the FE models are #3 bars with $As = 0.11\ in^2$ and a diameter of 0.375 in.

Table 21: Specimen Characteristics for FE Models

| SN. | Model ID | No. of rebar | Rebar distribution | | Lateral support | conc. Interface in one side | |
|---|---|---|---|---|---|---|---|
| | | | Rows | Columns | | b | h |
| 1 | FR441 | 4 | 4 | 1 | FREE | 4 | 10 |
| 2 | FB441 | 4 | 4 | 1 | Fixed base | 4 | 10 |
| 3 | FF441 | 4 | 4 | 1 | Fully fixed | 4 | 10 |
| 4 | FR422a | 4 | 2 | 2 | FREE | 4 | 10 |
| 5 | FR422b | 4 | 2 | 2 | FREE | 4 | 10 |
| 6 | FR623 | 6 | 2 | 3 | FREE | 4 | 10 |
| 7 | FR632 | 6 | 3 | 2 | FREE | 4 | 10 |
| 8 | FR441 | 4 | 2 | 2 | Fully fixed | 6 | 12 |
| 9 | FF441 | 4 | 4 | 1 | Fully fixed | 6 | 12 |

Each model name had two letters and three numbers, the two letters are to define the lateral supports conditions, where FR was used when the external concrete units were modeled without restraining the lateral movements, FB for models when all the nodes in the base of the two external concrete units were restrained against the lateral movements, and FF for models when all the nodes in the sides of the two external concrete units were restrained against the lateral movements. Three numbers following the first two represent

the number of #3 bars crossing each of the two interfaces, the number of rows of reinforcement, and the number of columns. Figure 48: Specimen Size and Rebar Details for FE Model shows the model size and rebar details.

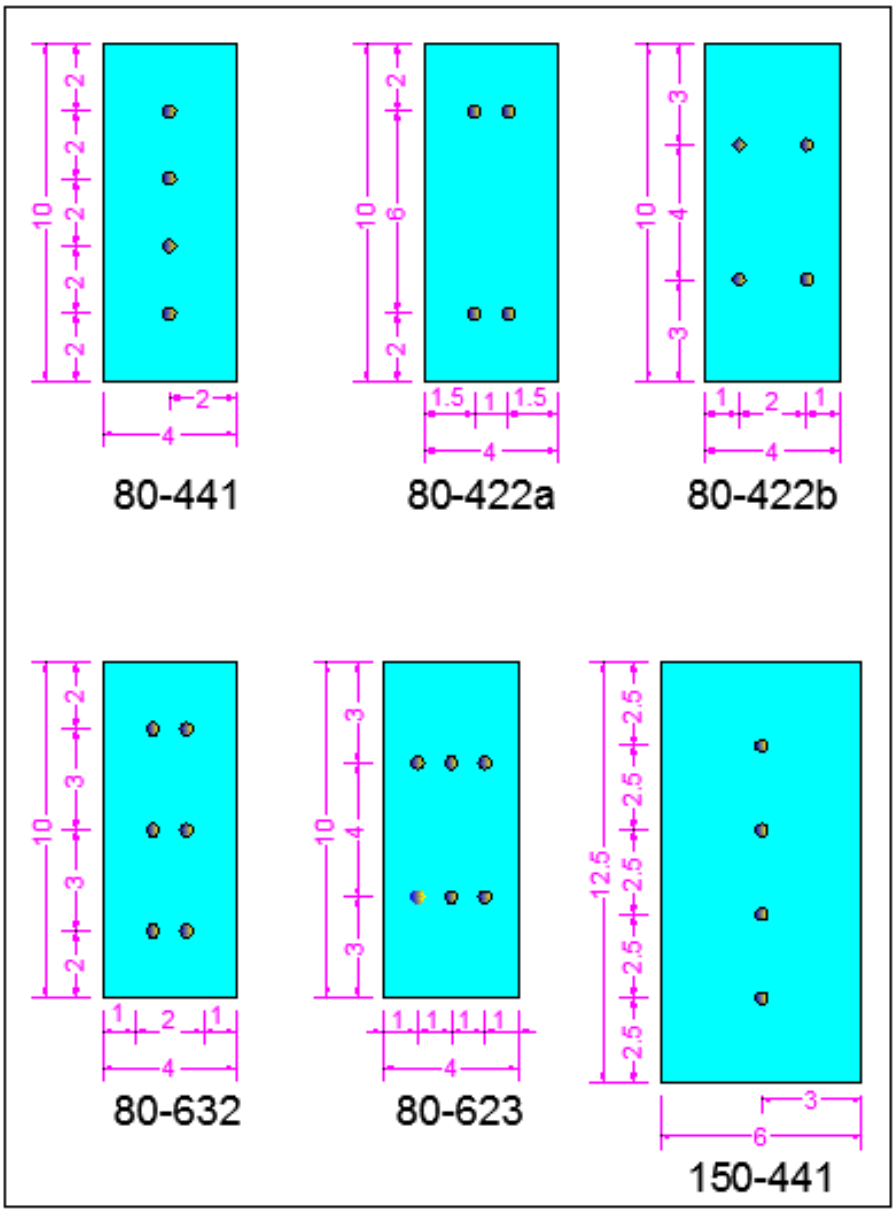


Figure 48: Specimen Size and Rebar Details for FE Model

### 4.5.4 Rebar Modeling

The rebar was modeled as 3D solid element with 8 nodes “C3D8R” with a diameter of 0.375” meshed into 12 symmetric elements in the cross section, meshed into 0.5” in the longitudinal direction.

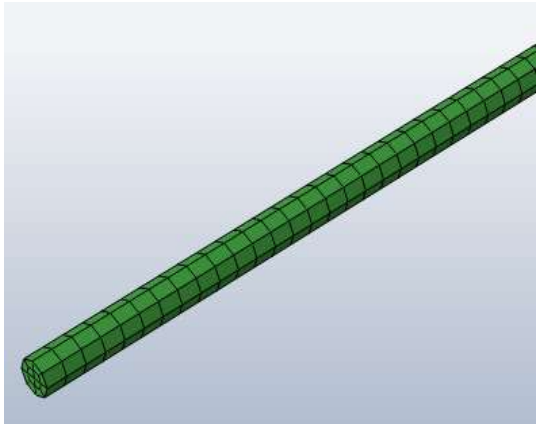

Figure 49: Rebar Mesh

### 4.5.5 Concrete Modeling

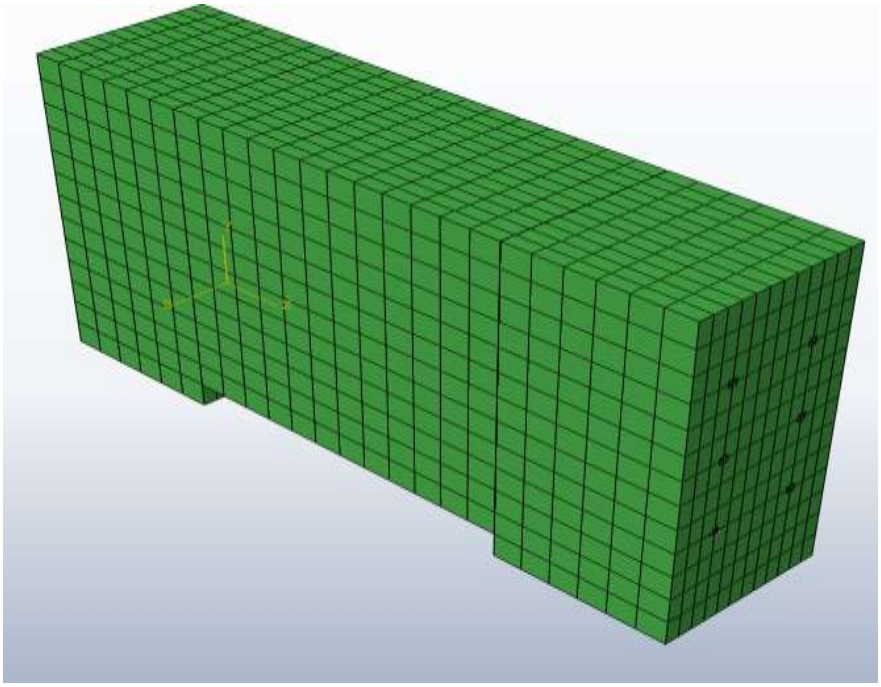

Figure 50: Concrete Model Mesh

The concrete blocks was modeled as 3D solid element using 8 nodes “C3D8R” with element size of 0.5”x1”x1” with aspect ratio of 2.0.

### 4.5.6 Boundary Conditions

The top of the middle concrete units was supported to restrain the translation in Y direction “vertical movement- u2”, the load was applied to the external concrete units as 0.5″ upward displacement which is higher than the possible slip in the interface between the concrete units. The analysis was expected to abort when the stresses in the rebar or the concrete units exceed the specified stress-strain input values for the defined material. The movement in the horizontal direction “U1” was studied in 3 cases; (a) with free external units, (b) with fully laterally supported sides; (c) when supporting the base only matching the fixation of the base provided by the contact with the testing machine.

### 4.5.7 Contact between Steel and Concrete

In the laboratory test a development length was provided to prevent the pull out of the rebar from the concrete; Hence in the computer model the rebar was defined as embedded in the concrete unit, only the 8 elements in the perimeter of the bars were included in this contact and the concrete units were defined as a host.

### 4.5.8 Friction between Concrete Surfaces

The interface contact for the concrete placed against hardened concrete with rough interface will provide shear strength; to account for that friction in the computer models, a friction module considering the master surface in the middle concrete unit and the slave surface in the external concrete units as shown in Figure 51 was used.

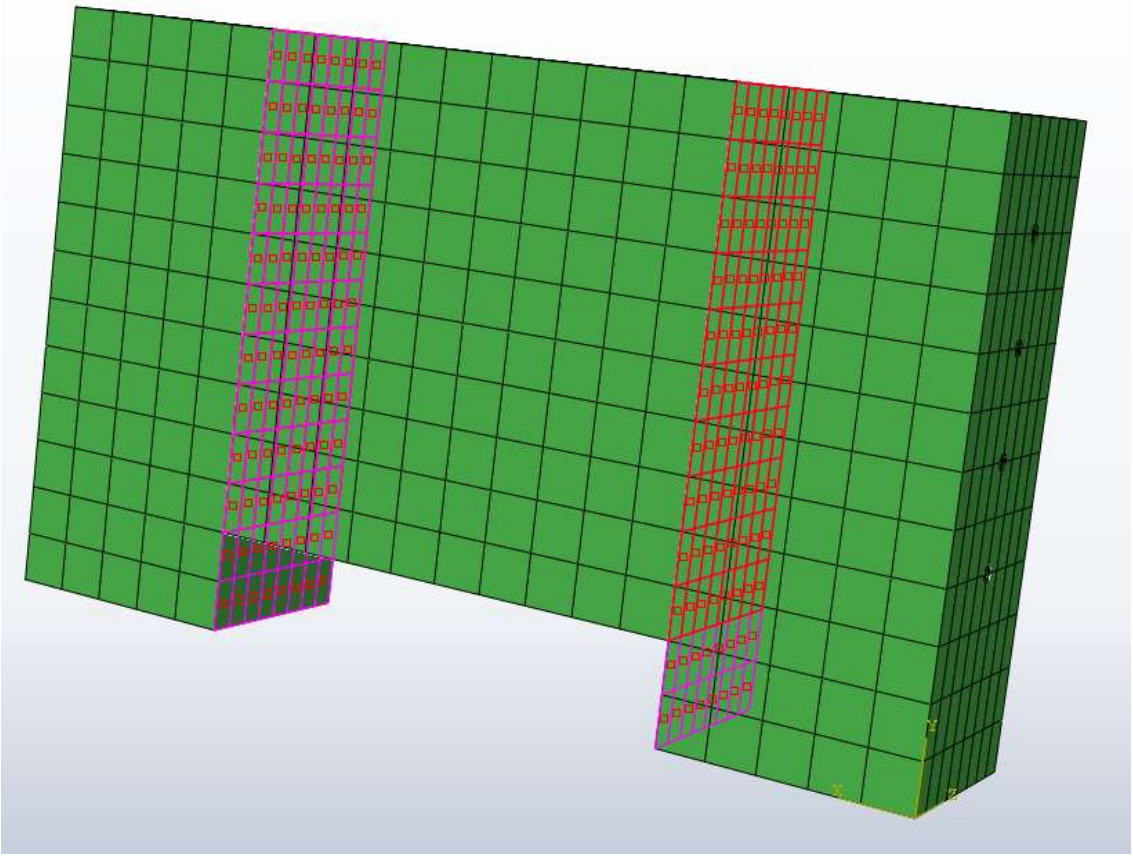

Figure 51: Interface Friction Surface

4.5.9 Analysis Results

The analysis of the model indicated large tensile stresses in the rebar, with lateral spread for the models with support condition “free to move laterally”, accompanied with vertical slip at the interface. The ultimate load and ultimate shear strength is reported in Table 22: FE Analysis Results.

Table 22: FE Analysis Results

| # | Model ID | ρ% | As ($in^2$) | Ac ($in^2$) | Load (lb) | Shear (psi) | Vertical disp. (in) | horizontal disp. (in) |
|---|---|---|---|---|---|---|---|---|
| 1 | FR441 | 1.1 | 0.88 | 80 | 46,599 | 582 | 0.00762958 | 0.0052 |
| 2 | FB441 | 1.1 | 0.88 | 80 | 63,101 | 789 | 0.0228885 | - |
| 3 | FF441 | 1.1 | 0.88 | 80 | 68,415 | 855 | 0.0415397 | - |
| 4 | FR422(a) | 1.1 | 0.88 | 80 | 51,888 | 649 | 0.0169456 | 0.0067 |
| 5 | FR422(b) | 1.1 | 0.88 | 80 | 55,548 | 694 | 0.0163237 | 0.0069 |
| 6 | FR623 | 1.65 | 1.32 | 80 | 65,593 | 820 | 0.0074532 | 0.0073 |
| 7 | FR632 | 1.65 | 1.32 | 80 | 75,637 | 945 | 0.012501 | 0.0097 |
| 8 | FR441 | 0.59 | 0.88 | 150 | 55,871 | 372 | 0.019399 | 0.0063 |
| 9 | FF441 | 0.59 | 0.88 | 150 | 87,594 | 584 | 0.051332 | - |

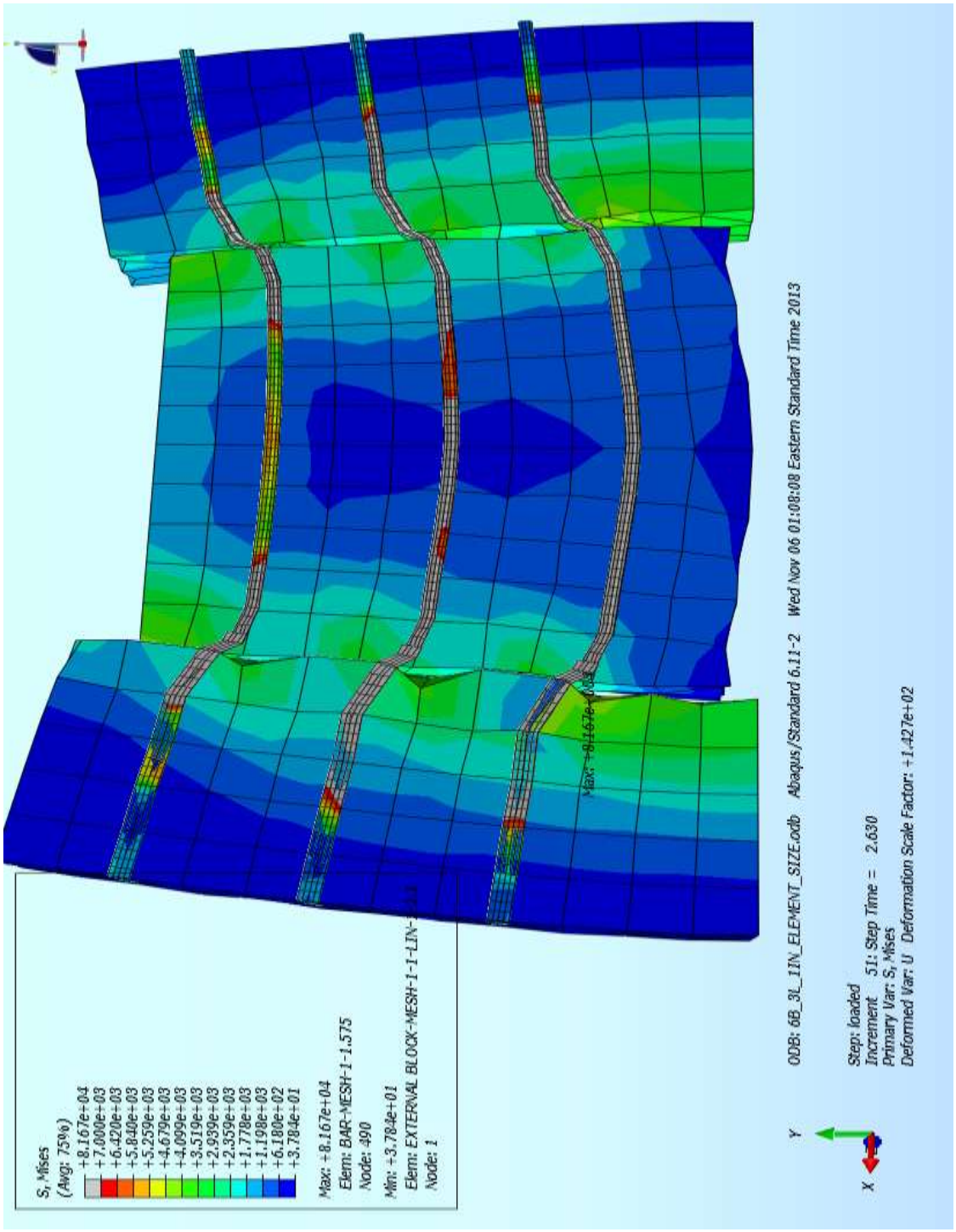


Figure 52: Steel and Concrete Stresses Distribution

Six models were analyzed with free lateral movement to the two external concrete units, a lateral separation range from 0.0052” to 0.0097”  at the bottom of the interface as shown in Figure 53. The load-slip relationships obtained from the finite element analyses are shown in Figures 54 and 55.

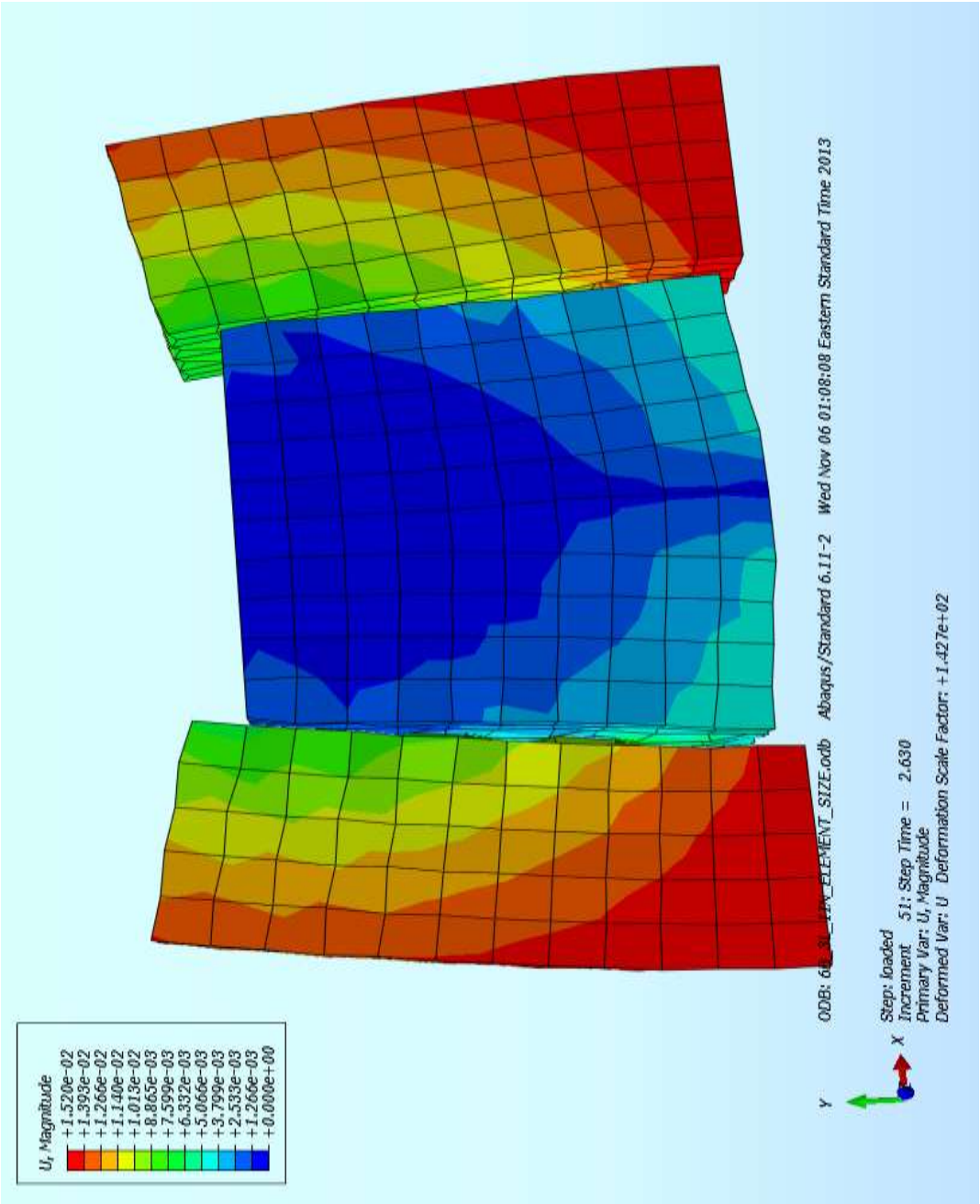


Figure 53: Lateral Displacement for FR441

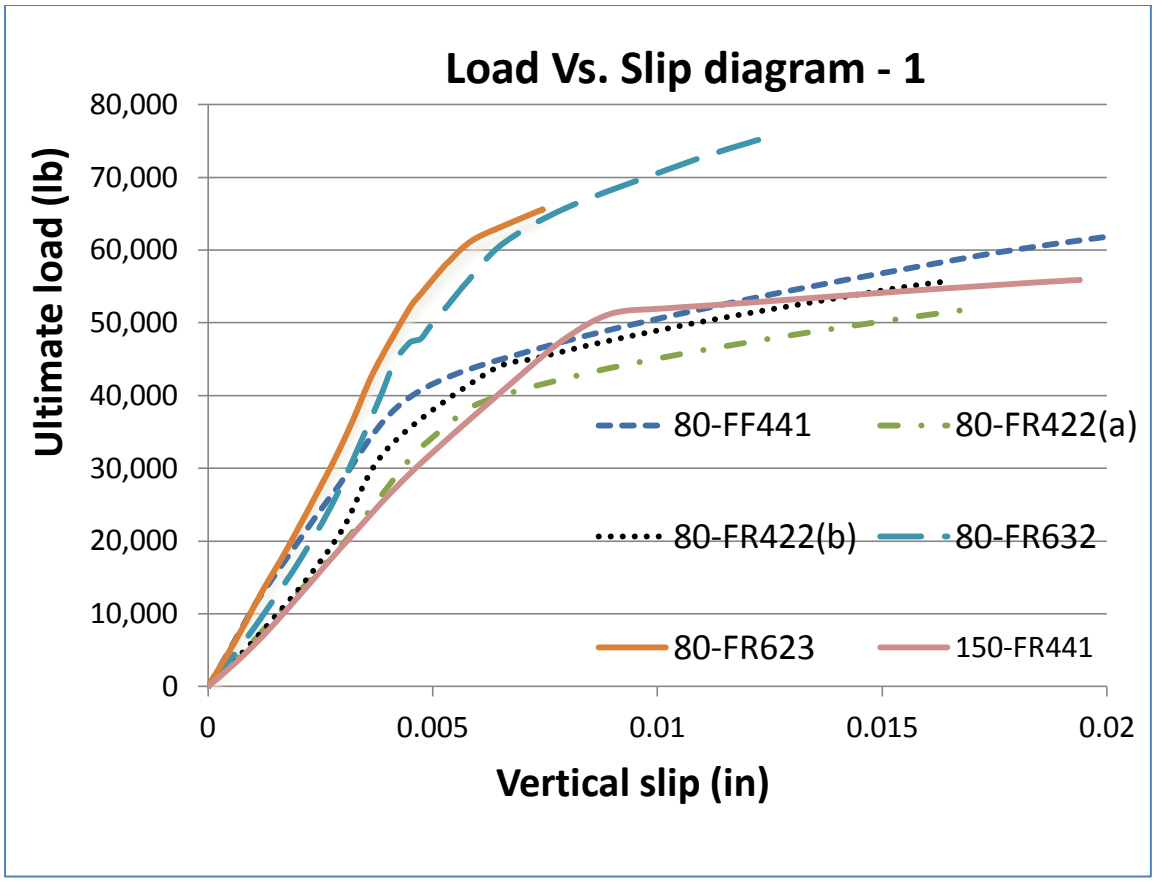


Figure 54: Load vs. Slip for FE Models - A

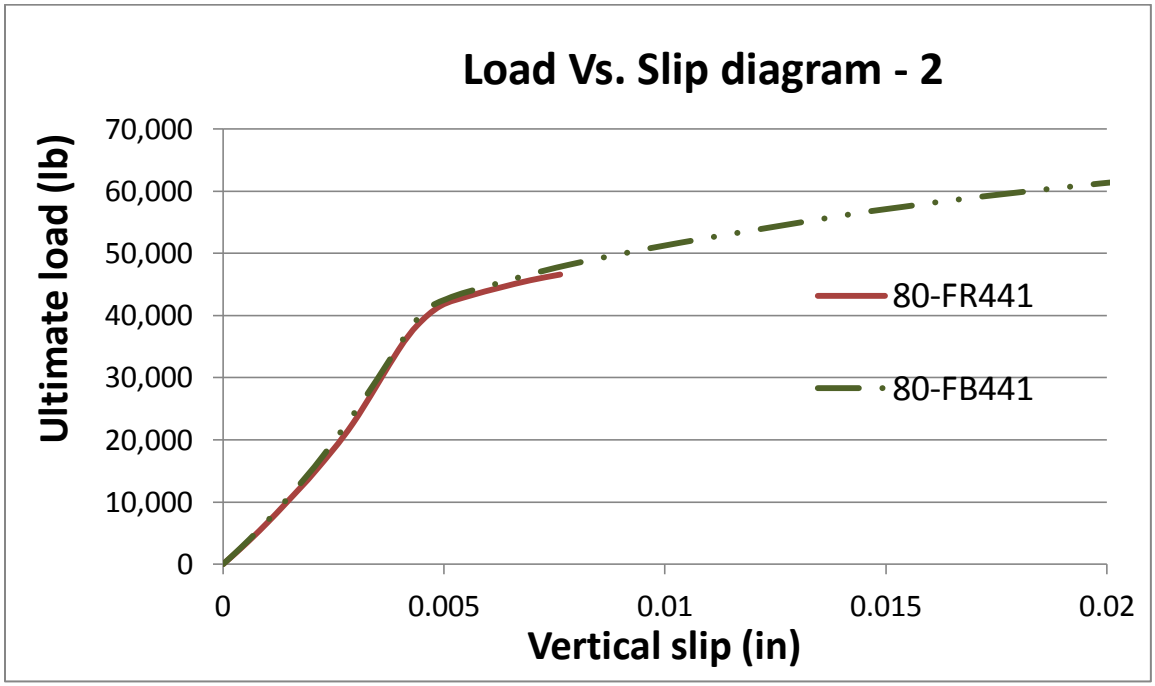


Figure 55: Load vs. Slip for FE Models - B

### 4.5.10 Discussion

The finite element analysis can demonstrate the effects of a) boundary conditions, b) reinforcement area, c) rebar distribution, and d) interface area.

#### 4.5.10.1 Boundary Condition

In the laboratory test as shown in Figure 17: Test setup, no lateral support was provided to the specimen. However the friction between the contact surfaces of the specimen and the lower platen of the test machine will provide some lateral fixity under the vertical load. The magnitude of this frictional resistance is difficult to estimate. Finite element models were able to demonstrate that lateral supports increased the shear strength, prevented the lateral separation of the concrete units. For the three comparable models with constant reinforcement and concrete interface area it was found that the model with restrained against lateral separation on the exterior blocks (FF441) has higher shear load and shear strength capacities of 68415 lb or 855 psi compared to the model with restrained only at the base (FB441) with strength of (63,101 lb or 789 psi). The model with restrained base (FB441) has higher shear load and shear strength (63,101 lb or 789 psi) compared to the model with unrestrained boundary conditions (FR441) with strength of 46,599 lb or 582 psi. Some of the results of the finite element analysis are shown in Figures 56 and 57.

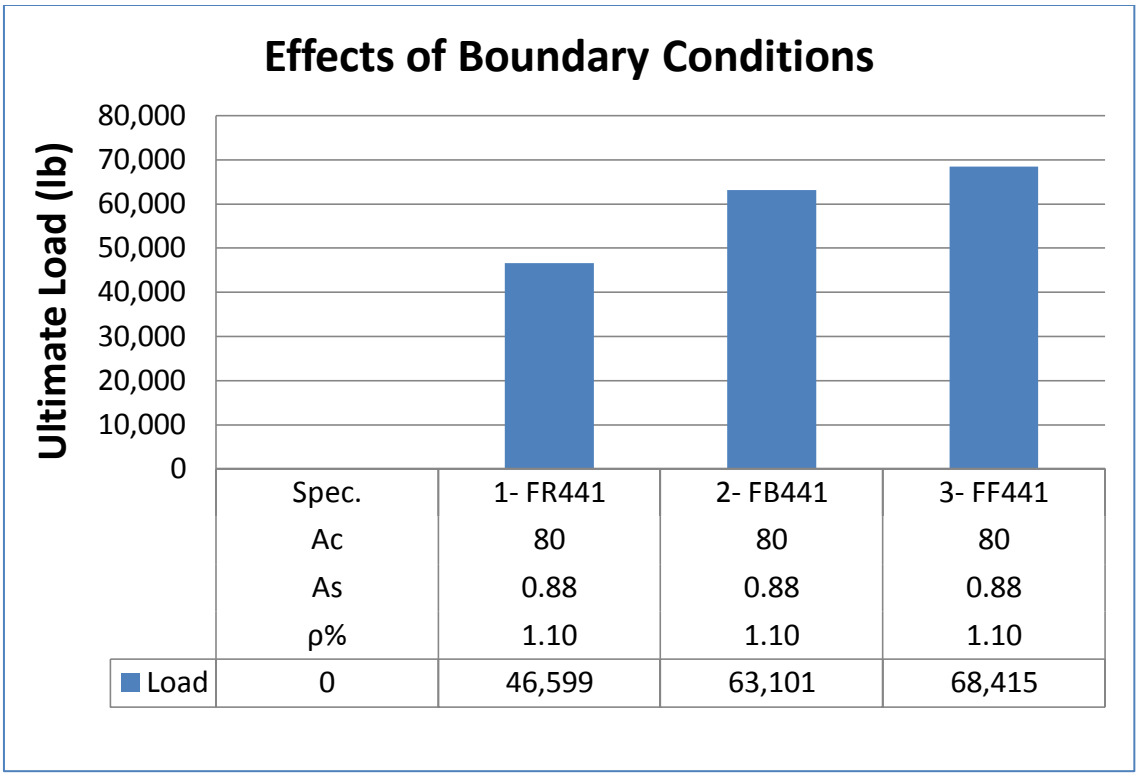


Figure 56: Boundary Condition and Load Carrying Capacity

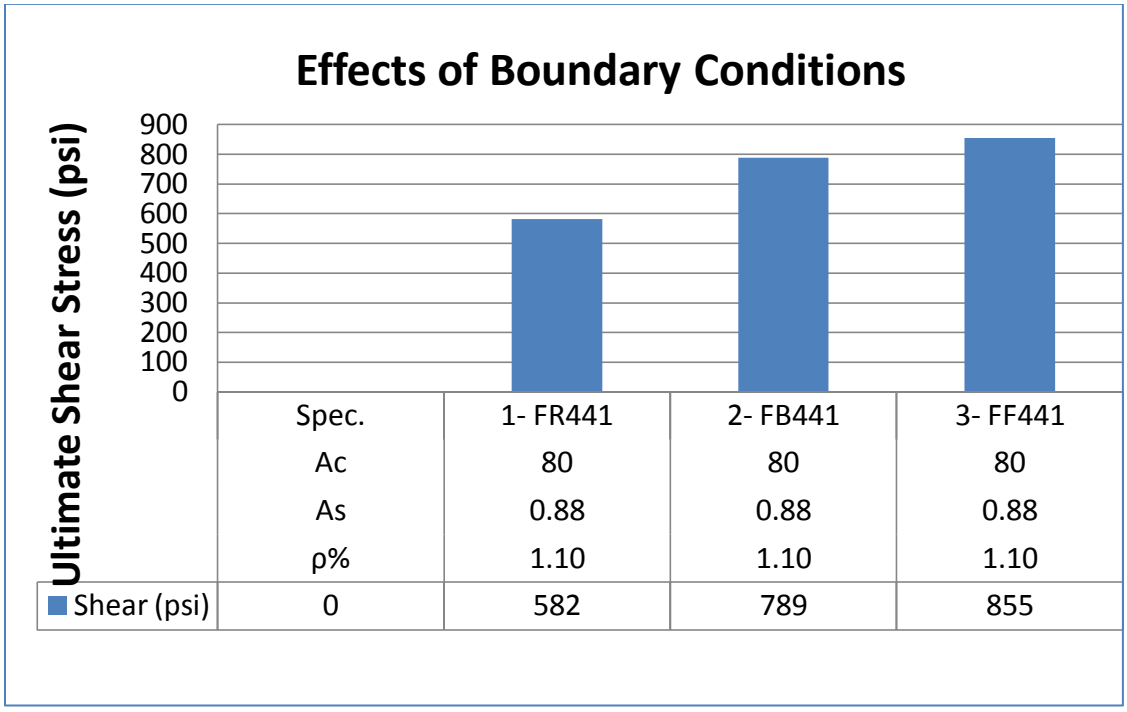


Figure 57: Boundary Conditions and Shear Strength

4. 5.10.2 Rebar Distribution and Reinforcement Area.

At fixed reinforcement areas and interface surfaces it was found that specimen FR441 with 4#3 bars placed in one column had shear load and strength equal to 46,955 lb or 582 psi which is less than placing the 4 bars in 2 rows and 2 columns in specimen 4-FR422 (a) with loading capacity of 51,888 lb or 649 psi. Changing the spacing between the rebar could change the shear strength which can be found by comparing 4-FR422(a) to 5-FR422(b) with load carrying capacity of 55,548 lb or 694 psi and also compared to 6-FR623 with two rows and 3 columns of rebar, had loading carrying capacity of 65,593 lb or 820 psi which is less than for model 7-FR635 with 3 rows and 2 columns with load carrying capacity of 75,637 lb or 945 psi. ACI 318-11 allows using the same expression for single layer of steel and for two layers of steel (ties), with no limits for the spacing between the layers.

The increase of the reinforcement area at a fixed concrete surface increased the value of $\rho$, increased the ultimate load and shear strength of the model. With concrete area of 80 $in^2$, the steel area increased from 0.88 to 1.32 $in^2$ and $\rho$ increased from 1.1% to 1.65%, for model FR441 to FR623. The corresponding load carrying capacity increased from 46,599 lbs to 65,593 lbs and the shear stress strength increased from 582 psi to 820 psi.

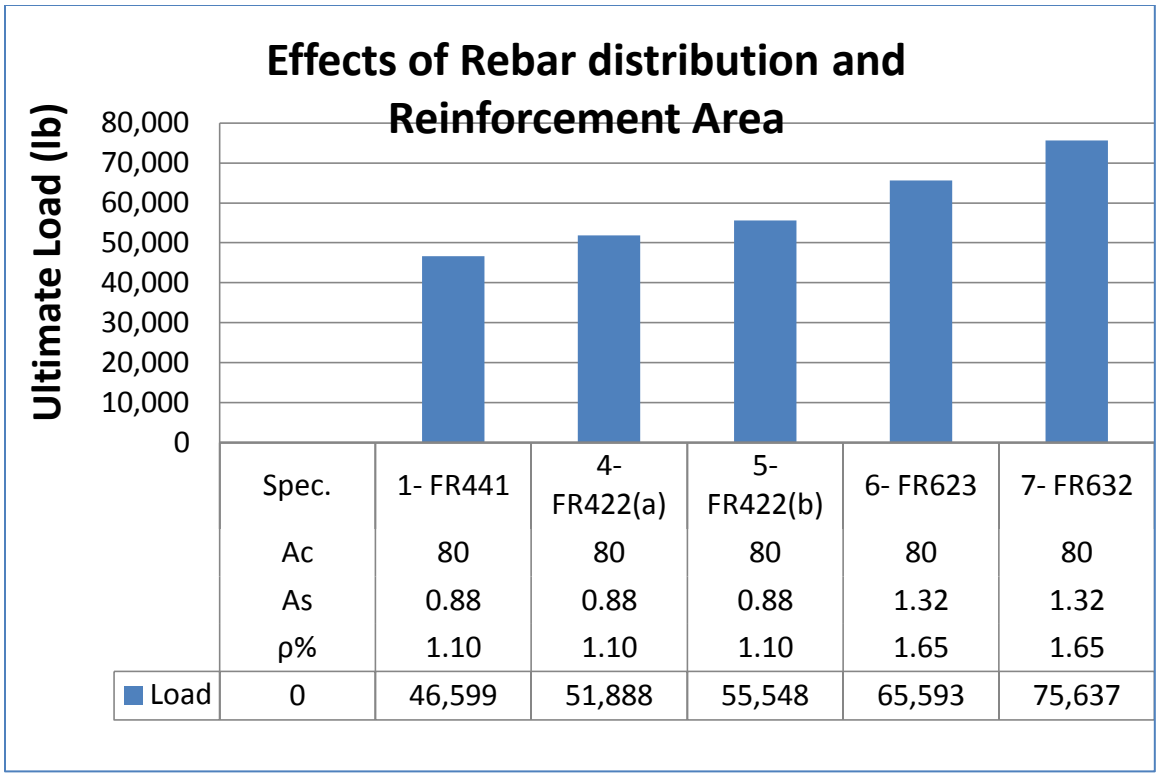


| Spec. | 1- FR441 | 4- FR422(a) | 5- FR422(b) | 6- FR623 | 7- FR632 |
|---|---|---|---|---|---|
| Ac | 80 | 80 | 80 | 80 | 80 |
| As | 0.88 | 0.88 | 0.88 | 1.32 | 1.32 |
| ρ% | 1.10 | 1.10 | 1.10 | 1.65 | 1.65 |
| Load | 0 | 46,599 | 51,888 | 55,548 | 65,593 | 75,637 |

Figure 58: Rebar Distribution and Reinforcement Area - Load

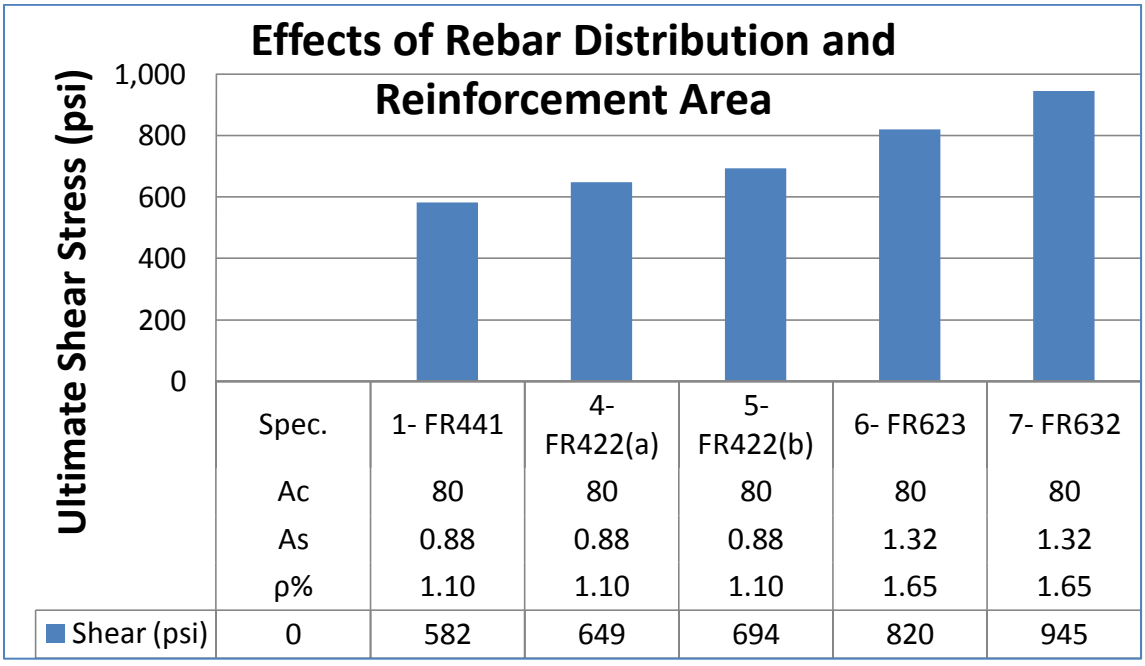


| Spec. | 1- FR441 | 4- FR422(a) | 5- FR422(b) | 6- FR623 | 7- FR632 |
|---|---|---|---|---|---|
| Ac | 80 | 80 | 80 | 80 | 80 |
| As | 0.88 | 0.88 | 0.88 | 1.32 | 1.32 |
| ρ% | 1.10 | 1.10 | 1.10 | 1.65 | 1.65 |
| Shear (psi) | 0 | 582 | 649 | 694 | 820 | 945 |

Figure 59: Rebar Distribution and Reinforcement Area - Shear

4.5.10.3 Interface Area

Using the same rebar area (4 bars, $A_s = 0.88$ in$^2$) the increase of the concrete area will increase the ultimate load applied to the specimen. However the reduction of ($\rho$=As/Ac) reduces the shear strength which is the case for specimen FF441 with $A_c = 80$ in$^2$. The ultimate load is 68,415 lb with shear strength of 855 psi when the concrete area was increased with the same reinforcement $\rho$ reduced from 1.1% to 0.59%. The ultimate load increased to 87,594 lb but the shear strength reduced to 584 psi. In general, the reduction of $\rho$ reduces the shear strength. The same trend exists in the case of FR441 Figure 60: Interface Area - Load and Figure 61: Interface Area - Shear. The bond and friction between concrete units has limited effect on the improvement of the strength compared to reinforcement area. It is believed by (Saemann & Washa, 1964) that the effect of roughness will reduce significantly with the increase of the reinforcement ratio. At high reinforcement ratios, a proper confinement surrounding the rebar is required not only for development of tensile stresses, but also to resist the compressive stresses transferred from the rebar to the surrounding concrete.

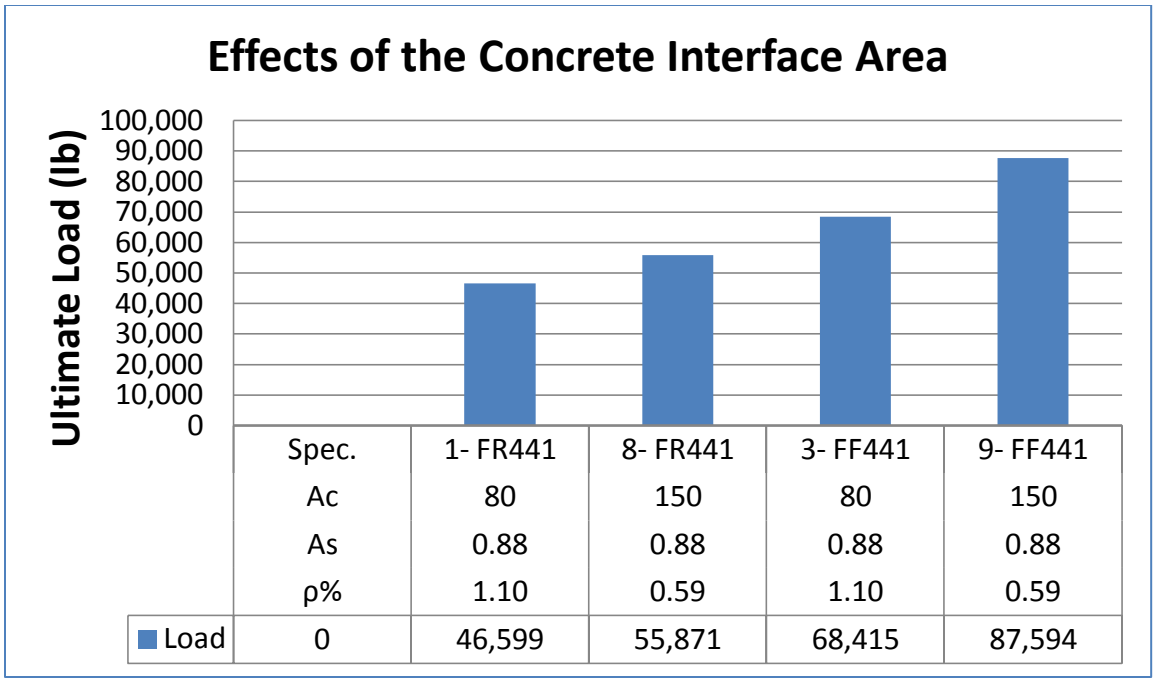


Figure 60: Interface Area - Load

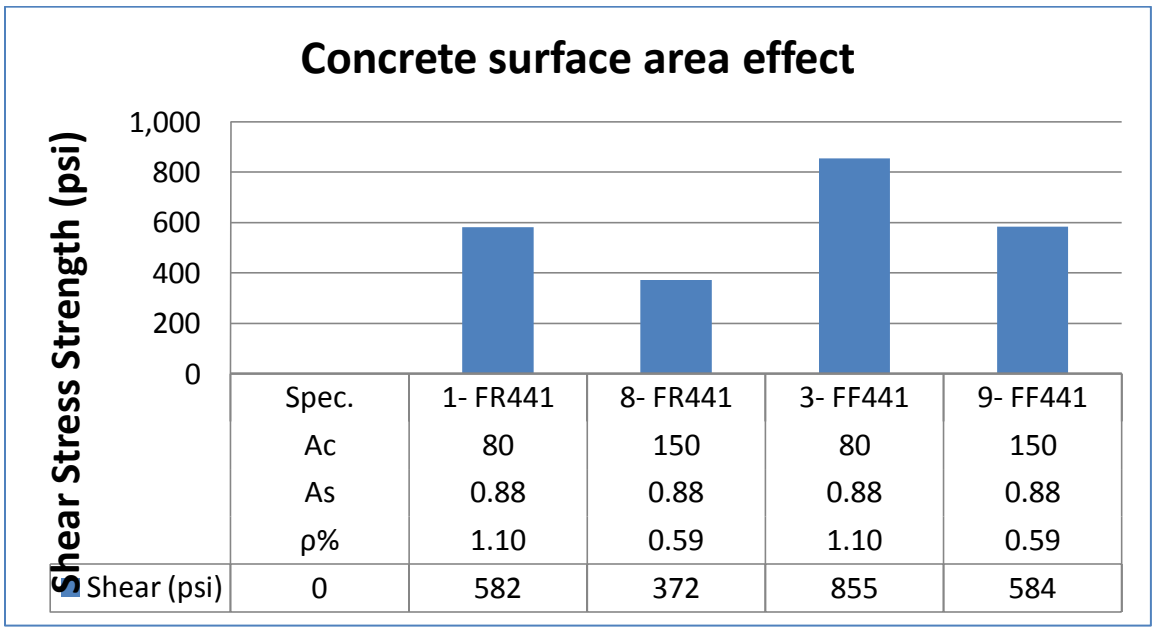


Figure 61: Interface Area - Shear

# CHAPTER V

# POTENTIAL APPLICATION FOR ADJACENT BOX BEAM GIRDER BRIDGES

## 5.1 Introduction

The use of cement based mortar is a common practice in construction especially when pre-cast concrete elements are used; the non-metallic non-shrink grouts are used to join adjacent precast reinforced concrete structural elements. A wide range of grout materials is available in the market. Non-metallic, non-shrink cement based grouts are specified by the departments of transportation in most of the states to reduce the shrinkage cracks and to avoid corrosion due to the exposure to weather conditions. The ultra-high performance concrete is a good alternative for the traditional grouts with higher bond strength with the concrete girders and higher resistance to the chloride penetration and low porosity because of the ingredients used in the mix design.

Key ways are formed in the structural elements to act as shear keys when filled with grouts. The grout is expected to have a perfect bond with the precast concrete units and to transfer the stresses from one girder to the adjacent girder to ensure that the structure acts as a single unit. An important application of using grouts in key ways is for the pre-cast pre-stressed bridge girders. Key ways can be in the longitudinal direction

joining adjacent box beams in the case of pre-cast pre-stressed box beam girders or in the transverse direction connecting beams in long span bridges. Transverse ties or prestressing strands are sometimes used to provide clamping force in the transverse direction in the case of adjacent pre-cast pre-stressed box beam girders to ensure the integrity of the structure in transferring the loads between the adjacent girders.

Joint performance depends on three factors:

1- Geometry of the key way

2- Properties of grout material

3- The amount of transverse force applied to the girder

The findings from the research described in this thesis are attempted to be applied to a practical application. That practical application is for key way joints of adjacent box beam bridges. The following sections outline the basis for potentially adopting some of the test results to adjacent box beam bridges. One of the common types of grout material used in the key ways of adjacent box beams is a normally a cementitious material that is similar to concrete. Wet grout placed against hardened concrete is expected to perform in a manner similar to wet concrete cast against hardened concrete. Therefore, preliminary work for the evaluation of key way grouted joints was done in this part of the project as a pilot study for a larger research project that will follow this work.

## 5.2 State-of-practice for key way geometry

Key way geometries in Figure 62: Examples of key Way Configurations and Figure 63: Different Key Way Geometries show that some states use a full depth key way and other states use a partial depth key way with wide range of widths.

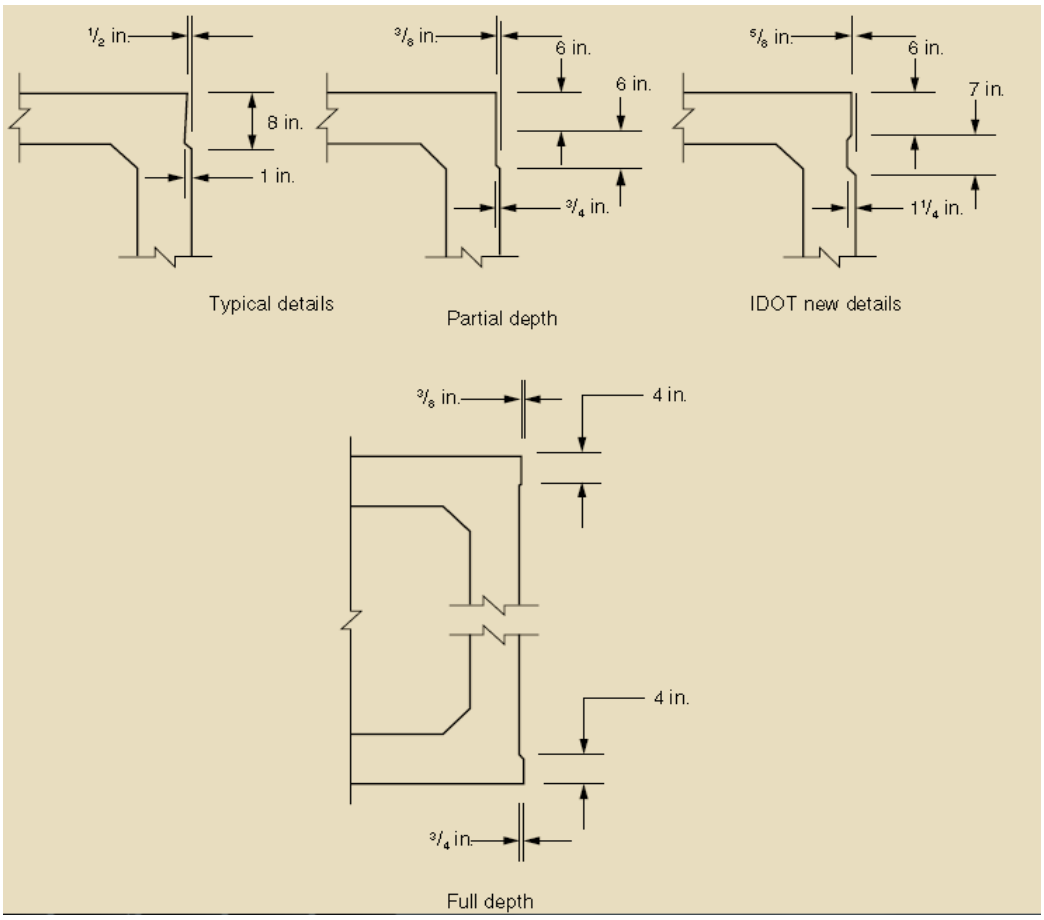


Figure 62: Examples of key Way Configurations (Henry, 2011)

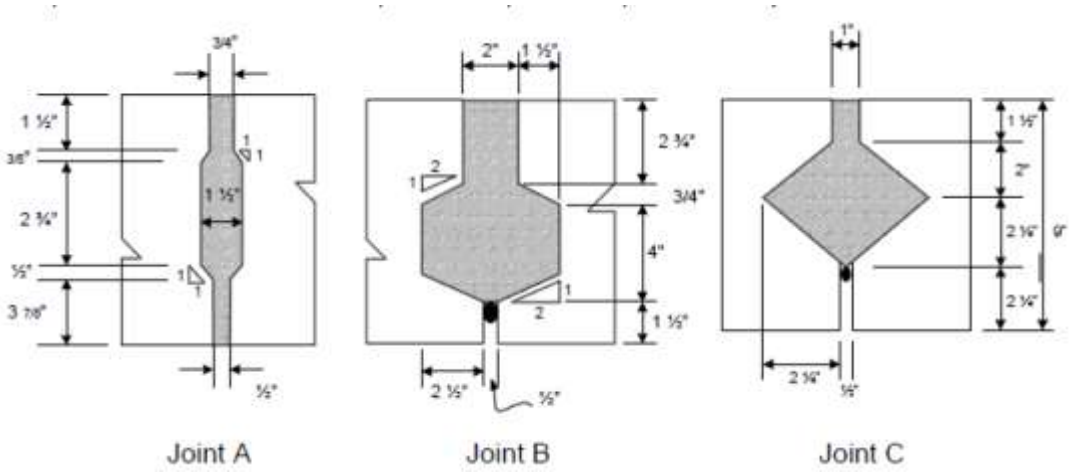


Figure 63: Different Key Way Geometries (Murphy, Kim, Zang, & Chao, 2010)

5.3 ODOT Current Practice

Ohio Department of Transportation has standard designs for box beam girders with standard key way geometries. For all 36" and 48" wide box beams with composite or non-composite beams, when the beam height is 12", 17", 21", *or* 27" the key way is 3" deep and 3/4" wide for the top opening to place the grout, below which a 4" of depth with 1.5" width. The key way depth is increased from total of $3 + 4 = 7"$ to $6 + 6 = 12"$ in case of deeper box beams with height of 33" *or* 42", a standard slope of 1: 1 for the chamfers at the transitions to change widths.

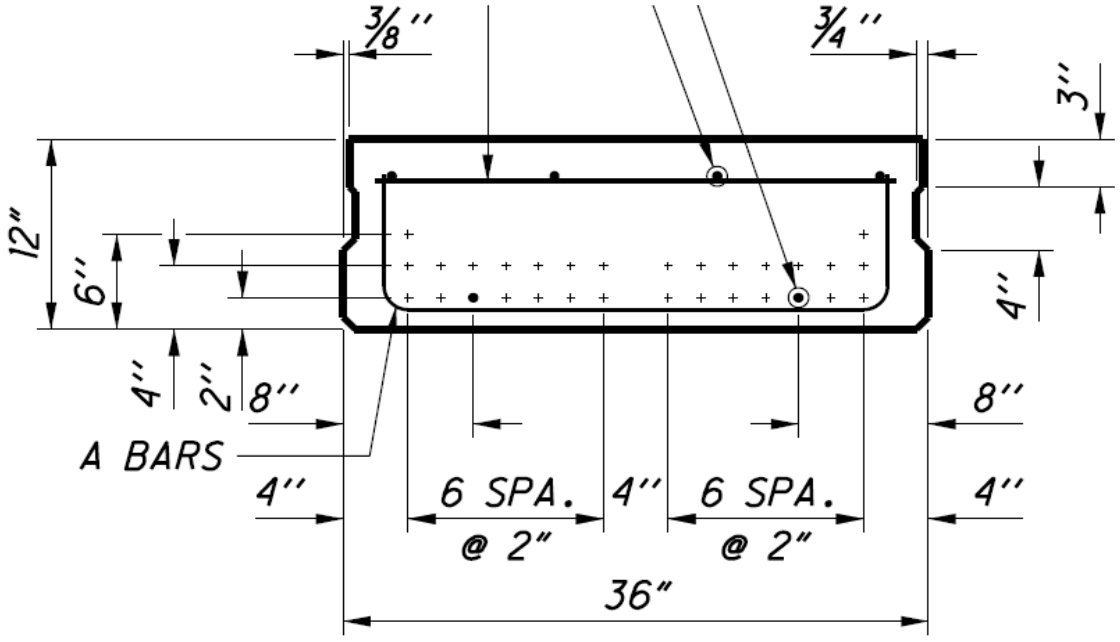


**B12-36**

(STRAND PATTERN TYPICAL FOR ALL 36" WIDE BEAMS)

Figure 64: Standard ODOT Key Way Geometry

5.4 Transverse Force

This information was gathered primarily from a survey of state highway agencies through the AASHTO Highway Subcommittee on Bridges and Structures and a review of the *AASHTO LRFD* Bridge Design Specifications (Henry, 2011). The locations for the ties were at the ends, mid span, quarter points, and third points, depending on the number of ties tying adjacent box beams. About 70% of the respondents reported that the ties were placed at mid-depth. If two strands or bars were used at one longitudinal location, they were placed at the third points in the depth. Other responses included specific location depths.

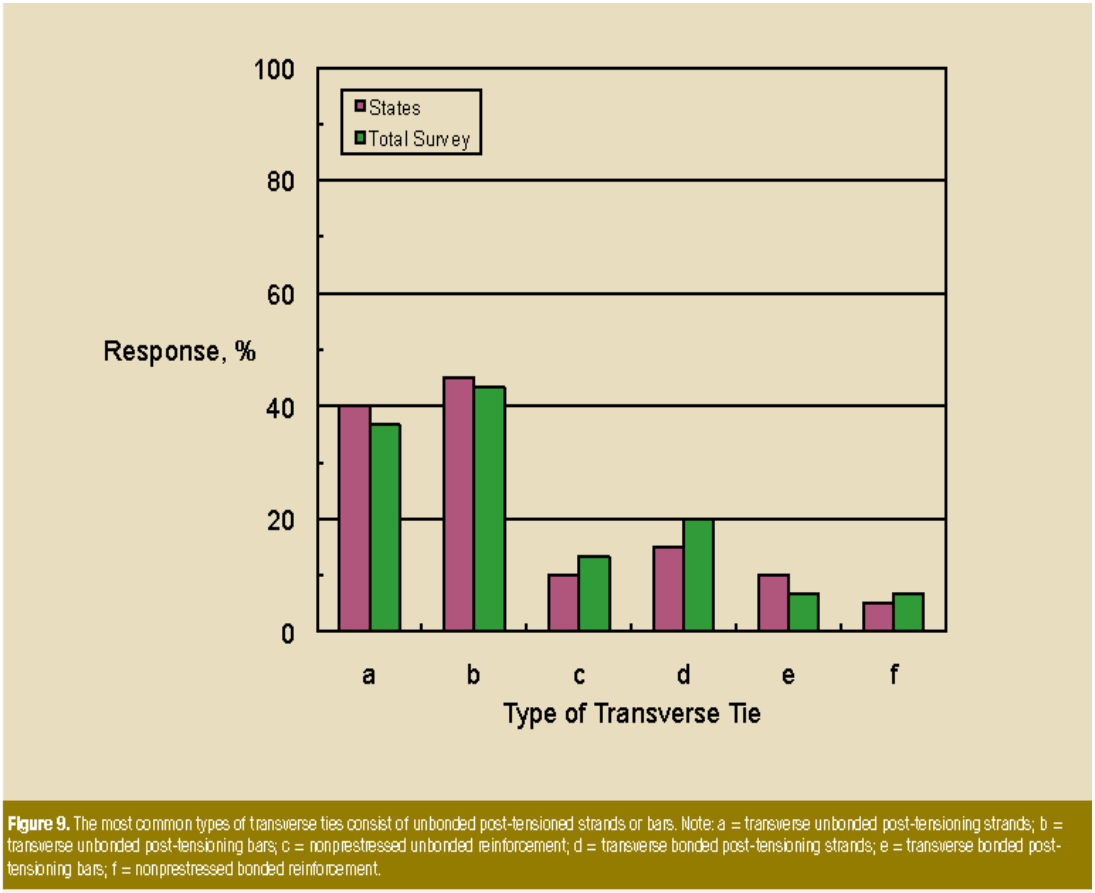


**Figure 9.** The most common types of transverse ties consist of unbonded post-tensioned strands or bars. Note: a = transverse unbonded post-tensioning strands; b = transverse unbonded post-tensioning bars; c = nonprestressed unbonded reinforcement; d = transverse bonded post-tensioning strands; e = transverse bonded post-tensioning bars; f = nonprestressed bonded reinforcement.

Figure 65: The Use of Transverse Force (Henry, 2011)

## 5.5 Design Criteria for Connections (Henry, 2011)

Eighty-one percent of states and 89% of the respondents to the survey stated that they did not make any design calculations to determine the amount of transverse ties between box beams. Some respondents provided information about the post-tensioning force used for each transverse tie and the spacing of ties. Based on this information, the average transverse force per unit length along the span for various numbers of ties was calculated. Figure 11 shows the results for 11 states. Where a single horizontal line is shown, it is based on the specified maximum spacing between ties. If the ties are closer than the minimum, the force will be higher than shown in the figure. Some states presented a range of forces because these states used a fixed number of ties for a range of span lengths. These are shown as a vertical band of color. A design chart to determine the required effective transverse post-tensioning force is provided in the PCI bridge design manual. This chart is based on the work of El- Remaily et al.

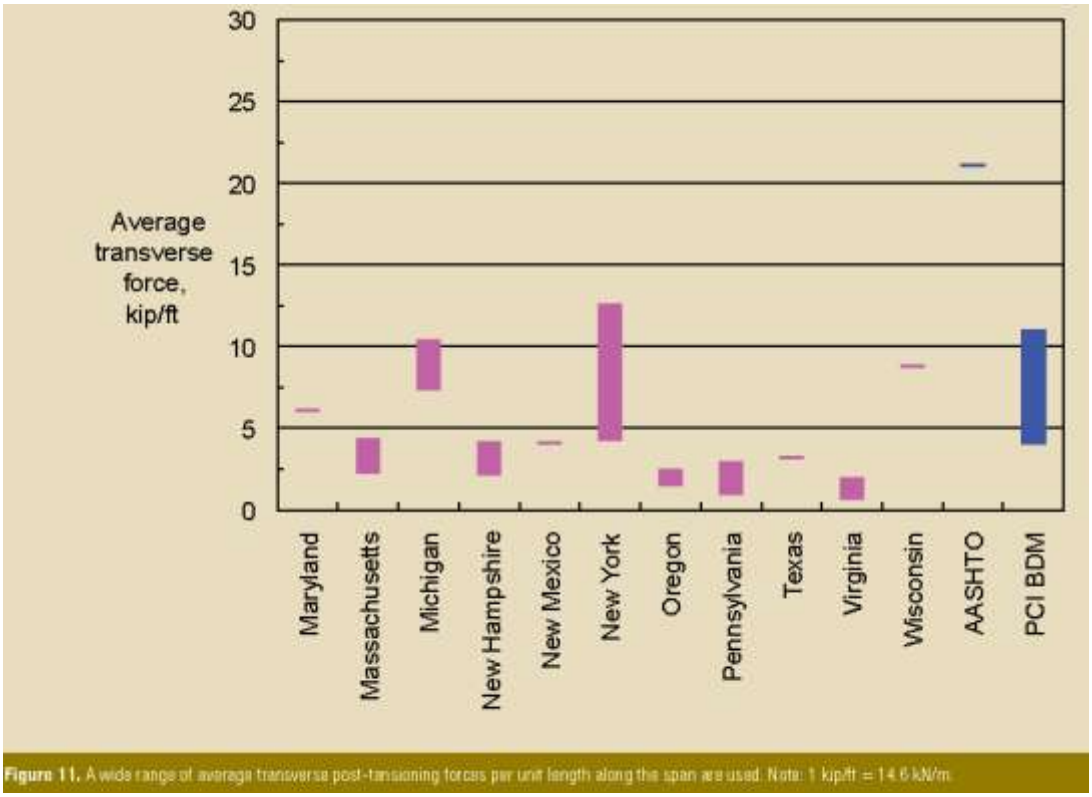


Figure 66: Average Transverse force (Henry, 2011)

5.6 Test Program

ODOT requires a one inch diameter tie-rod through two inch diameter hole in the transverse direction through the beams to provide a normal force of 15 kips that results from a torque of 250 lb-ft. In this test program, Grade B7 Alloy Steel threaded rods with ½" diameter and 20 threads per inch were used. The diameter of the hole in the concrete units for the tie rod was 1 inch with different amounts of applied torque of 100 lb-in, 200 lb-in, and 230 lb-in. The tie rod was placed at six inches from the top of the girder. This test specimen design was considered to be representative of the current practice and would possibly allow the application of the test results that were developed in this study (the test results were presented in earlier chapters).

5.7 Specimen Design

Each specimen comprised three concrete units, the external two units were of four inches length, four inches width, and 12 inches height with key way matching the current practice of ODOT as shown in Figure 67: Typical Geometry of Test Specimens and Figure 68: Test Specimen with a Tie Rod. Specimens S1 and S2 were joined using only the grout without tie rods. These specimens were used as the control test specimens. Five other specimens were joined with the grout and half inch diameter tie rod at six inches from the top. The applied torque was 230 (in-lb) for S3, S4, 200 (in-lb) for specimens S5, S6, and 100 (in-lb) for S7.

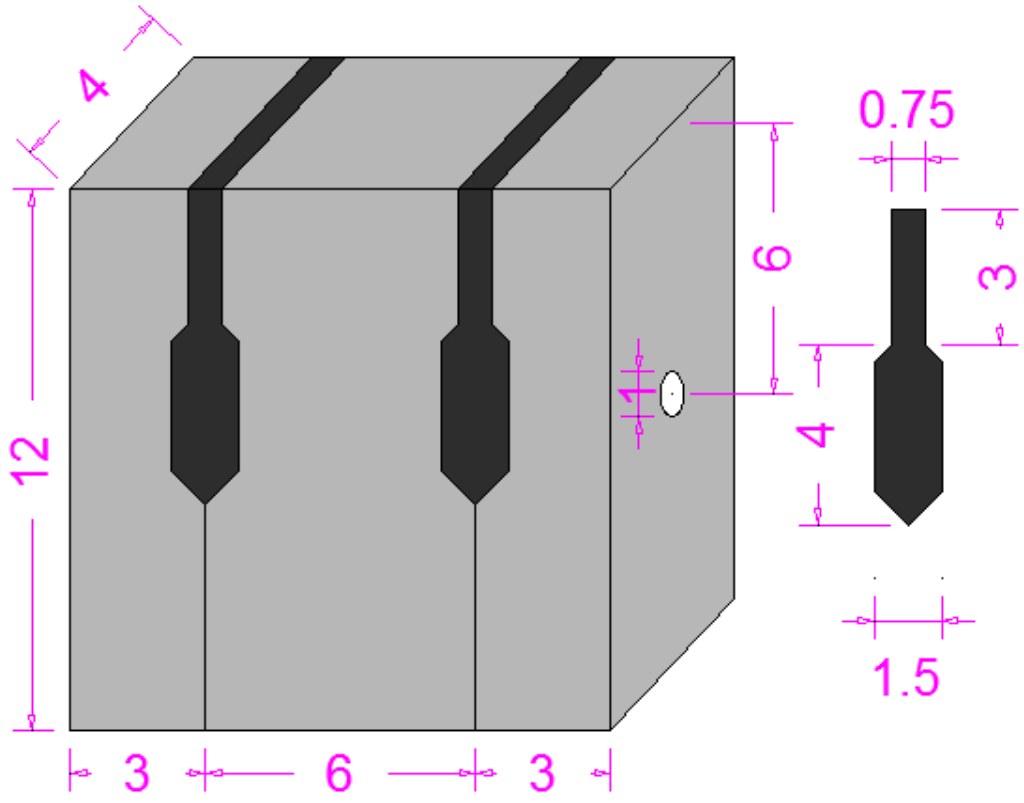


Figure 67: Typical Geometry of Test Specimens

.

Figure 68: Test Specimen with a Tie Rod

5.7.1Compressive strength of concrete units and grout

| | |
|---|---|
| Concrete Compressive Strength For S1,S2, S3, and S7 (psi) | 8,615 |
| Concrete Compressive Strength For S4,S5 (psi) | 8,686 |
| Grout (psi) | 7,477 |

5.7.2 Grout Material

Approved ODOT grout material was used based on the availability in the local market with reasonably high compressive strength; the average 28 day compressive strength of the grout was 7,477 psi.

5.8 Test Results

The results developed from the preliminary testing of the seven specimens are shown for failure condition in Table 23 and at first crack condition in Table 24.

Table 23: Results from the Key Way Shear Tests at Failure

| # | Concrete compressive strength (psi) | Grout compressive strength (psi) | Tie-rod torque | Failure load (lb) | Vertical displacement (in) | Top lateral displacement (in) | Bottom lateral displacement (in) |
|---|---|---|---|---|---|---|---|
| S1 | 8,615 | 7,477 | 0 | 4,940 | 0.0395 | Not measured | 0.004 |
| S2 | 8,615 | 7,477 | 0 | 8,530 | 0.03925 | Not measured | 0.014 |
| S3 | 8,615 | 7,477 | 230 | 23,050 | 0.1425 | 0.0425 | 0.092 |
| S4 | 8,686 | 7,477 | 230 | 23,068 | 0.13075 | Not measured | 0.055 |
| S5 | 8,686 | 7,477 | 200 | 23,838 | 0.11275 | 0.0315 | 0.07 |
| S6 | 8,686 | 7,477 | 200 | 29,133 | 0.13225 | 0.0165 | 0.078 |
| S7 | 8,615 | 7,477 | 100 | 25,691 | 0.09375 | 0.06 | 0.0445 |

Table 24: Results from the Key Way Shear Tests at First Crack

| # | Concrete compressive strength (psi) | Grout compressive strength (psi) | Tie-rod torque | First crack load (lb) | Vertical displacement (in) | Top lateral displacement (in) | Bottom lateral displacement (in) |
|---|---|---|---|---|---|---|---|
| S1 | 8,615 | 7,477 | 0 | 2,800 | 0.013 | Not measured | 0.0023 |
| S2 | 8,615 | 7,477 | 0 | 7,800 | 0.0245 | Not measured | 0.0055 |
| S3 | 8,615 | 7,477 | 230 | 18,000 | 0.0646 | 0.0045 | 0.0065 |
| S4 | 8,686 | 7,477 | 230 | 18,000 | 0.0635 | Not measured | 0.0065 |
| S5 | 8,686 | 7,477 | 200 | 18,000 | 0.05525 | 0.012 | 0.012 |
| S6 | 8,686 | 7,477 | 200 | 11,500 | 0.0555 | 0.0055 | 0.0055 |
| S7 | 8,615 | 7,477 | 100 | 13,500 | 0.033 | 0.017 | 0.003 |

Typical load-slip curves are shown in Figure 69 for specimens without tie rods and are shown in Figure 70 for specimens with tie rods

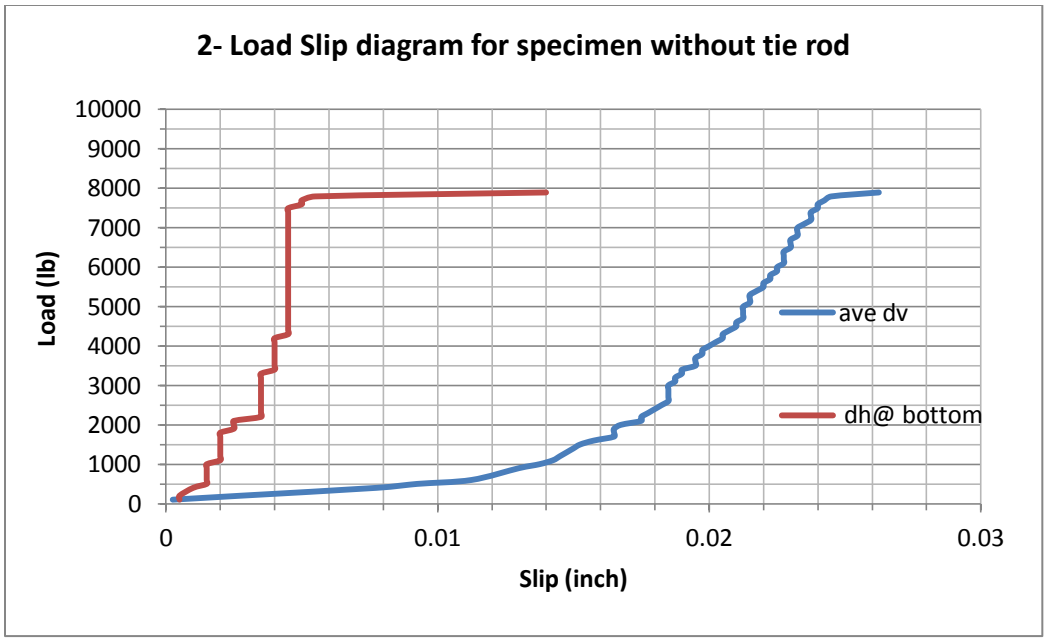


Figure 69: Typical Load-Slip Diagram for Specimens without Tie-Rod

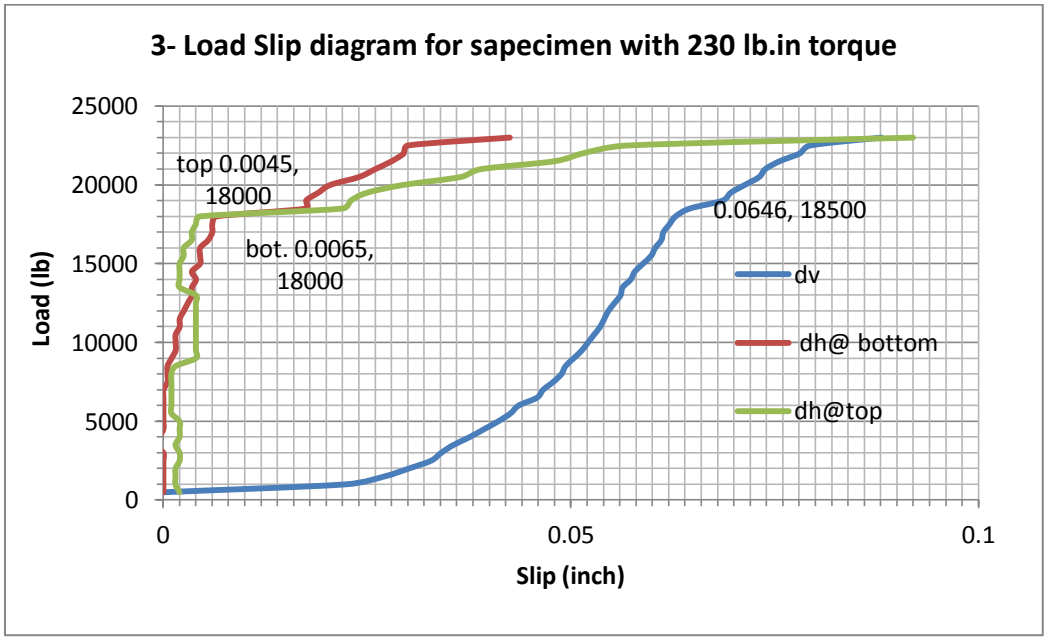


Figure 70: Typical Load-Slip Diagram for Specimens with Tie-Rod

## 5.9 Discussion

The listed concrete compressive strength is the least of the three average compressive strengths of the three concrete units. The middle concrete unit was supported at the top by the cross-head preventing it from vertical movement, while the load was applied to exterior two concrete units when the loading platen was moved upward. Dial gages were installed to measure the relative vertical slip between the three units, and the lateral spread or outward movements at the bottom. The top lateral movements were measured only in S3, S5, S6, and S7.

### 5.9.1 Load Transfer Mechanism

The specimen strength depends on the bond strength between the concrete and the grout material, the area of contact at the interface, bearing of grout on the chamfered base of concrete units, friction between the grout and concrete, shear resisted by steel cross-sectional area of the tie-rod crossing the interfaces. When loading is purely in shear, the primary difference between the specimens reported in previous chapters of this thesis and the key way joints is the additional bearing pressure mobilized on the chamfered base of concrete units.

### 5.9.2 Failure Modes

A sudden failure took place at the interface for the specimens without a tie-rod; concrete units and grout were not damaged or cracked as shown in Figure 72. For specimens with a tie rod, the specimens could be loaded until the concrete units were cracked or the tie-rod yielded. For specimen size used in this study, the concrete failed before steel as shown in Figure 71.

### 5.9.3 First Crack Load and Reserve Strength

A higher first crack load was recorded for the specimens with a tie rod compared to those without a tie rod. A load equal to 11,500 lb to 18,000 lb for specimens with tie rods was recorded as compared to 2,800 lb and 7,800 lb for the specimens without tie rod. The resulting higher load carrying capacity may be due to the contribution of the steel area of the tie-rod crossing the two interfaces and larger frictional resistance at the interface due to the clamping force applied through tie rod torque. The reserve strength "post-cracking load" was larger for the specimens with tie rod because the tie rod will provide lateral stability preventing the excessive lateral spread of the units at the bottom.


Figure 71: Typical failure mode for specimens with tie-rod

Figure 72: Typical failure mode for specimens without tie-rod

5.9.4 Vertical Displacement

Using a tie rod with the resulting clamping force allows larger vertical slip at first crack load. There was a trend also to increase the vertical slip as the clamping force is increased in all specimens. A vertical slip of 0.025 inch was the maximum slip recorded for specimens without tie rod, and increased to 0.033 inch for specimen S7 with 100 in-lb torque. For the specimens S5 and S6, with torque equal to 200 in-lb had the same amount of slip equal to 0.055". For the specimens S3 and S4 with 230 in-lb of torque, vertical slips equal to 0.063" and 0.064" were recorded. Increasing the clamping force using the same area of steel crossing the interface allowed larger vertical slip at first crack load.

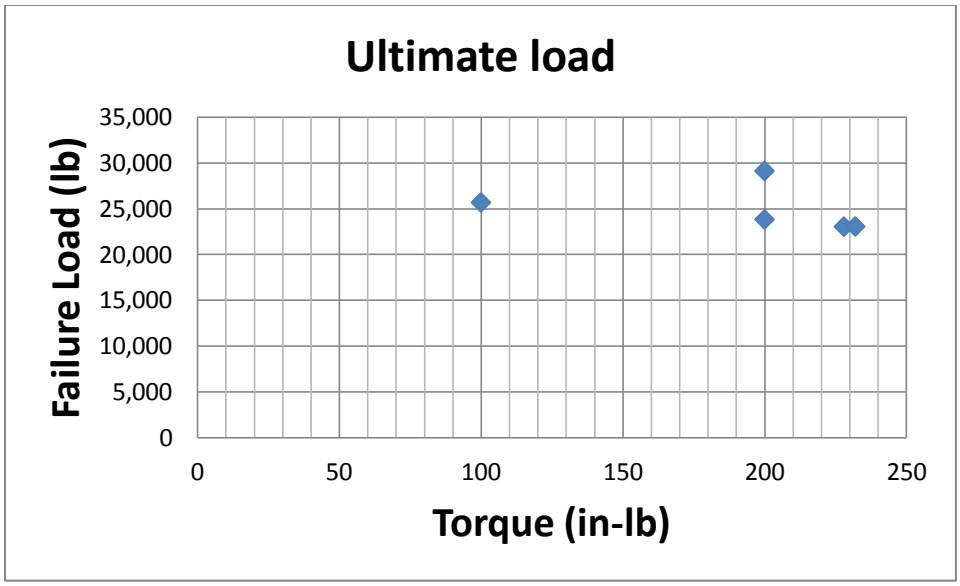


Figure 73: Failure load Vs. Torque

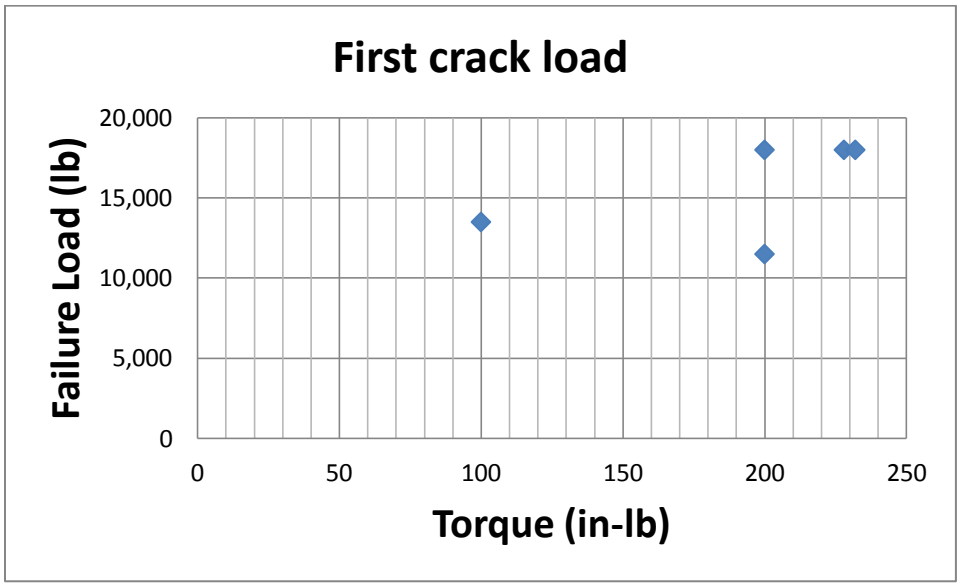


Figure 74: Ultimate load Vs. Torque

ACI 318-11 allows the interface shear transfer strength equation to design for the horizontal shear in flexure.

In “direct” shear along a shear plane, the increase in the load acting will reduce the frictional contribution due to lateral separation and vertical slip as found in all test specimens reported in this study unless the concrete blocks are supported in the horizontal direction to maintain full surface contact during the entire duration of the loading. This kind of restraint against separation at the interface is achievable in the case of precast-prestressed adjacent box beam girder bridges when ties or horizontal prestressing strands are used to tie the units together. The tie elevation and the compressive force applied to the box beams will influence the contribution from friction and crack width between the units.

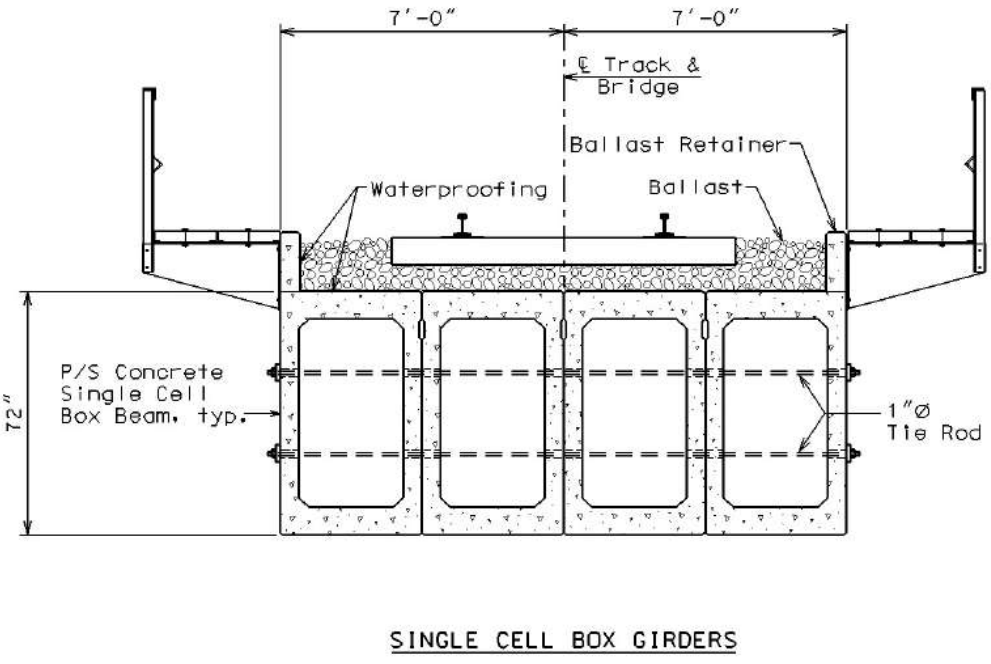


Figure 75: Ties in Box Beam Bridges (PCI, 2009)

An example of precompression across the interface for single cell box beams is shown in Figure 75: Ties in Box Beam Bridges (PCI, 2009) where two tie rods are used to prevent separation in the tensile and compression zones.

The equations evaluated in this study will form a basis for developing a prediction model in an upcoming research project on key way evaluation for determining the shear transfer strength of the longitudinal joints for adjacent box beam bridges.

# CHAPTER VI

# CONCLUSIONS AND RECOMMENDATIONS

The following conclusions may be drawn from the research study presented in this thesis. The study included an evaluation of the existing shear transfer strength equations for a smooth or rough interface and a carefully designed experimental work to determine the shear transfer strength of an interface with concrete cast against the surface of hardened concrete.

1. The horizontal shear strength equations for the prediction of the interface shear strength in composite concrete beams by Patnaik 2001 are suitable for predicting the shear transfer strength of a concrete interface.
2. Under a shear loading that is parallel to shear interface, tensile stresses across the interface will cause a lateral separation to develop resulting in a reduction of the shear strength.
3. The boundary conditions affect the shear strength; providing lateral supports in such way as to prevent separation at the interface can control the horizontal displacement; thereby maintaining the frictional contact between the two sides of an interface.

4. Applying an external clamping force perpendicular to the shear interface increases the shear strength of the interface. Such an external clamping force can be a substitute for the lateral supports for practical reasons. This aspect is particularly helpful in the case of precast-prestressed box beam girders for which it is not practical to provide lateral supports after installing the girders in place.
5. The distribution of the rebar crossing the shear interface will change the load path through the concrete section and a better distribution of the interface steel results in higher shear transfer strength of the concrete interface. Using strut and tie model for each individual situation to evaluate the compressive stresses in the struts and the tensile stresses in the rebar is a suitable approach, but a reasonable strut width needs to be considered based on the spacing of the reinforcing bars.
6. Detailing limits are needed for the spacing between the shear reinforcement crossing the interface to provide enough confinement and development length.
7. The higher the reinforcement ratio crossing the interface the lower the vertical slip, with more utilization of concrete strength at failure.
8. Suitable choice of key way depths and widths are needed to improve the shear strength and joint performance in precast-prestressed box beam bridges.

# REFERENCES


1 ACI. (2011). *Building code requirement for reinforced concrete.* Detroit: ACI 318-11.

2 Anderson, A. R. (1960). Composite design in precast cast-in-place concrete. *Prog Archit*, pp. 2(2):38-58.

3 Arafjo, D. L., & E1 Debs, M. K. (2005, March). Strength of shear connection in composite bridges with precast decks using high performance concrete and shear-keys. *Materials and Structures*, pp. 173-181.

4 Aziz, J. R. (2010). Shear Capacity of Concrete Prizms With Interface Joints. *Journal Of Engineering Volume 16*.

5 Birkeland, H. W. (1968). *Precast And Prestressed Concrete.* Class Notes For Course University of British Columbia.

6 Birkeland, P. W., & Birkeland, H. W. (1966). Connections in precast concrete structure. *ACI JOURNAL*, 63(3):345-68.

7 Eduardo, N. J., D, D.-d.-C. a., & Branco b, J. A. (2010). Accuracy of Design Code Expressions for Estimating Longitudinal Shear Strength of Strengthening Concrete Overlays. *Engineering Structures 32*.

8 Gaston, J. R., & Kriz, L. B. (1964). Connections in precast concrete strucures-scarf joints. *PCI J*.

9 Hanson, N. W. (1960). Precat Prestressed Concrete Bridges. 2. Horizontal Shear Connections. *Portland Cement Assoc*.

10 Henry, R. G. (2011). Adjacent precast concrete box-beam bridges: State of the practice. *PCI*, 75-91.

11 Hermansen, B. R., & Cowan, J. (1974). Modified shear-friction theory for bracket design,. *ACI Journal*, 71(2):55-60.

12 Khan, L. F., & Mitchell, A. D. (2002). Shear friction tests with high strength concrete. *ACI Structural Journal*, pp. 99(1):98-103.

13 Loov, R. E., & Patnaik, A. K. (1994). Horizontal Shear Strength of Composite Concrete Beams With Rough Interface. *PCI*, 39(1):48-69.

14 Mahmoud et al, M. (2013). Interfacial shear behavior of composite flanged concrete beams,. *HBRC*.

15 Mansur, M. A., Vinayagam, T., & Tan, K. H. (2008). Shear transfer across a crack in reinforced high strength concrete. *ACES J Material*, pp. 20(4):294–302.

16 Mattock, A. H. (1974). Shear tranfer in concrete having reinforcement at an angle to the shear plan. *ACI J. Special puplication 42-2*.

17 Mattock, A. H. (1994). Reader comments of paper "Horizontal shear strength of composite concrete beams with a rough interface" puplished in PCI Journal January- February 1994:39(1):48-69, by Loov RE, Patnaik AK. . *PCI Journal*, pp. 39(5):106-8.

18 Mattock, A. H. (2001). Shear friction and high strength concrete. *ACI Structural journal*.

19 Mattock, A., & Kaar, P. (1961). Shear test of continuous girders. *PCA*, 3(1) : 19-46.

20 Mitchell, G. (2002). Horizontal Shear Transfer Across a Roughenen Surface. *Cement & Concrete Composites*, 25 (2003) 379–385.

21 Murphy, M. l., Kim, J., Zang, Z., & Chao. (2010). *Deteminning more effective approaches of grouting shear keys of adjacent box beams.* Pennsylvanya Transportation Institute.

22 Naito Main, C. J. (n.d.). Retrieved from Google: http://www.google.com/imgres?newwindow=1&safe=off&hl=en&biw=1242&bih=545&tbm=isch&tbnid=BghQeccoJdC1iM%3A&imgrefurl=http%3A%2F%2Fwww.lehigh.edu%2F~cjn3%2Fpenndot.shtml&docid=dfi2nZhB6zCxFM&imgurl=http%3A%2F%2Fwww.lehigh.edu%2F~cjn3%2Fcorr.jpg&w=800&h=600&

23 Patnaik, A. H. (2001). Behavior of composite concrete beams with smooth interface. *ASEC J Struct Eng*.

24 PCI. (2009). The State of the Art of Precast/Prestressed Adjacent Box Beam Bridges.

25 Pedro, M. S., & Eduardo, N. B. (2011). Factors Affecting Bond Between Old And New Concrete. *ACI Material Journal*.

26 Pedro, M. S., & Eduardo, N. J. (2012). A state-of-the art review on shear friction . *Engineering Structures*.

27 Pedro, M. S., & Eduardo, N. J. (2013). A State of The Art Reviw on Roughness Quantification Method for Concrete Surfaces. *Construction and Building Materials 38 912-923*.

28 Raths, C. H. (1977). Reader comments of paper "Design proposals for reinforced concrete corbels" May-June 1976;21(3):18-42, by Mattock A PCI. *PCI*.

29 Saemann, J. C., & Washa, G. W. (1964). Horizontal shear connections between precast beams and cast in place slabs. *American Concrete Institute*, pp. 61(11):1309-83.

30 Scott, J. (2010). *Interface shear strength in lightweight concrete bridge girders.* Thesis submitted to the faculty of the Virginia Polytechnic Institute and State University.

31 Wall, J. S., & Shrive, N. G. (1988). Factors Affecting Bond Between Old and New Concrete. *ACI Material Journal*, 85-M15.

32 Wong, R., Ma, S., Wong, R., & Chau, K. T. (2007). *Shear strength components of concrete under direct shearing.* Cement and Concrete Research.

APPENDIX

Tensile test results

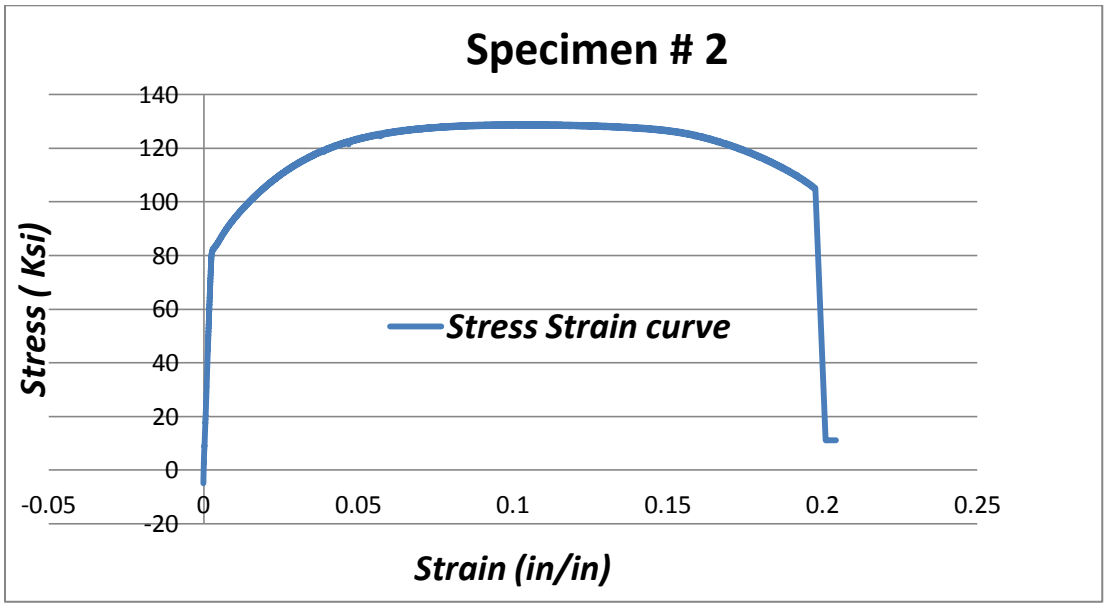

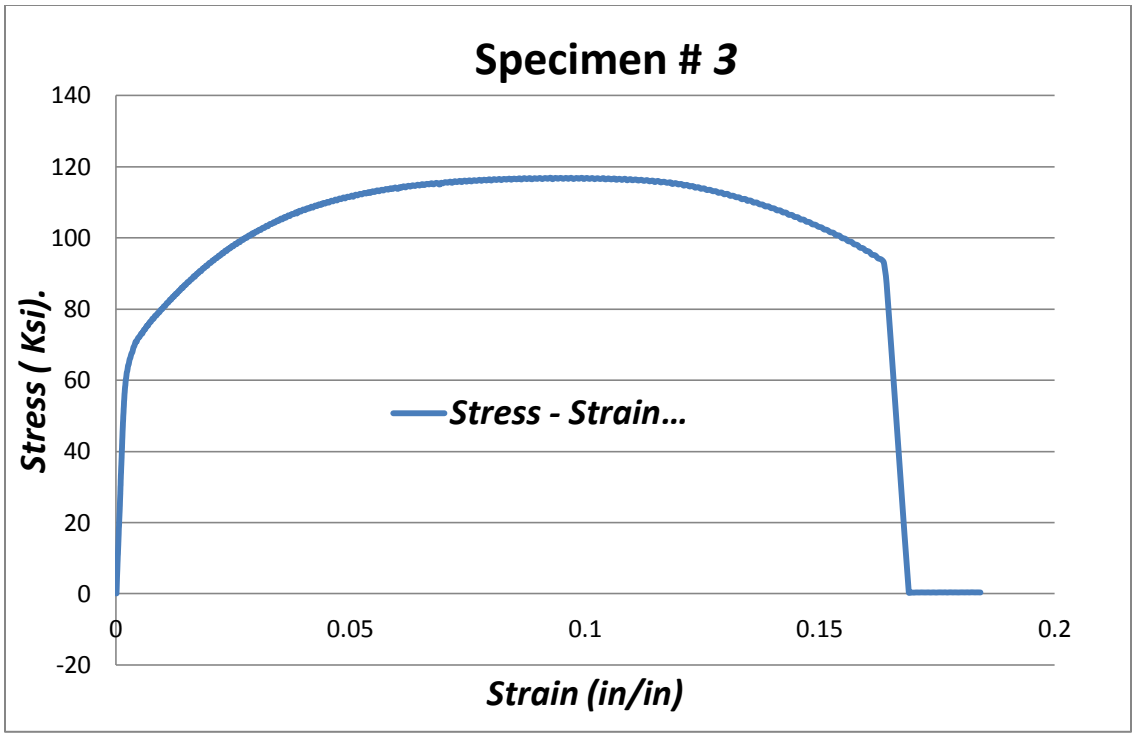


Selected data from Abaqus input file

** Generated by: Abaqus/CAE 6.11-2

*Preprint, echo=NO, model=NO, history=NO, contact=NO

** PARTS

*Part, name=bar-mesh-1

*Element, type=C3D8R

*Elset, elset=_PickedSet2, internal, generate

1, 1200, 1

** Section: steel

*Solid Section, elset=_PickedSet2, material=STEEL

*End Part

**

*Part, name="external unit-mesh-1"

```
*Node
      1,          5.,          12.,          4.
*Element, type=C3D8R
  1, 118, 119, 132, 131,   1,   2,  15,  14
480, 688, 689, 702, 701, 571, 572, 585, 584
*Elset, elset=_PickedSet2, internal, generate
   1,  480,    1
** Section: concrete
*Solid Section, elset=_PickedSet2, material=CONCRETE
*End Part
*Part, name="moddle part-mesh-1"
*Node
      1,          15.,          12.,          4.
   1089,          5.,          2.,          0.
*Element, type=C3D8R
  1,  100,  101,  112,  111,    1,    2,   13,   12
800, 1077, 1078, 1089, 1088,  978,  979,  990,  989
*Elset, elset=_PickedSet2, internal, generate
   1,  800,    1
*Nset, nset=supports, generate
    1,  1079,    11
** Section: concrete
*Solid Section, elset=_PickedSet2, material=CONCRETE
*End Part
** ASSEMBLY
```

*Assembly, name=Assembly

*Instance, name=bar-mesh-1-1, part=bar-mesh-1

0., 4., 2.

0., 4., 2., 0., 5., 2., 90.

*End Instance

*Instance, name="external unit-mesh-1-1", part="external unit-mesh-1"

*End Instance

*Instance, name="moddle part-mesh-1-1", part="moddle part-mesh-1"

*End Instance

*Instance, name="external unit-mesh-1-1-lin-1-2", part="external unit-mesh-1"

15., 0., 0.

*End Instance

*Instance, name=bar-mesh-1-1-lin-1-2, part=bar-mesh-1

0., 6., 2.

0., 6., 2., 0., 7., 2., 90.

*End Instance

*Instance, name=bar-mesh-1-1-lin-1-3, part=bar-mesh-1

0., 10., 2.

0., 10., 2., 0., 11., 2., 90.

*End Instance

*Instance, name=bar-mesh-1-1-lin-1-4, part=bar-mesh-1

0., 8., 2.

0., 8., 2., 0., 9., 2., 90.

*End Instance

*Elset, elset=_PickedSet31, internal, instance=bar-mesh-1-1-lin-1-2

1, 2, 3, 4, 5, 6, 7, 8, 9, 10, 11, 12, 13, 14, 15, 16

, 1200

*Elset, elset=_PickedSet31, internal, instance=bar-mesh-1-1

1, 2, 3, 4, 5, 6, 7, 8, 9, 10, 11, 12, 13, 14, 15, 16

1197, 1198, 1199, 1200

*Elset, elset=_PickedSet31, internal, instance=bar-mesh-1-1-lin-1-4

1, 2, 3, 4, 5, 6, 7, 8, 9, 10, 11, 12, 13, 14, 15, 16 ,1200

*Elset, elset=_PickedSet31, internal, instance=bar-mesh-1-1-lin-1-3

1, 2, 3, 4, 5, 6, 7, 8, 9, 10, 11, 12, 13, 14, 15, 16

, 1198, 1199, 1200

*Nset, nset=_PickedSet33, internal, instance="moddle part-mesh-1-1", generate

1, 1079, 11

*Nset, nset=_PickedSet35, internal, instance="external unit-mesh-1-1", generate

586, 702, 1

*Nset, nset=_PickedSet36, internal, instance="external unit-mesh-1-1-lin-1-2", generate

1, 117, 1

*Nset, nset=_PickedSet39, internal, instance="external unit-mesh-1-1", generate

13, 702, 13

*Nset, nset=_PickedSet39, internal, instance="external unit-mesh-1-1-lin-1-2", generate

13, 702, 13

*Elset, elset="_EXTERNAL block sufaces_S1", internal, instance="external block-mesh-1-1-lin-1-2", generate

385, 480, 1

*Elset, elset="_EXTERNAL block sufaces_S2", internal, instance="external block-mesh-1-1", generate

1, 96, 1

*Surface, type=ELEMENT, name="EXTERNAL block sufaces"

"_EXTERNAL block sufaces_S1", S1

"_EXTERNAL block sufaces_S2", S2

*Elset, elset="_middle block surface_S1", internal, instance="moddle part-mesh-1-1", generate

 721,  800,    1

*Elset, elset="_middle block surface_S2", internal, instance="moddle part-mesh-1-1", generate

  1,  80,   1

*Surface, type=ELEMENT, name="middle block surface"

"_middle block surface_S1", S1

"_middle block surface_S2", S2

** Constraint: Constraint-1

*Embedded Element, absolute exterior tolerance=0.01, exterior tolerance=0.01, roundoff tolerance=0.01

_PickedSet31

*End Assembly

** MATERIALS

*Material, name=CONCRETE

*Concrete

   2925.,      0.

4949.07, 0.0037

*Failure Ratios

 1.16,   0.09,   1.28, 0.3333

*Shear Retention

1., 0.01

*Tension Stiffening

1.,  0.

0., 0.002

*Elastic

4.64539e+06, 0.18

*Material, name=STEEL

*Elastic

2.9e+07, 0.28

*Plastic

89096.,  0.

113339., 0.17717

** INTERACTION PROPERTIES

*Surface Interaction, name=friction

1.,

*Friction, slip tolerance=0.005

0.9,

** BOUNDARY CONDITIONS

** Name: U1-U3 Type: Displacement/Rotation

*Boundary

_PickedSet35, 1, 1

_PickedSet35, 3, 3

** Name: U2 Type: Displacement/Rotation

*Boundary

_PickedSet33, 2, 2

** Name: u1 Type: Displacement/Rotation

*Boundary

_PickedSet36, 1, 1

** INTERACTIONS

** Interaction: FRICTION

*Contact Pair, interaction=friction, type=SURFACE TO SURFACE

"EXTERNAL block sufaces", "middle block surface"

** STEP: loaded

*Step, name=loaded, inc=1000000

*Static

0.001, 100., 0.0001, 1.

** BOUNDARY CONDITIONS

** Name: DISPLACEMENT Type: Displacement/Rotation

*Boundary

_PickedSet39, 2, 2, 0.5

** OUTPUT REQUESTS

*Restart, write, frequency=0

** FIELD OUTPUT: F-Output-1

*Output, field, variable=PRESELECT

** HISTORY OUTPUT: H-Output-1

*Output, history, variable=PRESELECT

*End Step